YEAST-BASED VACCINE APPROACHES TO CANCER IMMUNOTHERAPY

by

MASSACHUSETTS INSTITUTE OF TECHNOLOGY
OCT 31 2008
LIBRARIES

Shanshan W. Howland

B.S. and M.S. Chemical Engineering
Stanford University, 2001

Submitted to the Department of Biological Engineering in
Partial Fulfillment of the Requirements for the Degree of

Doctor of Philosophy in Biological Engineering

at the

Massachusetts Institute of Technology

September 2008

© 2008 Shanshan W. Howland. All rights reserved.

The author hereby grants to MIT permission to reproduce and to distribute publicly
paper and electronic copies of this thesis document in whole or in part
in any medium now known or hereafter created.

Signature of Author: _____
Department of Biological Engineering
June 30, 2008

Certified by: _____
K. Dane Wittrup
C.P. Dubbs Professor of Chemical Engineering & Biological Engineering
Thesis Supervisor

Accepted by: _____
Alan J. Grodzinsky
Professor of Electrical, Mechanical & Biological Engineering
Chair, Course XX Graduate Program Committee

ARCHIVES

Thesis committee members:

Jianzhu Chen
Cottrell Professor of Immunology, Department of Biology

Herman N. Eisen
Professor Emeritus and Senior Lecturer, Department of Biology

Darrell J. Irvine
Eugene Bell Associate Professor of Tissue Engineering, Departments of Materials Science & Engineering and Biological Engineering

YEAST-BASED VACCINE APPROACHES TO CANCER IMMUNOTHERAPY

by

Shanshan W. Howland

Submitted to the Department of Biological Engineering
On June 30, 2008 in Partial Fulfillment of the
Requirements for the Degree of Doctor of Philosophy in
Biological Engineering

ABSTRACT

Saccharomyces cerevisiae stimulates dendritic cells and represents a promising candidate for cancer immunotherapy development. Effective cross-presentation of antigen delivered to dendritic cells is necessary for successful induction of cellular immunity. Using a yeast vaccine model, we investigated the phagosome-to-cytosol pathway of cross-presentation. We demonstrate that the rate of antigen release from phagocytosed yeast directly affects cross-presentation efficiency, with an apparent time limit of about 25 min post-phagocytosis for antigen release to be productive. Antigen expressed on the yeast surface is cross-presented much more efficiently than antigen trapped in the yeast cytosol by the cell wall. The cross-presentation efficiency of yeast surface-displayed antigen can be increased by the insertion of linkers susceptible to cleavage in the early phagosome. Antigens indirectly attached to yeast through antibody fragments are less efficiently cross-presented when the antibody dissociation rate is extremely slow.

Next, we present a yeast-based cancer vaccine approach that is independent of yeast's ability to express the chosen antigen, which is instead produced separately and conjugated to the yeast cell wall. The conjugation method is site-specific (based on the SNAP-tag) and designed to facilitate antigen release in the dendritic cell phagosome and subsequent translocation for cross-presentation. Phagosomal antigen release was further expedited through the insertion of the invariant chain ectodomain as a linker, which is rapidly cleaved by Cathepsin S. The dose of delivered antigen was increased in several ways: by using yeast strains with higher surface amine densities, by using yeast cell wall fragments instead of whole cells, and by conjugating multiple layers of antigen. The novel multi-layer conjugation scheme is site-specific and takes advantage of Sfp phosphopantetheinyl transferase, enabling the antigen dose to grow linearly. We show that whole yeast cells coated with one layer of the cancer-testis antigen NY-ESO-1 and yeast hulls bearing three layers were able to cross-prime naïve $CD8^+$ T cells *in vitro*, with the latter resulting in higher frequencies of antigen-specific cells after ten days. This cross-presentation-efficient antigen conjugation scheme is not limited to yeast and can readily be applied towards the development of other particulate vaccines.

Thesis supervisor: K. Dane Wittrup
Title: C.P. Dubbs Professor of Chemical Engineering & Biological Engineering

Table of Contents

Chapter 1

Introduction

1.1 Cancer Immunotherapy

The idea that the immune system defends the body from not just infections but also cancer is almost one century old (1). Since then, extensive data has been collected showing that immunodeficient mice are particularly susceptible to both carcinogen-induced and spontaneous tumors (2). Three lines of evidence support the role of cancer immunosurveillance in humans (reviewed in (3)). First, the incidence of cancer is elevated in immunodeficient individuals and in immunosuppressed transplant recipients. Second, some cancer patients have developed detectable humoral or cellular responses against their own tumors, demonstrating that the immune system can differentiate between normal and transformed cells and leading to the discovery of hundreds of tumor-associated antigens (TAAs). Third, numerous studies have demonstrated a positive correlation between the presence of tumor-infiltrating lymphocytes and patient prognosis, suggesting that anti-tumor immune responses are not merely incidental but can be protective. The growing field of cancer immunotherapy addresses the challenge of harnessing the immune system to treat cancer.

Cancer immunotherapy may be classified into passive and active strategies. In passive immunotherapy, the effectors of immunity—antibodies, cytokines, or even T cells—are generated outside the body for introduction into the patient. The goal of active immunotherapy, or cancer vaccination, is to stimulate the body into mounting an adaptive immune response against one or more TAAs. While passive immunotherapy technology is more mature, with multiple monoclonal antibodies and cytokines already on the market, the elusive allure of cancer vaccines lies in their potential ability to confer long-lasting protection against tumor recurrence.

Amongst the immune system's arsenal, cytotoxic T lymphocytes (CTLs) are the most direct weapon against tumor cells. Humoral immunity is limited to cell membrane-expressed targets and the therapeutic effects mediated by growth inhibition, antibody-dependent cytotoxicity and complement-dependent cytotoxicity vary considerably between antibodies (4). Therefore, understanding how professional antigen-presenting cells (APCs) trigger T cell activation is critical to cancer vaccine development.

Dendritic cells (DCs) have been described as "nature's best APCs" (5) and until recently were thought to be the only APCs known to activate naïve T cells (6). Since the immune system often appears to be ignorant of tumor antigens, especially in early stage solid tumors (7), DCs are crucial to the success of cancer vaccines. In their immature state, DCs reside in the blood and peripheral tissues, constantly sampling the microenvironment for antigens. In the absence of infection or inflammation, small numbers of these resting DCs travel to secondary lymphoid organs to contribute towards peripheral tolerance of self-antigens. In the presence of an infection, DCs mature in response to inflammatory stimuli and pathogen-associated "danger signals". They migrate to the draining lymph nodes to present foreign antigen, thus stimulating lymphocyte proliferation. The two-signal model of lymphocyte activation explains how such different outcomes can arise from DC-T cell interaction. In this model, mature DCs presenting both peptide-MHC complexes (signal 1) and costimulatory molecules (signal 2) to T cells stimulate proliferation, whereas immature DCs presenting signal 1 without signal 2 induce T cell anergy. This model has been refined over time but it remains the prevailing paradigm. In a striking demonstration by Dhodapkar et al., injection of immature DCs pulsed with influenza matrix peptide inhibited CTL function in human volunteers, whereas mature DCs pulsed with the same antigen boosted the number of specific CTLs (8). Therefore, DC maturation status and the choice

of adjuvants warrant special consideration in cancer vaccine design, particularly when pre-existing immune tolerance to tumors has to be overcome (9).

1.2 The Cancer Vaccine Landscape

Historically, non-specific stimulators of the immune system have been reported to be beneficial in treating cancer, beginning with Coley's toxins in the 1890s. William Coley developed a mixture of two heat-killed bacterial strains to treat bone sarcoma, which was widely used until radiation therapy and chemotherapy emerged (10). Bacillus Calmette-Guerin (BCG, inactivated tuberculosis bacteria) is still part of the standard of care for superficial bladder cancer. The cytokines IFN-α and IL-2 are FDA-approved treatments for specific types of cancers. While all these treatments are thought to boost the immune response against cancer, they are not true cancer vaccines in that they are not targeted against TAAs. Gardasil® is sometimes described as the first cancer vaccine on the market, but it is really a vaccine preventing infection by certain strains of human papillomavirus and will neither prevent nor treat cervical cancer in individuals already infected. Despite intense research and optimism, no cancer vaccines have been approved until very recently, and none by the FDA. In April 2008, Oncophage®, peptide-heat shock protein complexes isolated from each patient's tumor cells, was approved to treat renal cell carcinoma in Russia. In May, OncoVAX®, a preparation made from irradiated autologous tumor cells, was licensed to be commercialized in Switzerland followed by seven Eastern European countries.

Many different strategies for cancer vaccination are under investigation. Before TAAs were identified, whole tumor cells (often irradiated) and tumor cell lysates were used. Early efforts to increase their immunogenicity centered on genetic engineering of the tumor cells to express cytokines, MHC molecules and costimulatory molecules (11, 12). Vaccines made from

autologous tumor cells remain attractive because they are personalized and contain a wider variety of antigens (including unidentified antigens and those bearing unique mutations); however, obtaining enough cells can be difficult and the risk of an autoimmune response may be higher than when only defined TAAs are present (13).

SEREX (serological identification of antigens by recombinant expression cloning (14)) and other methods to discover TAAs opened up the floodgates for the development of a new generation of cancer vaccines. Synthetic peptides representing T cell epitopes are relatively easy to produce and thus have been widely studied in clinical trials. To increase immunogenicity, peptide vaccines are frequently co-administered with cytokines, "classical" adjuvants (e.g. alum, incomplete Freund's adjuvant) or Toll-like receptor ligands mimicking danger signals from pathogens. Although peptide vaccination frequently results in marked expansion of specific $CD8^+$ T cells, up to 5-10% of circulating $CD8^+$ T cells in some cases, clinical responses have been disappointing (15). Often, the expanded T cells have low avidity and recognize peptide-pulsed target cells but not unmodified tumor cells with lower surface levels of the peptide-MHC; this problem is thought to arise because peptide vaccination results in APCs with unusually high surface levels of peptide-MHC complexes that then activate these "low quality" CTLs (16). Ironically, the fact that minimal peptide-epitope vaccines do not need to be processed by APCs may turn out to be problematic rather than advantageous. Other issues with peptide vaccines include the narrow immune response (easily evaded by tumors) and the lack of helper epitopes. Recombinant proteins representing full-length TAAs or parts thereof partially address these problems. Like peptides, they do not inherently mature DCs and have to be combined with one or more adjuvants. Recombinant proteins may also be produced as fusions to sequences with a variety of functions, such as antibodies against DC receptors (17), heat shock proteins (18),

protein transduction domains (19), the bacterial danger signal flagellin (20) and chemokines (21). Another tactic to increase the efficacy of protein vaccines is to mix them with antibodies to form immune complexes that both mature DCs and enhance uptake by interaction with Fc receptors (22, 23); this is also applicable to whole cell vaccines (24).

Recombinant proteins can be expensive to produce and purify and have a limited shelf-life. DNA vaccination is a cheaper and more stable alternative, whereby genes encoding TAAs are introduced into the body, usually in the form of plasmids. The TAAs may be expressed and processed directly in DCs or they may be expressed or secreted by other cell types prior to uptake by DCs. Much of the research in DNA vaccine development focuses on ways to increase transfection efficiency and transgene expression levels, in particular, by using different delivery methods such as injection, electroporation or particle bombardment of naked DNA or the delivery of DNA complexed with polymers or lipids (25). Molecular adjuvants such as cytokines and chemokines may be encoded on the same or separate plasmid.

Viral vaccines are another way to deliver TAA genes, typically with much higher transfection rates than those achieved by non-viral methods. Although recombinant viruses are much more difficult to manufacture than plasmid DNA, they by nature contain or induce danger signals and are adept at entering cells. The advantages and disadvantages of various viral vectors, including vaccinia, fowlpox and adenovirus, are beyond the scope of this overview and are discussed in recent reviews (26-29). Although viral vectors used for cancer immunotherapy are generally replication-defective, safety issues and regulatory hurdles remain significant concerns. Pre-existing immunity to some viral vectors can limit the potential patient pool and neutralizing antibody responses may prevent the same viral vector from being used twice in the same patient.

Like viral vectors, recombinant microorganisms share the appeal of being "self-adjuvented". The microorganisms may be dead, functioning as APC-targeted carriers of danger signals and antigen expressed recombinantly (30, 31) or in plasmid form (32). Certain strains of bacteria possessing functions that can be exploited for antigen delivery are delivered live, such as *Listeria monocytogenes* that can inhabit the cytosol of APCs (33, 34) and *Salmonella typhimurium* that can inject proteins into the host cell cytosol (35, 36). Yeast-based vaccines will be discussed in more detail later. Many of the same strategies used by the drug delivery field are being explored to package antigen (and sometimes adjuvant) into nano- or microparticles, such as liposomes and other lipid-based carriers (37) and encapsulation by biodegradable (38, 39) or pH-sensitive polymers (40, 41).

Finally, with DC vaccines, DCs or their precursors (e.g. monocytes, $CD34^+$ progenitors) are isolated from the patient, cultured, loaded with antigen and matured *ex vivo*, and re-administered into the body. Any of the above cancer vaccine strategies can be used to deliver TAAs directly to the DCs. In addition, DCs may be transfected with mRNA isolated from tumors (42), or even fused with tumor cells (43). The stand-out advantage of DC vaccines is the ability to control and monitor antigen loading and DC maturation state, whereas the obvious drawbacks are the high cost and difficulty of scaling up the approach.

1.3 Cross-presentation

To provide the first signal required to activate CTLs, APCs need to process and present antigen as peptide-MHC class I complexes. This presents a challenge for cancer vaccine development because MHC class I molecules are conventionally loaded with endogenous antigens generated within the cell, for example, during viral infections. The mechanisms by which exogenous antigens can be processed and presented on MHC class I molecules, i.e cross-

presented, are not as well characterized. The requirement for cross-presentation can be circumvented by vaccinating with peptides that represent defined epitopes, such that no antigen processing is required. This approach requires knowledge of these epitopes and is limited to patients with corresponding HLA haplotypes. Alternatively, viral or non-viral vectors can be used to transfect APCs with TAA genes; however, outside of an *ex vivo* approach, the difficulty lies in targeting gene transfer to rare APC cells. Therefore, cross-presentation is likely to remain key to cancer vaccine development, especially as it has turned out to be unexpectedly efficient (44-46). Teleologically, cross-presentation needs to be effective because uptake and processing of virus-infected cells would be critical for protection against viruses that either do not infect APCs or that block antigen presentation in infected APCs (47).

Exogenous proteins may be taken up by APCs by a number of mechanisms, including receptor-mediated endocytosis and macropinocytosis, but we will focus on phagocytosis as the mechanism relevant to yeast-based vaccines. Early reports of cross-presentation at times disagreed as to whether proteasomes and TAP were required, leading to the elucidation of two distinct pathways. In the phagosome-to-cytosol route, internalized antigens are transported to the cytosol surrounding the phagosome through a size-selective but as yet unidentified "pore" (48). The proteins are thought to be polyubiquitinated and thus targeted for proteasomal cleavage. Three independent reports in 2003 demonstrated that MHC class I molecules and the cellular machinery required for loading them were present in early phagosomes, likely as a result of the endoplasmic reticulum (ER) fusing with the nascent phagosome (49-51). The cleaved peptides are then transported back into the ER-phagosome compartment (or perhaps the ER itself as this fusion event has been disputed (52)) and loaded onto MHC class I molecules with the help of TAP and tapasin. Although this has yet to be proven for phagocytosed antigens, peptides

generated from antigens endocytosed by the mannose receptor were recently shown to be loaded by endosomal TAP to form complexes that trafficked from the endosome to the cell membrane (53). In the alternative vacuolar pathway, antigens remain in the phagosome as it matures by fusion with late endosomes and lysosomes (54). Like in the MHC class II pathway, endolysosomal proteases cleave antigen proteins into peptides. The peptides are thought to be loaded onto recycling MHC class I molecules, perhaps by peptide exchange at low pH, and trafficked to the surface (55).

1.4 NY-ESO-1 as a Cancer Immunotherapy Target

NY-ESO-1 is an attractive target for cancer immunotherapy because it is one of the most immunogenic TAAs known, with an unusually large proportion of advanced patients developing spontaneous humoral and cellular immune responses (56, 57). As a testament to its appeal, when the Cancer Vaccine Collaborative decided to focus its efforts on a single antigen, NY-ESO-1 was selected (58). A member of the cancer/testis family of TAAs, its expression is restricted to the germ cells of the testes and perhaps the ovaries and placenta in normal tissues (59-61). On the other hand, NY-ESO-1 mRNA has been detected in 20-30% of a broad range of tumors, including melanomas, hepatocellular carcinoma, breast, prostate, bladder, ovarian, lung, and thyroid cancers (60). NY-ESO-1 is an 18 kDa protein expressed in the cytosol or nucleus; it has no known murine homologue and its function is unknown (61).

In a clinical trial of vaccination with HLA-A2-restricted NY-ESO-1 peptides and GM-CSF as an adjuvant, four out of seven initially NY-ESO-1 seronegative patients mounted $CD8^+$ T cell responses (57). However, further research has shown that the peptide-induced CTLs are inconsistent in their ability to recognize and kill tumor cells (62), and that their TCRs have different structural features compared to spontaneously generated CTLs (63). Vaccination

strategies involving recombinant NY-ESO-1 protein appear to be more promising. In a clinical trial, ten out of sixteen patients with resected, NY-ESO-1-positive melanomas immunized with NY-ESO-1 protein complexed with ISCOMATRIX adjuvant developed $CD8^+$ T cell responses, compared to one out of sixteen who received protein alone (64). Even though the trial was not designed to assess clinical efficacy, it was very encouraging that only two out of nineteen NY-ESO-1/ISCOMATRIX-vaccinated melanoma patients relapsed during follow-up, compared to nine out of sixteen who received NY-ESO-1 without adjuvant and five out of seven who received a placebo. Other NY-ESO-1 vaccination strategies that are currently in phase I or II clinical trials include formulation with cholesterol-bearing hydrophobized pullulan, live recombinant *Salmonella typhimurium* and a vaccinia/fowlpox prime-boost strategy (58).

A recent preliminary study proposes that targeting NY-ESO-1-expressing tumor cells may be akin to attacking "cancer's Achilles' heel" (65). Cebon et. al sorted a series of melanoma cell lines for subpopulations that highly expressed CD133 (65). CD133 is expressed by a wide variety of normal stem cells and may also be a cancer stem cell marker (66). These CD133hi cells that were clonogenic in soft agar culture were also highly enriched for NY-ESO-1 and could be selectively killed by NY-ESO-1-specific CTLs. This suggests that even though tumors are heterogeneous in NY-ESO-1 expression, vaccinating against NY-ESO-1 could prevent tumor growth and metastasis by eliminating the cancer stem cells.

1.5 Yeast as an Adjuvant and Vaccine

Saccharomyces cerevisiae embodies many of the qualities desired in vaccines: it is non-pathogenic, Generally Recognized as Safe (GRAS) by the FDA, well-characterized and cheap to produce. The adjuvant qualities of yeast have long been recognized; zymosan, a cell wall preparation of *S. cerevisiae* composed largely of β-glucans, has been used for over 50 years to

stimulate inflammatory cytokine production (67, 68). However, the wide variety of DC receptors that are engaged by *S. cerevisiae* and other fungi are only recently being defined. Dectin-1, a lectin receptor recognizing fungal β-glucan, has been found to cooperate with Toll-like receptors 2 and 6 to stimulate secretion of the Th1 cytokines IL-12 and TNF-α in response to zymosan (68). Zymosan has also been found to co-engage Dectin-1 and another lectin receptor, DC-SIGN, to stimulate biosynthesis of arachidonic acid (a precursor to prostaglandin E2 required for migration) in human DCs (69). The mannan fraction of yeast cell walls has been shown to stimulate proinflammatory cytokine production in monocytes (70) and dendritic cells (71). Production of mannosylated recombinant antigens in *S. cerevisiae* (72) or *Pichia pastoris* (73) yeast is a tactic used to enhance uptake by the mannose receptor, although this receptor is dispensable for cell-associated antigen (74).

In 2001, Stubbs et al. pioneered the use of recombinant yeast to induce cellular immunity (75). Immunization of mice with *S. cerevisiae* yeast expressing ovalbumin intracellularly was demonstrated to protect against subsequent challenge by ovalbumin-expressing tumor cells. They also showed that yeast was a powerful stimulator of murine DC maturation and IL-12 secretion. More recently, yeast expressing mutated Ras oncoprotein was shown to induce shrinkage of carcinogen-induced lung tumors in mice (76). There is clearly room for improvement because only about one-quarter of the tumors were eradicated despite an intense dosing regiment of ten weekly injections (76). The same group observed that prior immunization with control yeast did not reduce the potency of subsequent immunization with antigen-expressing yeast, suggesting that any immune responses mounted against yeast itself are non-neutralizing (77). In the past year, two more TAAs were expressed intracellularly in yeast, the melanoma antigen MART-1 and carcinoembryonic antigen; both induced $CD4^+$ and $CD8^+$ T cells in vaccinated mice (78, 79).

This technology is currently being tested in a phase I clinical trial against chronic hepatitis C, and no dose-limiting toxicity was observed after subcutaneous injection of heat-killed *S. cerevisiae* (80).

1.6 Introduction to the Thesis

The goal of this thesis project is to use *S. cerevisiae* as a vaccine development platform to evaluate factors that affect cross-presentation and to demonstrate proof-of-concept using the cancer-testis antigen, NY-ESO-1. While several reports on yeast-based vaccines are described above, improvements in the technology have essentially been limited to efforts to increase intracellular antigen expression levels (e.g. gene copy number, promoter choice) (80). We believe that cross-presentation can be made more efficient by designing antigen delivery vectors that manipulate the kinetics of rate-limiting processes. In the proteasome-dependent route of cross-presentation, the egress of antigen from the phagosome to the cytosol appears to be one such process. Yeast surface display technology developed in the Wittrup laboratory enables us to not only quantify and monitor antigen levels but also to manipulate the kinetics of antigen release in the DC phagosome.

1.7 References

1. Erhlich, P. 1909. Ueber den jetzigen Stand der Karzinomforschung. *Ned. Tijdschr. Geneeskd.* 5: 273-290.
2. Dunn, G. P., C. M. Koebel, and R. D. Schreiber. 2006. Interferons, immunity and cancer immunoediting. *Nat Rev Immunol* 6: 836-848.
3. Dunn, G. P., L. J. Old, and R. D. Schreiber. 2004. The Three Es of Cancer Immunoediting. *Annual Review of Immunology* 22: 329-360.
4. Strome, S. E., E. A. Sausville, and D. Mann. 2007. A Mechanistic Perspective of Monoclonal Antibodies in Cancer Therapy Beyond Target-Related Effects. *Oncologist* 12: 1084-1095.
5. Whiteside, T., and C. Odoux. 2004. Dendritic cell biology and cancer therapy. *Cancer Immunology, Immunotherapy* 53: 240-248.
6. Guermonprez, P., J. Valladeau, L. Zitvogel, C. Thery, and S. Amigorena. 2002. Antigen presentation and T cell stimulation by dendritic cells. *Annual Review of Immunology* 20: 621-667.
7. Ochsenbein, A. F. 2005. Immunological ignorance of solid tumors. *Springer Semin Immunopathol* 27: 27.
8. Dhodapkar, M. V., R. M. Steinman, J. Krasovsky, C. Munz, and N. Bhardwaj. 2001. Antigen-specific Inhibition of Effector T Cell Function in Humans after Injection of Immature Dendritic Cells. *J. Exp. Med.* 193: 233-238.
9. Engleman, E. G., J. Brody, and L. Soares. 2004. Using signaling pathways to overcome immune tolerance to tumors. *Sci STKE* 2004: pe28.
10. McCarthy, E. F. 2006. The toxins of William B. Coley and the treatment of bone and soft-tissue sarcomas. *Iowa Orthop J* 26: 154-158.
11. Pardoll, D. 1992. New strategies for active immunotherapy with genetically engineered tumor cells. *Curr Opin Immunol* 4: 619-623.
12. Baskar, S. 1996. Gene-modified tumor cells as cellular vaccine. *Cancer Immunol Immunother* 43: 165-173.
13. Gilboa, E. 2001. The risk of autoimmunity associated with tumor immunotherapy. *Nat Immunol* 2: 789-792.
14. Sahin, U., O. Tureci, H. Schmitt, B. Cochlovius, T. Johannes, R. Schmits, F. Stenner, G. Luo, I. Schobert, and M. Pfreundschuh. 1995. Human Neoplasms Elicit Multiple Specific Immune Responses in the Autologous Host. *Proceedings of the National Academy of Sciences* 92: 11810-11813.
15. Slingluff, C. L., Jr., and D. E. Speiser. 2005. Progress and controversies in developing cancer vaccines. *J Transl Med* 3: 18.
16. Celis, E. 2002. Getting peptide vaccines to work: just a matter of quality control? *J Clin Invest* 110: 1765-1768.

17. Keler, T., L. He, V. Ramakrishna, and B. Champion. 2007. Antibody-targeted vaccines. *Oncogene* 26: 3758-3767.

18. Suzue, K., X. Zhou, H. N. Eisen, and R. A. Young. 1997. Heat shock fusion proteins as vehicles for antigen delivery into the major histocompatibility complex class I presentation pathway. *Proceedings of the National Academy of Sciences* 94: 13146-13151.

19. Shibagaki, N., and M. C. Udey. 2002. Dendritic Cells Transduced with Protein Antigens Induce Cytotoxic Lymphocytes and Elicit Antitumor Immunity. *J Immunol* 168: 2393-2401.

20. Cuadros, C., F. J. Lopez-Hernandez, A. L. Dominguez, M. McClelland, and J. Lustgarten. 2004. Flagellin Fusion Proteins as Adjuvants or Vaccines Induce Specific Immune Responses. *Infect. Immun.* 72: 2810-2816.

21. Biragyn, A., K. Tani, M. C. Grimm, S. Weeks, and L. W. Kwak. 1999. Genetic fusion of chemokines to a self tumor antigen induces protective, T-cell dependent antitumor immunity. *Nat Biotechnol* 17: 253-258.

22. Schuurhuis, D. H., A. Ioan-Facsinay, B. Nagelkerken, J. J. van Schip, C. Sedlik, C. J. M. Melief, J. S. Verbeek, and F. Ossendorp. 2002. Antigen-Antibody Immune Complexes Empower Dendritic Cells to Efficiently Prime Specific CD8+ CTL Responses In Vivo. *J Immunol* 168: 2240-2246.

23. Regnault, A., D. Lankar, V. Lacabanne, A. Rodriguez, C. Thery, M. Rescigno, T. Saito, S. Verbeek, C. Bonnerot, P. Ricciardi-Castagnoli, and S. Amigorena. 1999. Fcgamma Receptor-mediated Induction of Dendritic Cell Maturation and Major Histocompatibility Complex Class I-restricted Antigen Presentation after Immune Complex Internalization. *J. Exp. Med.* 189: 371-380.

24. Akiyama, K., S. Ebihara, A. Yada, K. Matsumura, S. Aiba, T. Nukiwa, and T. Takai. 2003. Targeting Apoptotic Tumor Cells to Fc{gamma}R Provides Efficient and Versatile Vaccination Against Tumors by Dendritic Cells *J Immunol* 170: 1641-1648.

25. Belakova, J., M. Horynova, M. Krupka, E. Weigl, and M. Raska. 2007. DNA vaccines: are they still just a powerful tool for the future? *Arch Immunol Ther Exp (Warsz)* 55: 387-398.

26. Harrop, R., J. John, and M. W. Carroll. 2006. Recombinant viral vectors: cancer vaccines. *Adv Drug Deliv Rev* 58: 931-947.

27. Eisenberger, A., B. M. Elliott, and H. L. Kaufman. 2006. Viral Vaccines for Cancer Immunotherapy. *Hematology/Oncology Clinics of North America* 20: 661-687.

28. Harrop, R., and M. W. Carroll. 2006. Viral vectors for cancer immunotherapy. *Front Biosci* 11: 804-817.

29. Collins, S. A., B. A. Guinn, P. T. Harrison, M. F. Scallan, G. C. O'Sullivan, and M. Tangney. 2008. Viral vectors in cancer immunotherapy: which vector for which strategy? *Curr Gene Ther* 8: 66-78.

30. Radford, K. J., A. M. Jackson, J. H. Wang, G. Vassaux, and N. R. Lemoine. 2003. Recombinant E. coli efficiently delivers antigen and maturation signals to human dendritic cells: presentation of MART1 to CD8+ T cells. *Int J Cancer* 105: 811-819.

31. Mayr, U. B., P. Walcher, C. Azimpour, E. Riedmann, C. Haller, and W. Lubitz. 2005. Bacterial ghosts as antigen delivery vehicles. *Advanced Drug Delivery Reviews* 57: 1381-1391.

32. Ebensen, T., S. Paukner, C. Link, P. Kudela, C. de Domenico, W. Lubitz, and C. A. Guzman. 2004. Bacterial Ghosts Are an Efficient Delivery System for DNA Vaccines. *J Immunol* 172: 6858-6865.

33. Paterson, Y., and P. C. Maciag. 2005. Listeria-based vaccines for cancer treatment. *Curr Opin Mol Ther* 7: 454-460.

34. Singh, R., and Y. Paterson. 2006. Listeria monocytogenes as a vector for tumor-associated antigens for cancer immunotherapy. *Expert Rev Vaccines* 5: 541-552.

35. Rüssmann, H., H. Shams, F. Poblete, Y. Fu, J. E. Galán, and R. O. Donis. 1998. Delivery of Epitopes by the Salmonella Type III Secretion System for Vaccine Development. *Science* 281: 565-568.

36. Nishikawa, H., E. Sato, G. Briones, L. M. Chen, M. Matsuo, Y. Nagata, G. Ritter, E. Jager, H. Nomura, S. Kondo, I. Tawara, T. Kato, H. Shiku, L. J. Old, J. E. Galan, and S. Gnjatic. 2006. In vivo antigen delivery by a Salmonella typhimurium type III secretion system for therapeutic cancer vaccines. *J Clin Invest* 116: 1946-1954.

37. Copland, M. J., T. Rades, N. M. Davies, and M. A. Baird. 2005. Lipid based particulate formulations for the delivery of antigen. *Immunol Cell Biol* 83: 97-105.

38. Shen, H., A. L. Ackerman, V. Cody, A. Giodini, E. R. Hinson, P. Cresswell, R. L. Edelson, W. M. Saltzman, and D. J. Hanlon. 2006. Enhanced and prolonged cross-presentation following endosomal escape of exogenous antigens encapsulated in biodegradable nanoparticles. *Immunology* 117: 78-88.

39. Waeckerle-Men, Y., E. U.-v. Allmen, B. Gander, E. Scandella, E. Schlosser, G. Schmidtke, H. P. Merkle, and M. Groettrup. 2006. Encapsulation of proteins and peptides into biodegradable poly(d,l-lactide-co-glycolide) microspheres prolongs and enhances antigen presentation by human dendritic cells. *Vaccine* 24: 1847-1857.

40. Haining, W. N., D. G. Anderson, S. R. Little, M. S. von Berwelt-Baildon, A. A. Cardoso, P. Alves, K. Kosmatopoulos, L. M. Nadler, R. Langer, and D. S. Kohane. 2004. pH-Triggered Microparticles for Peptide Vaccination. *J Immunol* 173: 2578-2585.

41. Hu, Y., T. Litwin, A. R. Nagaraja, B. Kwong, J. Katz, N. Watson, and D. J. Irvine. 2007. Cytosolic Delivery of Membrane-Impermeable Molecules in Dendritic Cells Using pH-Responsive Core-Shell Nanoparticles. *Nano Lett.* 7: 3056-3064.

42. Gilboa, E., and J. Vieweg. 2004. Cancer immunotherapy with mRNA-transfected dendritic cells. *Immunological Reviews* 199: 251-263.

43. Rosenblatt, J., D. Kufe, and D. Avigan. 2005. Dendritic cell fusion vaccines for cancer immunotherapy. *Expert Opinion on Biological Therapy* 5: 703-715.

44. Ackerman, A. L., and P. Cresswell. 2004. Cellular mechanisms governing cross-presentation of exogenous antigens. *Nat Immunol* 5: 678-684.

45. Larsson, M., J. F. Fonteneau, S. Somersan, C. Sanders, K. Bickham, E. K. Thomas, K. Mahnke, and N. Bhardwaj. 2001. Efficiency of cross presentation of vaccinia virus-derived antigens by human dendritic cells. *Eur J Immunol* 31: 3432-3442.

46. Storni, T., and M. F. Bachmann. 2004. Loading of MHC Class I and II Presentation Pathways by Exogenous Antigens: A Quantitative In Vivo Comparison. *J Immunol* 172: 6129-6135.

47. Guermonprez, P., and S. Amigorena. 2005. Pathways for antigen cross presentation. *Springer Semin Immunopathol* 26: 257-271.

48. Rodriguez, A., A. Regnault, M. Kleijmeer, P. Ricciardi-Castagnoli, and S. Amigorena. 1999. Selective transport of internalized antigens to the cytosol for MHC class I presentation in dendritic cells. *Nat Cell Biol* 1: 362-368.

49. Guermonprez, P., L. Saveanu, M. Kleijmeer, J. Davoust, P. Van Endert, and S. Amigorena. 2003. ER-phagosome fusion defines an MHC class I cross-presentation compartment in dendritic cells. *Nature* 425: 397-402.

50. Houde, M., S. Bertholet, E. Gagnon, S. Brunet, G. Goyette, A. Laplante, M. F. Princiotta, P. Thibault, D. Sacks, and M. Desjardins. 2003. Phagosomes are competent organelles for antigen cross-presentation. *Nature* 425: 402-406.

51. Ackerman, A. L., C. Kyritsis, R. Tampe, and P. Cresswell. 2003. Early phagosomes in dendritic cells form a cellular compartment sufficient for cross presentation of exogenous antigens. *Proc Natl Acad Sci U S A* 100: 12889-12894.

52. Touret, N., P. Paroutis, M. Terebiznik, R. E. Harrison, S. Trombetta, M. Pypaert, A. Chow, A. Jiang, J. Shaw, and C. Yip. 2005. Quantitative and Dynamic Assessment of the Contribution of the ER to Phagosome Formation. *Cell* 123: 157-170.

53. Burgdorf, S., C. Scholz, A. Kautz, R. Tampe, and C. Kurts. 2008. Spatial and mechanistic separation of cross-presentation and endogenous antigen presentation. *Nat Immunol* 9: 558-566.

54. Shen, L., L. J. Sigal, M. Boes, and K. L. Rock. 2004. Important Role of Cathepsin S in Generating Peptides for TAP-Independent MHC Class I Crosspresentation In Vivo. *Immunity* 21: 155-165.

55. Lin, M.-L., Y. Zhan, J. A. Villadangos, and A. M. Lew. 2008. The cell biology of cross-presentation and the role of dendritic cell subsets. 86: 353-362.

56. Gnjatic, S., D. Atanackovic, E. Jager, M. Matsuo, A. Selvakumar, N. K. Altorki, R. G. Maki, B. Dupont, G. Ritter, Y. T. Chen, A. Knuth, and L. J. Old. 2003. Survey of naturally occurring CD4+ T cell responses against NY-ESO-1 in cancer patients: correlation with antibody responses. *Proc Natl Acad Sci U S A* 100: 8862-8867.

57. Jager, E., S. Gnjatic, Y. Nagata, E. Stockert, D. Jager, J. Karbach, A. Neumann, J. Rieckenberg, Y.-T. Chen, G. Ritter, E. Hoffman, M. Arand, L. J. Old, and A. Knuth. 2000. Induction of primary NY-ESO-1 immunity: CD8+ T lymphocyte and antibody

responses in peptide-vaccinated patients with NY-ESO-1+ cancers. *Proc Natl Acad Sci U S A* 97: 12198-12203.

58. Old, L. J. 2008. Cancer vaccines: an overview. *Cancer Immun* 8 Suppl 1: 1.

59. Bolli, M., E. Schultz-Thater, P. Zajac, U. Guller, C. Feder, F. Sanguedolce, V. Carafa, L. Terracciano, T. Hudolin, G. C. Spagnoli, and L. Tornillo. 2005. NY-ESO-1/LAGE-1 coexpression with MAGE-A cancer/testis antigens: A tissue microarray study. *Int J Cancer* 115: 960-966.

60. Chen, Y.-T., M. J. Scanlan, U. Sahin, O. Tureci, A. O. Gure, S. Tsang, B. Williamson, E. Stockert, M. Pfreundschuh, and L. J. Old. 1997. A testicular antigen aberrantly expressed in human cancers detected by autologous antibody screening. *Proc Natl Acad Sci U S A* 94: 1914-1918.

61. Nicholaou, T., L. Ebert, I. D. Davis, N. Robson, O. Klein, E. Maraskovsky, W. Chen, and J. Cebon. 2006. Directions in the immune targeting of cancer: Lessons learned from the cancer-testis Ag NY-ESO-1. *Immunol Cell Biol* 84: 303-317.

62. Dutoit, V., R. N. Taub, K. P. Papadopoulos, S. Talbot, M.-L. Keohan, M. Brehm, S. Gnjatic, P. E. Harris, B. Bisikirska, P. Guillaume, J.-C. Cerottini, C. S. Hesdorffer, L. J. Old, and D. Valmori. 2002. Multiepitope CD8+ T cell response to a NY-ESO-1 peptide vaccine results in imprecise tumor targeting. *J. Clin. Invest.* 110: 1813-1822.

63. Le Gal, F. A., M. Ayyoub, V. Dutoit, V. Widmer, E. Jager, J. C. Cerottini, P. Y. Dietrich, and D. Valmori. 2005. Distinct structural TCR repertoires in naturally occurring versus vaccine-induced CD8+ T-cell responses to the tumor-specific antigen NY-ESO-1. *J Immunother* 28: 252-257.

64. Davis, I. D., W. Chen, H. Jackson, P. Parente, M. Shackleton, W. Hopkins, Q. Chen, N. Dimopoulos, T. Luke, R. Murphy, A. M. Scott, E. Maraskovsky, G. McArthur, D. MacGregor, S. Sturrock, T. Y. Tai, S. Green, A. Cuthbertson, D. Maher, L. Miloradovic, S. V. Mitchell, G. Ritter, A. A. Jungbluth, Y.-T. Chen, S. Gnjatic, E. W. Hoffman, L. J. Old, and J. S. Cebon. 2004. Recombinant NY-ESO-1 protein with ISCOMATRIX adjuvant induces broad integrated antibody and CD4+ and CD8+ T cell responses in humans. *Proc Natl Acad Sci U S A* 101: 10697-10702.

65. Cebon, J., C. Gedye, I. Davis, J. Quirk, W. Chen, A. Simpson, O. Caballero, and L. J. Old. 2007. Vaccinating against cancer's Achilles' heel. *Cancer Immun* 7 Suppl 1: 13.

66. D Mizrak, M. B., MR Alison,. 2008. CD133: molecule of the moment. *The Journal of Pathology* 214: 3-9.

67. Underhill, D. M. 2003. Macrophage recognition of zymosan particles. *J Endotoxin Res* 9: 176-180.

68. Gantner, B. N., R. M. Simmons, S. J. Canavera, S. Akira, and D. M. Underhill. 2003. Collaborative induction of inflammatory responses by dectin-1 and Toll-like receptor 2. *J Exp Med* 197: 1107-1117.

69. Valera, I., N. Fernandez, A. G. Trinidad, S. Alonso, G. D. Brown, A. Alonso, and M. S. Crespo. 2008. Costimulation of Dectin-1 and DC-SIGN Triggers the Arachidonic Acid Cascade in Human Monocyte-Derived Dendritic Cells. *J Immunol* 180: 5727-5736.

70. Tada, H., E. Nemoto, H. Shimauchi, T. Watanabe, T. Mikami, T. Matsumoto, N. Ohno, H. Tamura, K. Shibata, S. Akashi, K. Miyake, S. Sugawara, and H. Takada. 2002. Saccharomyces cerevisiae- and Candida albicans-derived mannan induced production of tumor necrosis factor alpha by human monocytes in a CD14- and Toll-like receptor 4-dependent manner. *Microbiol Immunol* 46: 503-512.

71. Sheng, K.-C., D. S. Pouniotis, M. D. Wright, C. K. Tang, E. Lazoura, G. A. Pietersz, and V. Apostolopoulos. 2006. Mannan derivatives induce phenotypic and functional maturation of mouse dendritic cells. *Immunology* 118: 372-383.

72. Wadle, A., G. Held, F. Neumann, S. Kleber, B. Wuellner, A. M. Asemissen, B. Kubuschok, C. Scheibenbogen, T. Breinig, A. Meyerhans, and C. Renner. 2006. Cross-presentation of HLA class I epitopes from influenza matrix protein produced in Saccharomyces cerevisiae. *Vaccine* 24: 6272-6281.

73. Lam, J. S., M. K. Mansour, C. A. Specht, and S. M. Levitz. 2005. A Model Vaccine Exploiting Fungal Mannosylation to Increase Antigen Immunogenicity. *J Immunol* 175: 7496-7503.

74. Burgdorf, S., V. Lukacs-Kornek, and C. Kurts. 2006. The Mannose Receptor Mediates Uptake of Soluble but Not of Cell-Associated Antigen for Cross-Presentation. *J Immunol* 176: 6770-6776.

75. Stubbs, A. C., K. S. Martin, C. Coeshott, S. V. Skaates, D. R. Kuritzkes, D. Bellgrau, A. Franzusoff, R. C. Duke, and C. C. Wilson. 2001. Whole recombinant yeast vaccine activates dendritic cells and elicits protective cell-mediated immunity. *Nat Med* 7: 625-629.

76. Lu, Y., D. Bellgrau, L. D. Dwyer-Nield, A. M. Malkinson, R. C. Duke, T. C. Rodell, and A. Franzusoff. 2004. Mutation-selective tumor remission with Ras-targeted, whole yeast-based immunotherapy. *Cancer Res* 64: 5084-5088.

77. Franzusoff, A., R. C. Duke, T. H. King, Y. Lu, and T. C. Rodell. 2005. Yeasts encoding tumour antigens in cancer immunotherapy. *Expert Opinion on Biological Therapy* 5: 565-575.

78. Riemann, H., J. Takao, Y. G. Shellman, W. A. Hines, C. K. Edwards, D. A. Norris, and M. Fujita. 2007. Generation of a prophylactic melanoma vaccine using whole recombinant yeast expressing MART-1. *Experimental Dermatology* 16: 814-822.

79. Bernstein, M. B., M. Chakraborty, E. K. Wansley, Z. Guo, A. Franzusoff, S. Mostbock, H. Sabzevari, J. Schlom, and J. W. Hodge. 2008. Recombinant Saccharomyces cerevisiae (yeast-CEA) as a potent activator of murine dendritic cells. *Vaccine* 26: 509-521.

80. Munson, S., J. Parker, T. H. King, Y. Lio, V. Kelley, Z. Guo, V. Borges, and A. Franzusoff. 2008. Coupling innate and adaptive immunity with yeast-based cancer immunotherapy. In *Cancer Vaccines and Tumor Immunity*. R. Orentas, J. W. Hodge, and B. D. Johnson, eds. Wiley-Liss, New York, p. 131-149.

Chapter 2

Establishing the Experimental System

2.1 Introduction

When this thesis project was first proposed, we decided to study antigen cross-presentation and adjuvant effects using human cells, and if possible, with NY-ESO-1 instead of a model antigen. If testing in an animal model became a compelling next step, our collaborators were experienced in vaccinating HLA-A2-expressing transgenic mice (1, 2). In our own laboratory, we planned to directly measure cross-presentation of NY-ESO-1 by human dendritic cells (DCs) using an antibody fragment recognizing the NY-ESO-$1_{157\text{-}165}$/HLA-A2 complex (3). This approach turned out to be unfeasible, and this chapter describes our preliminary work in establishing a functional experimental system.

2.2 Human Monocyte-derived DCs

At the time, human DCs could be purchased from two companies: MatTek (Ashland, MA) supplied DCs generated from umbilical cord blood progenitors and Lonza (Basel, Switzerland) supplied DCs isolated from peripheral blood. However, these were prohibitively expensive and DCs differentiated from human monocytes by culture with IL-4 and GM-CSF (4) were much more prominent in the literature. Monocytes are typically enriched from peripheral blood mononuclear cells (PBMCs) by either plastic adherence or magnetic-activated cell sorting for $CD14^+$. To greatly increase the flexibility and convenience of performing DC experiments, we instead purchased a large batch (~10^9 cells) of monocytes purified by counter-flow centrifugal elutriation (Advanced Biotechnologies Inc, Columbia, MD) and cryopreserved these in aliquots.

An initial experiment was performed to culture these monocytes in media containing 1000 U/ml each of IL-4 and GM-CSF for one week and to characterize the resulting cells by flow cytometry. The floating and loosely adherent cells acquired an irregular morphology with some visible dendrites (Fig. 2.1A) and had a surface antigen profile consistent with immature monocyte-derived DCs: $CD1a^{variable}$, $CD11a^{high}$, $CD14^{low}$, $DC\text{-}SIGN^{hi}$, $HLA\text{-}DR^{low}$ (Fig. 2.1B). In contrast, the undifferentiated monocytes expressed CD14 at a much higher level but did not express either DC-SIGN or CD1a (not shown). The protocol for generating monocyte-derived DCs was standardized and is provided in detail in Appendix B.1.

2.3 DC Maturation by Yeast

Next, we wished to verify that human monocyte-derived DCs phagocytose yeast cells and mature in response to this stimulus. At this point (2004), there were no published reports of the effects of *Saccharomyces cerevisiae* cells on human DCs, although Stubbs et. al had reported that this yeast activated murine bone marrow-derived DCs (5) and several groups had investigated the interaction between *Candida albicans* and human DCs (6-8). Before we could proceed, we needed a way to render the yeast non-viable, to prevent them from overwhelming DCs in cell culture. Heat inactivation and antifungal agents were not optimal because of protein denaturation and possible side effects, respectively; instead, we investigated inactivation by UV-irradiation. Dose-response experiments exposing 10^7 yeast cells to 254 nm UV light in a Stratalinker UV Crosslinker (Stratagene) showed that 1000-1200 J/m^2 reduced the number of colony forming units to the single digits. Higher doses could not consistently eliminate colony growth, but simply performing the 1000 J/m^2 irradiation twice, swirling the dish in between, solved the problem of yeast growth in DC culture.

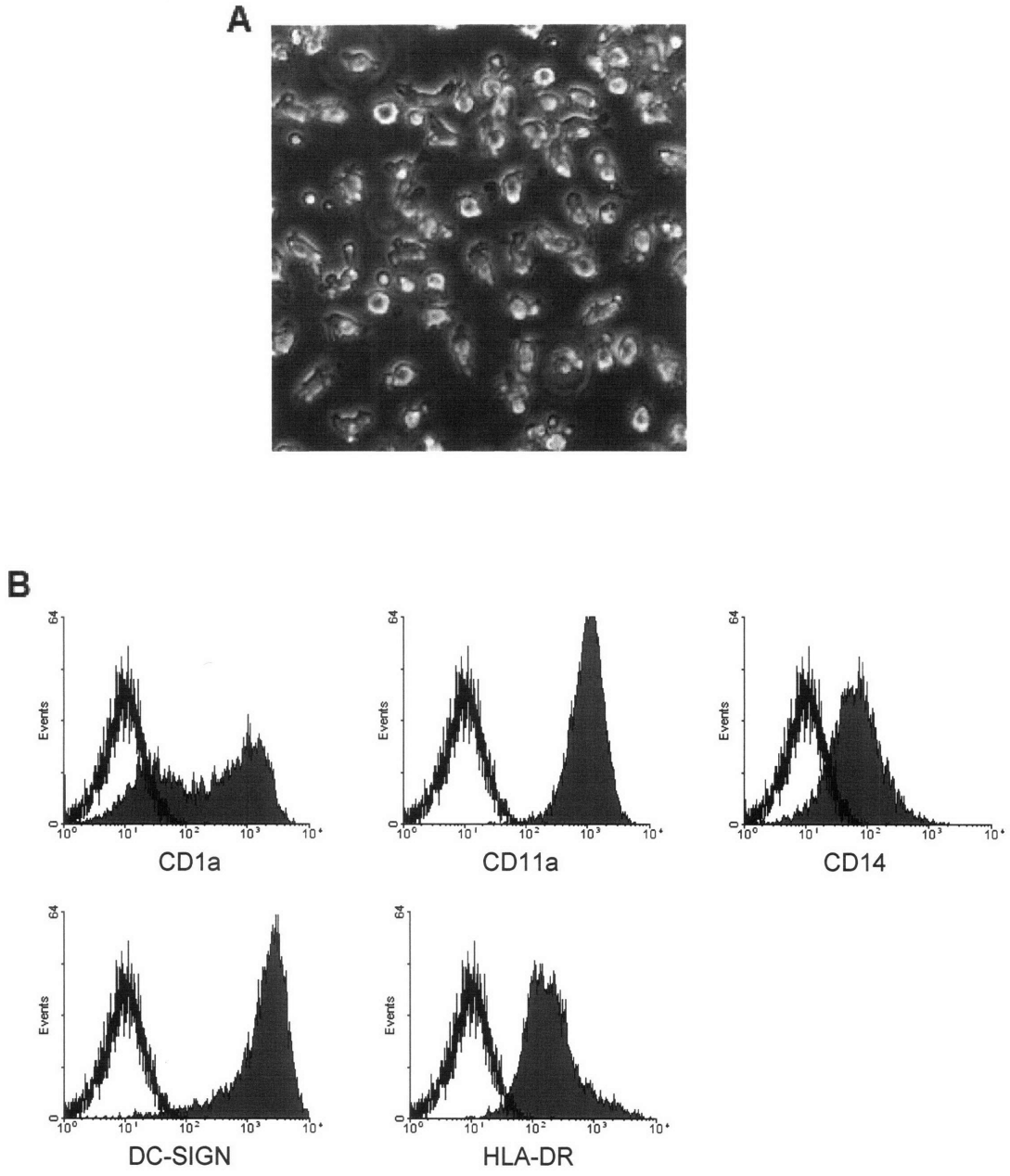

Figure 2.1, Phenotype of monocyte-derived DCs. Human monocytes were cultured in C10 medium (see Appendix B.1) with 1000 U/ml each of IL-4 and GM-CSF for 7 days.
A, Morphology of the resulting immature DCs as viewed by phase contrast microscopy.
B, The cells were labeled with PE-conjugated monoclonal antibodies against the indicated surface markers and analyzed by flow cytometry. The clear histogram indicates staining with goat α-mouse-PE, used here as a non-binding control.

Yeast surface-displaying a truncated form of NY-ESO-1 were UV-irradiated and added to immature monocyte-derived DCs at different ratios. After 48 h, the DCs were analyzed by flow cytometry for the expression of five surface markers of DC maturation: CD40, CD80, CD83, CD86, and HLA-DR. As shown in Fig. 2.2A, across a broad range of doses from 2 to 20 yeast per DC, DC upregulation of these maturation markers was comparable to that induced by a strong Toll-like receptor agonist, lipopolysaccharide (LPS), with 5-10 yeast per DC being optimal. We had previously found that the number of unphagocytosed yeast cells increased sharply when the yeast-to-DC ratio increased above 20:1, which may reflect the maximum DC phagocytic capacity. Consistent with the findings of Stubbs et al. using murine DCs (5), yeast cells induced human DCs to secrete much more IL-12 than did LPS (Fig. 2.2B). In conclusion, yeast cells exerted a strong, Th1 adjuvant effect on human monocyte-derived DCs.

2.4 Yeast Surface Display of NY-ESO-1 Variants

Yeast surface display of NY-ESO-1 as a fusion to Aga2p was first performed by Renner et al., who demonstrated the feasibility of using such yeast to screen patient sera for antibodies against cancer antigens (9). However, in our own laboratory, we found NY-ESO-1 yeast surface display levels to be barely detectable (Fig. 2.3C) and unsuitable for antigen production or for studying cross-presentation (10). Therefore, post-doctoral fellow Andrea Piatesi undertook the task of engineering better expressing NY-ESO-1 mutants (10). To summarize his results, he hypothesized that the cysteine cluster (CCRC) at positions 75-78 was a bottleneck for expression and rationally designed three mutants: NY-ESO-CS and NY-ESO-CA, where these Cys residues were substituted with Ser or Ala residues, respectively, and NY-ESO-T, where the unstructured N-terminal region up to the cysteine cluster was deleted (Figs. 2.3A, B).

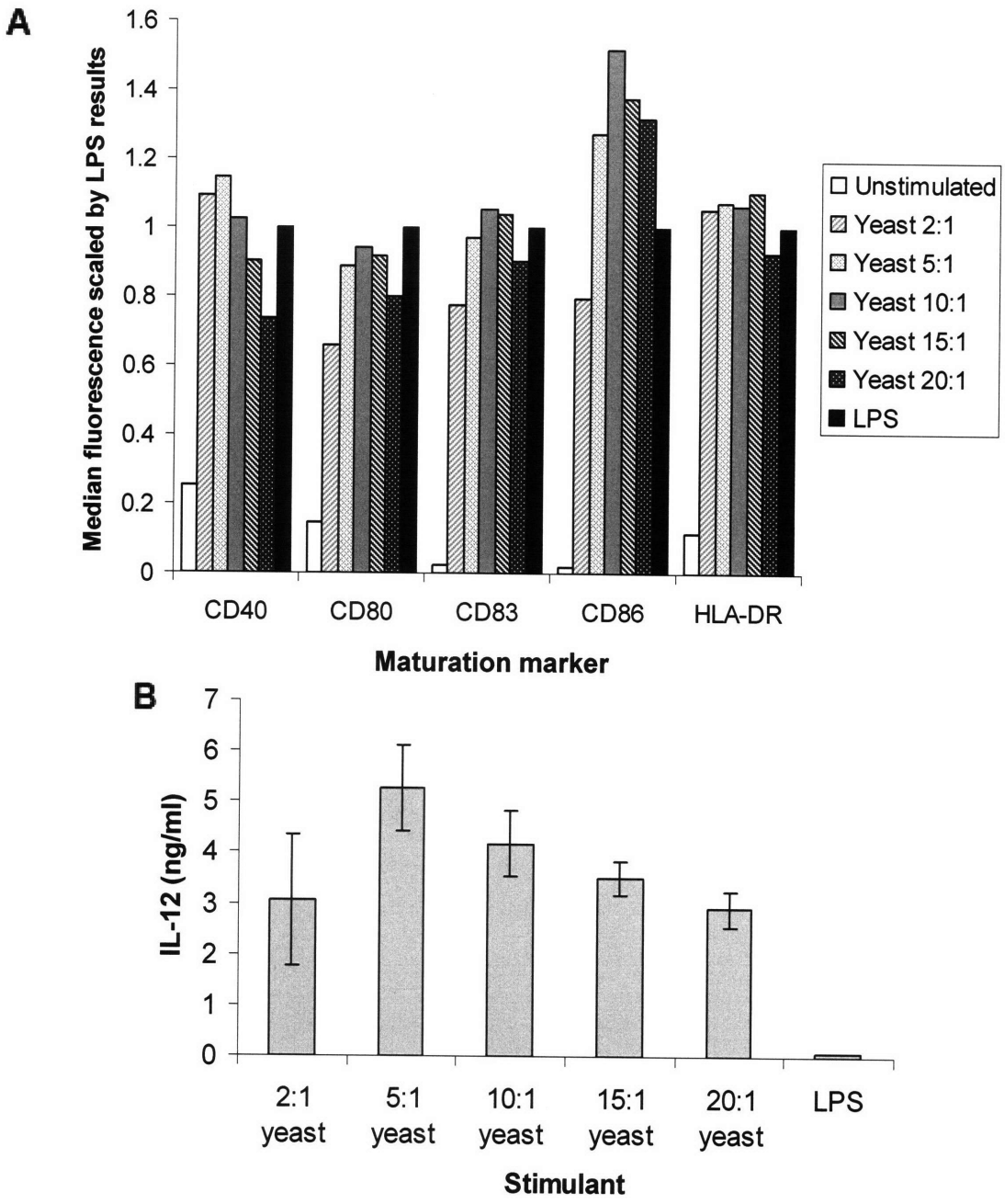

Figure 2.2, DC maturation in response to yeast. Human monocyte-derived DCs were seeded in a 24-well plate (5×10^5 DCs in 1 ml per well), and LPS (1 μg/ml) or UV-irradiated pCT-ESO-T yeast (at the indicated ratios) were added.

A, After 48 h, the cells from duplicate wells were pooled and divided into aliquots, each of which was labeled with α-DC-SIGN-FITC and a PE-conjugated antibody against a DC maturation marker. The cells were analyzed by flow cytometry and gated by DC-SIGN expression to exclude unphagocytosed yeast; PE fluorescence was scaled by the results of the LPS positive control.

B, IL-12p70 ELISA was performed on the cell culture supernatants. Error bars indicate the SD of duplicate wells.

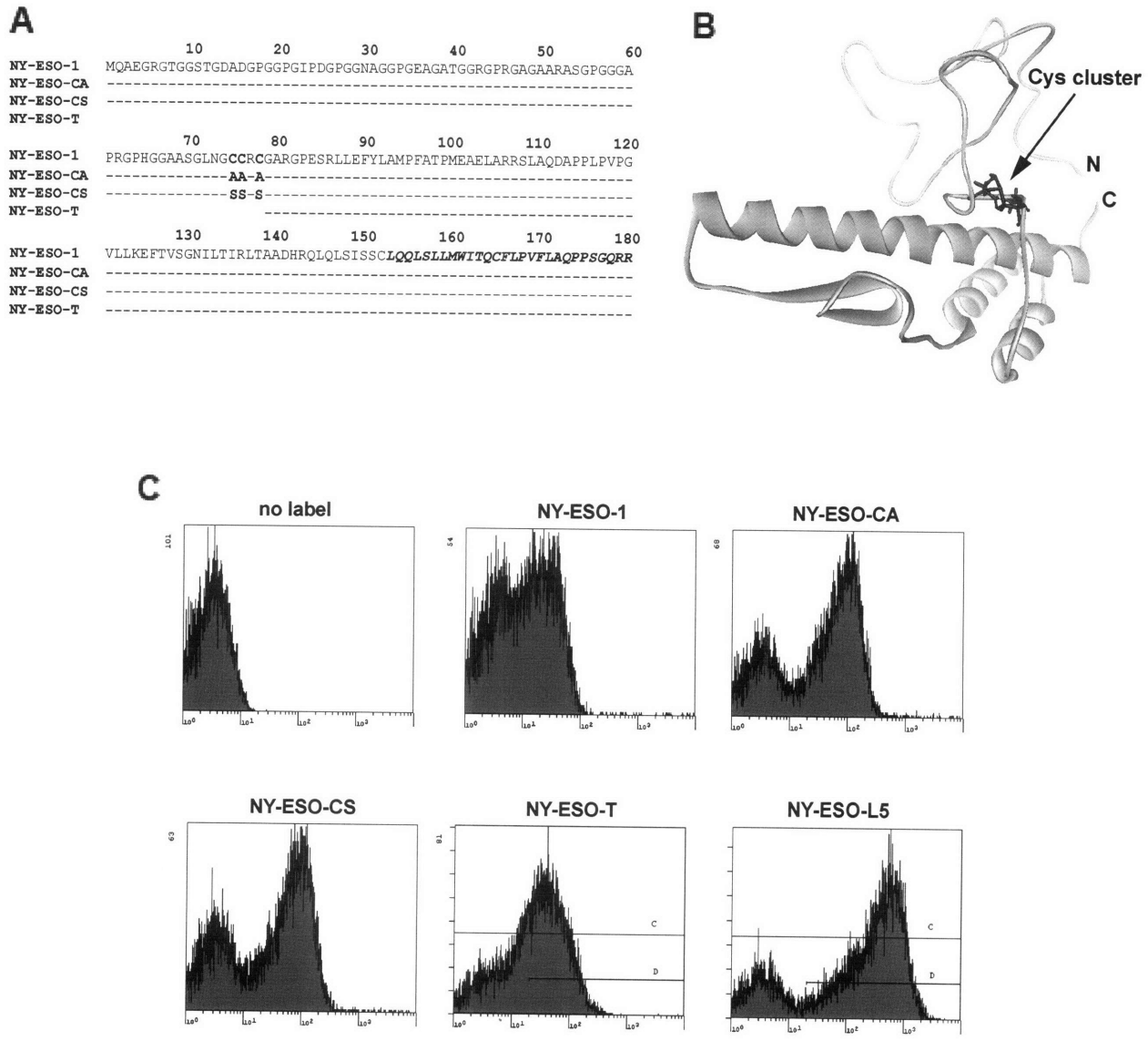

Figure 2.3, Mutants of NY-ESO-1 with improved yeast surface display levels.
A, Sequence alignment of NY-ESO-1 with three rationally designed mutants. Dashes indicate no change from NY-ESO-1.
B, Structure of NY-ESO-1 as predicted by the Rosetta algorithm, with the cysteine cluster highlighted.
C, Flow cytometry histograms of yeast surface-displaying NY-ESO-1 and variants, labeled with α-c-myc and a PE-conjugated secondary antibody.
Panels A and B are reproduced with permission from Fig. 1 of ref. (10) and panel C is adapted from Figs. 2A and 4.

To further improve upon the surface display levels, Piatesi performed directed evolution on each of the three mutants, generating libraries by error-prone PCR and repeatedly sorting for the highest expressing cells (10). The full-length NY-ESO-1 variants that were obtained had mutations at either position 153 (Leu to His) or 156 (Leu to His/Arg) on an NY-ESO-CS or NY-ESO-CA background. The position 156 mutation was less desirable because it had a higher likelihood of affecting the processing and immunogenicity of the most widely studied MHC class I epitope (157-165). The variant named NY-ESO-L5 ($C^{75}A/C^{76}A/C^{78}A/L^{153}H$), with a near 100-fold increase in surface display level over wild type (Fig. 2.3C), was selected for further study.

2.5 Attempts to Detect NY-ESO-1 Peptide-MHC by Antibody Labeling

Now that we had both functional human DCs and yeast surface-displaying a high level of an NY-ESO-1 variant, we could proceed with the proposed plan to detect cross-presentation by directly labeling yeast-fed DCs with 3M4E5, a Fab fragment binding to the NY-ESO-$1_{157-165}$/HLA-A2 complex (3). Biotinylated 3M4E5 (b-3M4E5) was kindly provided to us by the Renner lab. We were unable to detect an increase in 3M4E5 labeling between HLA-A2 DCs that had phagocytosed yeast surface-displaying NY-ESO-L5 as compared to wild type yeast despite extensive troubleshooting. For example, Fig. 2.4A shows the median fluorescence of DCs that had been exposed to NY-ESO-L5-displaying or wild type yeast for various time periods and subsequently labeled with b-3M4E5-streptavidin-PE complexes. Pre-incubating the b-3M4E5 at a 4:1 stoichiometric ratio with streptavidin-PE was a strategy to increase the avidity (as opposed to sequentially labeling with b-3M4E5 followed by streptavidin-PE). At none of the seven time points was the signal caused by NY-ESO-L5-displaying yeast higher than the control.

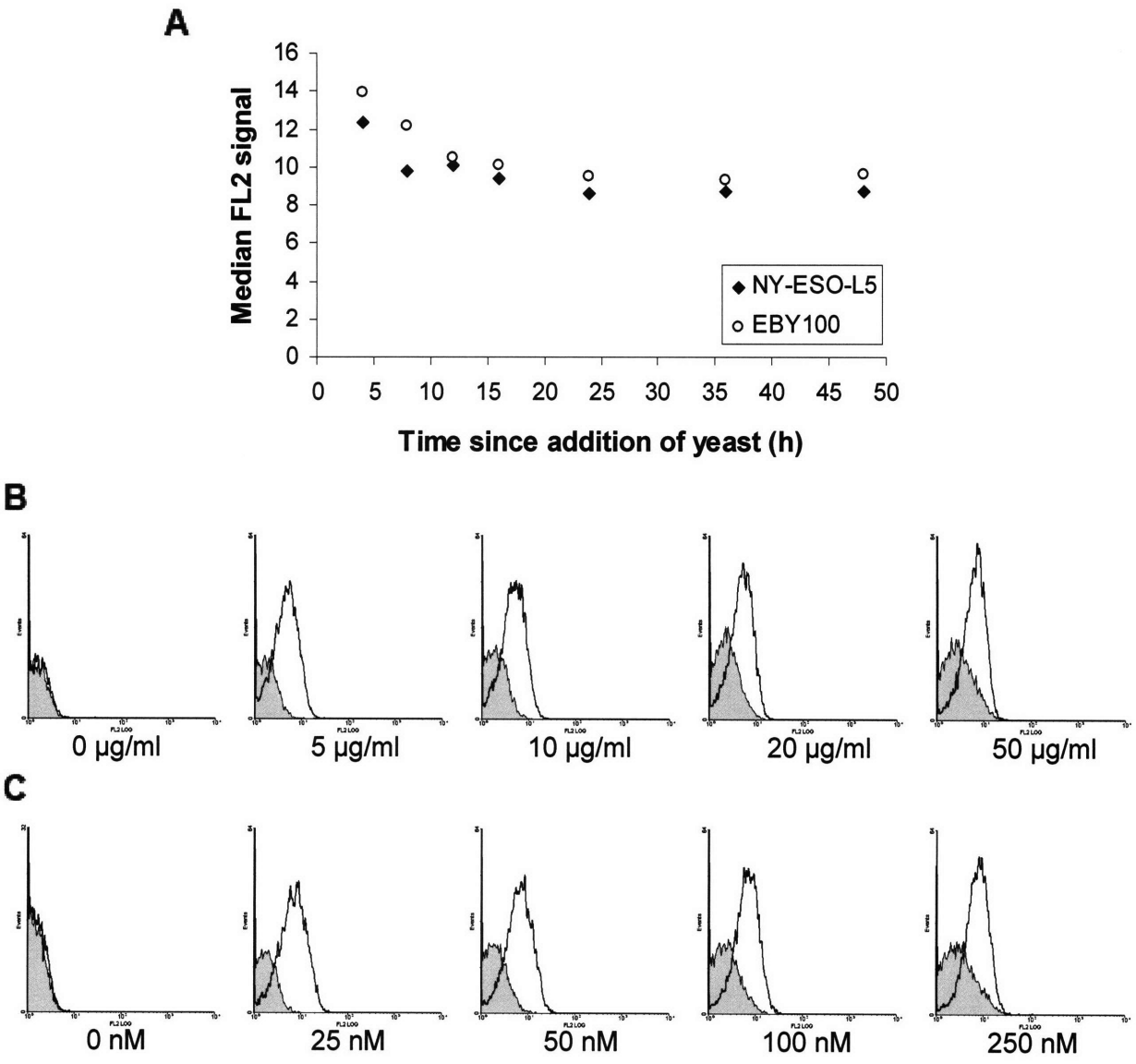

Figure 2.4, Low sensitivity of 3M4E5 labeling.

A, NY-ESO-L5-expressing or wild type EBY100 yeast were UV-irradiated and added to HLA-A2 monocyte-derived DCs at a 10:1 ratio. After the indicated time, the DCs were labeled with α-DC-SIGN-FITC and 100 nM of streptavidin-PE pre-loaded with a 4-fold molar ratio of b-3M4E5. The cells were analyzed by flow cytometry and the median PE fluorescence of the FITC-gated events was plotted. B and C, T2 cells were pulsed with 20 µg/ml of SLLMWITQA peptide for 2 h in serum-free medium.

B, The T2 cells were labeled with the indicated concentration of b-3M4E5, washed, and then labeled with 10 µg/ml of streptavidin-PE. C, The T2 cells were labeled with the indicated concentration of streptavidin-PE that had been pre-loaded with b-3M4E5. Gray histograms indicate unpulsed T2 cells labeled under the same conditions.

Since the failure to detect a difference in 3M4E5 labeling may lie in insufficient cross-presentation levels rather than the detection scheme, we also investigated labeling of peptide-pulsed T2 cells, which express HLA-A2. Regardless of whether we sequentially labeled with b-3M4E5 followed by streptavidin-PE or with pre-formed complexes, across a range of concentrations, there was less than a log of difference in fluorescence between the peptide-pulsed T2 cells and the unpulsed controls (Figs. 2.4B, C). Peptide pulsing results in an unphysiologically large fraction of surface MHC class I molecules forming complexes with that peptide, hence this low level of sensitivity did not bode well for detecting the much smaller numbers of peptide-MHC complexes generated by cross-presentation. We finally abandoned this strategy for detecting cross-presentation when Andreas Wadle from the Renner group brought their materials (DCs, yeast-produced NY-ESO-1 and fresh b-3M4E5) to our laboratory but was unable to demonstrate a significant difference in labeling (not shown).

2.6 Detection of Cross-presentation using a Model Antigen T Cell Clone

It was unclear whether problems with the reagent, such as inadequate affinity or batch-specific issues like misfolding, degradation or incomplete biotinylation, contributed towards the low levels of labeling with b-3M4E5. Nevertheless, we hypothesized that even an ideal antibody against a peptide-MHC complex may not be sensitive enough to quantitatively measure cross-presentation levels. Fewer than a hundred, and perhaps even just a single peptide-MHC complex on a DC can trigger $CD8^+$ T cell activation (11, 12), whereas flow cytometers typically require at least hundreds of fluorophore molecules per cell for detection. We therefore explored the use of T cell activation as an indirect measure of cross-presentation. Limited access to NY-ESO-1-specific T cells prompted us to select a model antigen for which T cell clones or lines were readily available. Monoclonal $CD8^+$ T cells recognizing the immunodominant, HLA-A*0201-

restricted peptide NLVPMVATV (N9V), derived from cytomegalovirus (CMV) phosphoprotein pp65, are available commercially (Proimmune, Oxford, UK). Two clones against Epstein-Barr virus epitopes are also available, but the prevalence of CMV infection combined with the high frequency of N9V-specific CTLs in infected individuals (13) allows for research continuity even if the T cell clone were to become unavailable.

The extended peptide ARNLVPMVATVQGQN that was consistently immunogenic in HLA-A*0201, CMV-positive individuals (14) was expressed in the yeast surface display system. The surface display level was very high, exceeding that of NY-ESO-L5 (Fig. 2.5A). In the pilot experiment, yeast surface-displaying N9V and wild type yeast were fed to HLA-A*0201 monocyte-derived DCs at three different doses. After either 3 h or 48 h, the DCs were co-cultured with N9V-specific $CD8^+$ T cells for 4 h in the presence of Brefeldin A. Intracellular IFNγ staining of fixed and permeabilized cells revealed that at 3 h post-feeding, a modest but consistently higher than background level of T cell activation could be detected (Fig. 2.5B). At the 48 h time point, the percentage of IFN-γ-positive T cells was much greater and increased with yeast dosage (Fig. 2.5C). This experiment proved that cross-presentation levels can be measured by detecting IFNγ secretion by activated cognate $CD8^+$ T cells, paving the way for the work described in the subsequent chapters. The assay protocol was altered to use a cytokine secretion-capture kit rather than intracellular cytokine staining and is detailed in Appendix B.2.

2.7 Production of Yeast-expressed NY-ESO-L5

Although NY-ESO-L5 was not ultimately used to study cross-presentation, Piatesi's work in engineering NY-ESO-1 variants that are highly expressed in yeast (10) also served

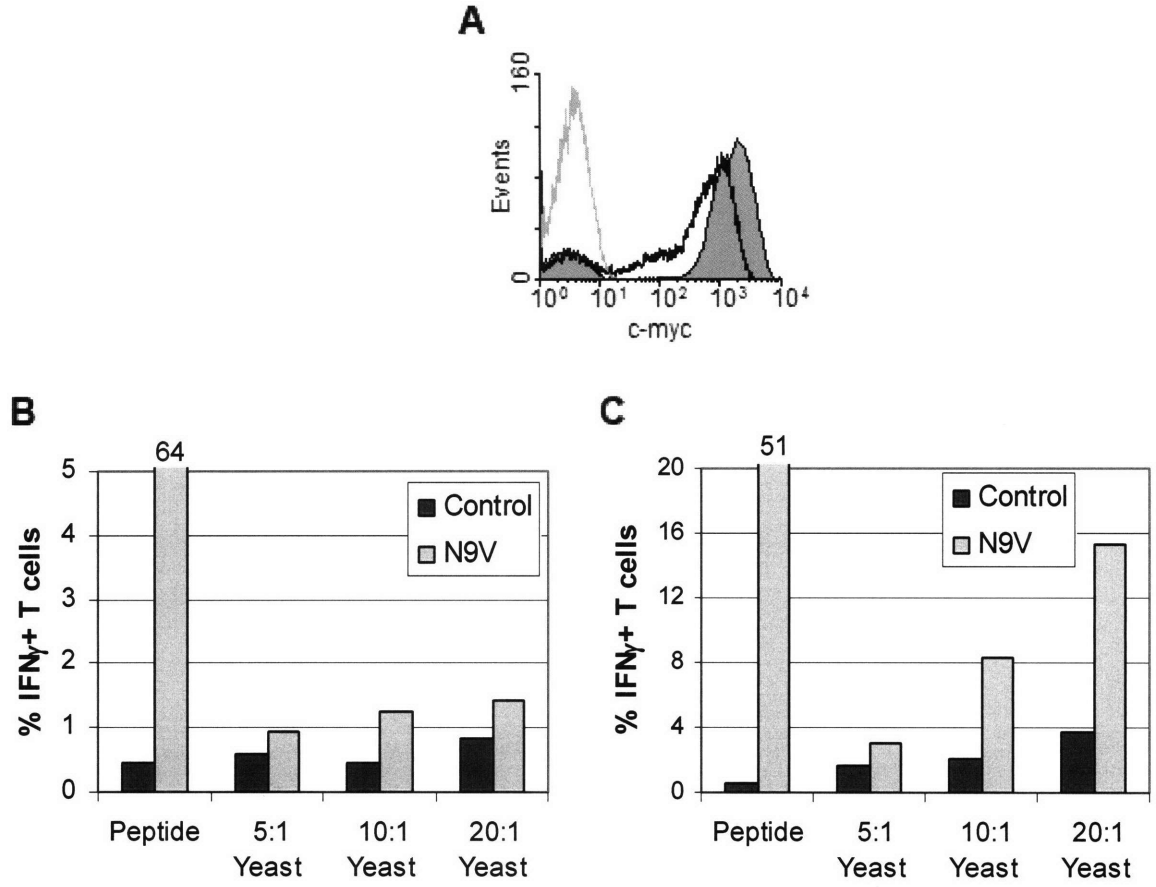

Figure 2.5, Detecting cross-presentation of the N9V epitope displayed on yeast using an antigen-specific T cell clone.

A, The high yeast surface display level of N9V (gray fill) as detected by labeling with chicken α-c-myc. Black line: yeast surface-displaying NY-ESO-L5; gray line: wild type yeast.

B and C, N9V-displaying yeast or control plasmidless yeast were added to HLA-A*0201 monocyte-derived DCs at the indicated ratios. The positive control DCs were pulsed with 1 μg/ml synthetic N9V peptide and 30 μg/ml poly I:C. N9V-specific T cells and Brefeldin A were added either 3 h (B) or 48 h (C) later. After 4 h of co-culture, the cells were stained with α-CD8-FITC, fixed and permeabilized, then stained with α-IFNγ-PE and analyzed by flow cytometry. The T cells were gated by FS/SS and CD8 labeling and the percentage of IFNγ-positive T cells was determined.

another purpose. NY-ESO-1 protein used in human vaccination trials is expressed in bacteria and purified from inclusion bodies (15). This material is of limited purity (perhaps due to the extreme hydrophobicity of the C-terminus of NY-ESO-1), which raises concerns over the generation of immune responses against bacterial contaminants (16). In particular, false positive reactions can occur when the same material is then used to perform Delayed Type Hypersensitivity (DTH) skin tests to monitor the anti-NY-ESO-1 immune response. Therefore, a source of NY-ESO-1 antigen produced in a non-bacterial host such as yeast is desirable. The rest of this chapter describes our work in developing a strategy to produce yeast-expressed NY-ESO-L5, which was previously published in ref. (10).

Initial attempts to secrete NY-ESO-L5 in yeast were unsuccessful: the yield was extremely low and comparable to the CS-engineered variant (data not shown). An alternative production strategy became necessary, as it appeared that the strong improvement in the display level was insufficient to boost the production of NY-ESO-L5 to useful levels. Since the directed evolution approach that we used is based on the display of the protein of interest as an Aga2p-fusion, we tested secretion of the whole display fusion (Aga2p-Xa-HA-$(G_4S)_3$-NY-ESO-1-c-*myc*) by transforming the pCT-constructs of NY-ESO-1, NY-ESO-CS and NY-ESO-L5 in BJ5464α. This yeast strain is Aga1p-deficient, allowing the secretion of the fusion directly into the media. Small scale secretion experiments were performed for the NY-ESO-1, NY-ESO-CS and NY-ESO-L5 display fusions, and the resulting Western blots are shown in Fig. 2.6A. Interestingly, only the NY-ESO-L5 fusion was efficiently secreted (Fig. 2.6A, lane 4). Both, the wt and the CS fusions were nearly undetectable (Fig. 2.6A, lanes 2 and 3) suggesting that the $L^{153}H$ mutation is largely responsible for the improved secretion of this antigen. The apparent MW of the fusion observed on the Western blot was much higher than expected (≈ 150 kDa instead of ≈ 30kDa),

presumably due to the extensive glycosylation of Aga2p and of the Xa-HA-$(G_4S)_3$-linker. Aga2p is a small glycoprotein (69 residues after cleavage of an 18-residue signal sequence) that is known to be highly *O*-glycosylated (17). At least 10 of the 21 serine and threonine residues in Aga2p are glycosylated showing an apparent mass of 33 kDa on SDS-PAGE (18). Initial attempts to purify the NY-ESO-L5 display fusion by size-exclusion chromatography and/or by metal-affinity chromatography of the same fusion with a C-terminal His_6-tag were of limited success (data not shown). In order to simplify the purification process, the original display vector was modified by introducing a more specific protease cleavage site (human rhino virus 3C; HRV 3C) right before the N-terminus of NY-ESO-L5. Moreover, the [Xa-HA-$(G_4S)_3$] sequence was shortened to a single G_4S repeat and a His_6-tag was added just upstream of the HRV 3C site. The C-terminal c-*myc*-tag was eliminated so that after HRV 3C cleavage, NY-ESO-L5 would be released without any tag sequences. Finally, to improve retention on a metal-affinity column, an additional His_6-tag was added at the N-terminus of Aga2p (following the signal peptide), leading to the generation of the pHAH-L5 display construct [His_6-Aga2p-G_4S-His_6-(HRV 3C)-(NY-ESO-L5)]. While maintaining an essentially identical NY-ESO-L5 display and secretion level compared to the original pCT-display construct (data not shown), this newly designed display fusion is significantly smaller and allows a simple purification of NY-ESO-L5. We found that instead of secreting the NY-ESO-L5 fusion from BJ5464α cells, higher purities can be achieved by reductively cleaving the fusion protein from the surface of EBY100 cells (data not shown). The reduction of the Aga2p-Aga1p disulfide bonds with TCEP yielded the NY-ESO-L5 fusion protein in a concentrated and partially purified form. The additional metal-affinity chromatography step results in the specific enrichment of the NY-ESO-L5 display fusion and allows the efficient isolation of NY-ESO-L5 by on-column

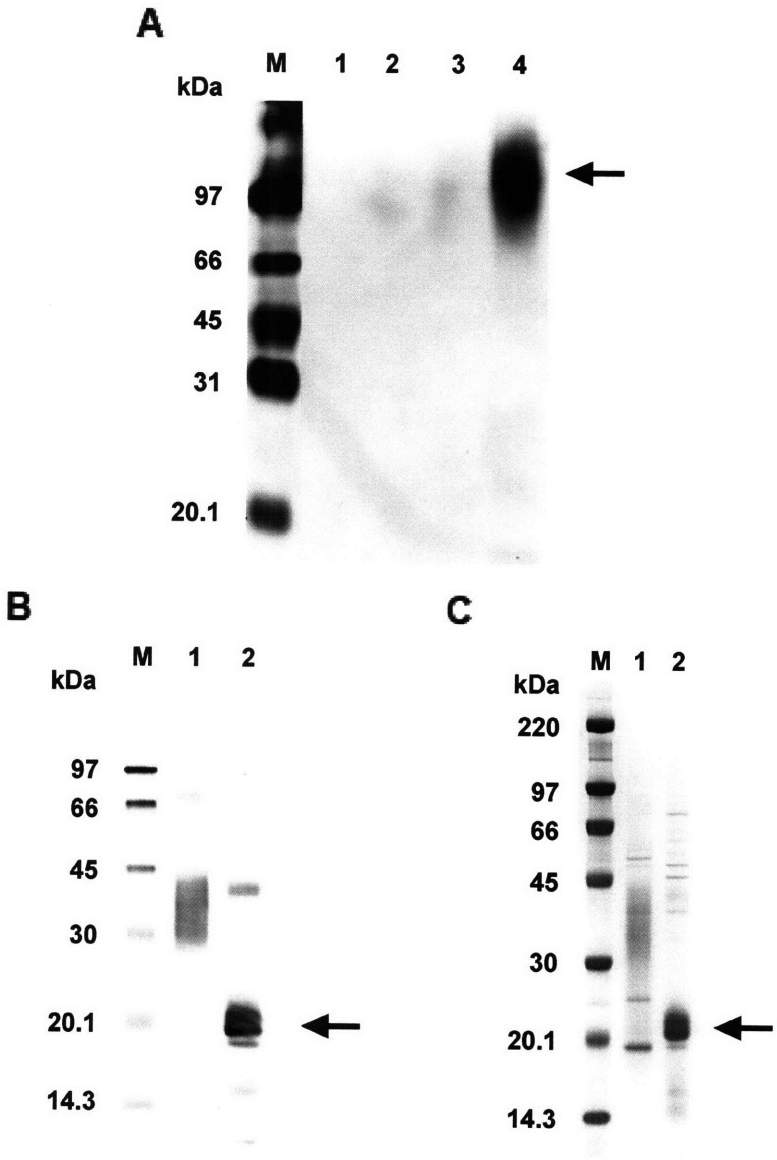

Figure 2.6, Secretion and purification of NY-ESO-L5 from yeast.
A, Western blot analysis of the NY-ESO-1, NY-ESO-CS and NY-ESO-L5 original display fusions ([Aga2p-Xa-HA-$(G_4S)_3$-(NY-ESO-1)-c-*myc*] fusions) secreted in BJ5464α. M: ECL-marker; lane 1: SG-CAA media ; lane 2: NY-ESO-1; lane 3: NY-ESO-CS; lane 4: NY-ESO-L5. Arrow shows the strong signal generated by the NY-ESO-L5 fusion.
B, Western blot analysis of the re-designed NY-ESO-L5 fusion ([His_6-Aga2p-G_4S-His_6-(HRV 3C)-(NY-ESO-L5)]) reduced from the surface of yeast with TCEP and purified by metal-affinity chromatography (lane 1). Lane 2 shows the same sample after on column digestion with HRV 3C protease instead of imidazole elution. Arrow indicates the band corresponding to NY-ESO-L5. All Western blots were performed using mAb E978 as the primary anti- NY-ESO-1 detection reagent.
C, SDS-PAGE analysis (Coomassie blue stain) of the same samples shown in (B).
Reproduced with permission from ref. (10).

digestion with HRV 3C protease. Western blot and SDS-PAGE analyses of the reduced fusion purified by metal-affinity chromatography confirmed the presence of a diffuse band between 30 and 45 kDa (Fig. 2.6B, lane 1 and Fig. 2.6C, lane 1). When the metal-bound display fusion was treated with HRV 3C protease, the released NY-ESO-L5 ran at around 20 kDa and was recognized by α-NY-ESO-1 monoclonal antibody (Fig. 2.6B, lane 2 and Fig. 2.6C, lane 2). Moreover, SDS-PAGE analysis shown in Figure 2.6C demonstrates that the obtained NY-ESO-L5 is highly enriched (yield ≈ 50 μg/L of NY-ESO-L5) and the antigen purity is significantly improved compared to the established cGMP purification of recombinant NY-ESO-1 from inclusion bodies (15).

Recombinant *E. coli*-derived NY-ESO-1 protein has been shown to be efficiently cross-presented when formulated in ISCOMATRIX (IMX) or as an immune complex (IC) (19). To be considered a viable vaccine or DTH alternative it is critical to demonstrate that the NY-ESO-L5 mutant can also be processed for class I MHC-restricted presentation to NY-ESO-1-specific $CD8^+$ T cells. Therefore, NY-ESO-L5 protein and the Aga2p-NY-ESO-L5 fusion protein were tested for efficiency of cross-presentation, to ensure that the $Leu^{153}His$ mutation and the AARA cluster (75-78) did not alter antigen processing and loading. The results (Fig. 2.7) are from two HLA-A2+ DC donors and are comparisons of the 157-165 NY-ESO-1 peptide *vs.* recombinant NY-ESO-1/IMX *vs.* each of the mutant proteins added together with empty IMX. The peptide response is taken as maximum response for each donor. Clearly, the mutations in the L5 version of NY-ESO-1 do not ablate the presentation of the same peptide antigen recognized from wild-type NY-ESO-1 protein.

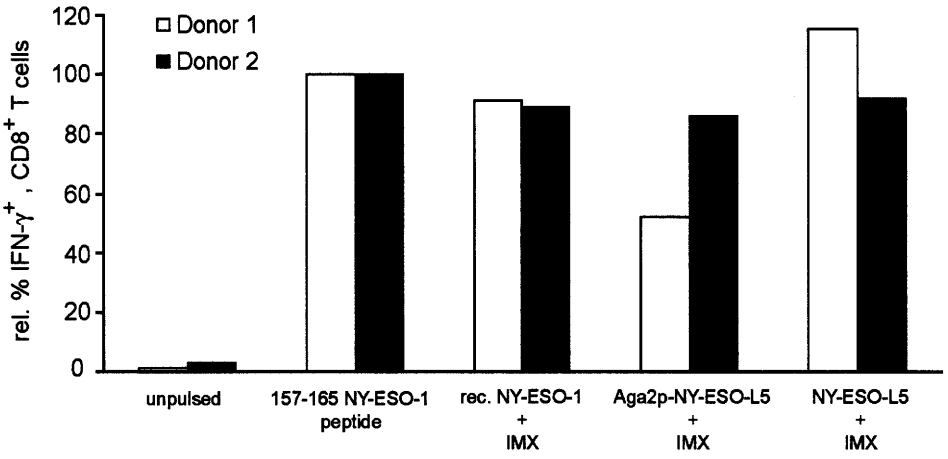

Figure 2.7, Cross-presentation of different NY-ESO-1 protein formulations. The 157-165 NY-ESO-1 peptide was used as a positive control. Recombinant NY-ESO-1, Aga2p-NY-ESO-L5 and NY-ESO-L5 mixed with an equimolar amount of IMX (10 μg/mL) were used to pulse monocyte-derived DCs from 2 HLA-$A2^+$ donors. Antigen-pulsed DCs were co-cultured with 157-165 NY-ESO-1 peptide specific $CD8^+$ T cells and induction of IFN-γ production assessed by intracellular cytokine staining. Reproduced with permission from ref. (10). This experiment was performed by N. Robson and J. Cebon, Ludwig Institute for Cancer Research, Melbourne, Australia.

2.8 References

1. Mateo, L., J. Gardner, Q. Chen, C. Schmidt, M. Down, S. L. Elliott, S. J. Pye, H. Firat, F. A. Lemonnier, J. Cebon, and A. Suhrbier. 1999. An HLA-A2 Polyepitope Vaccine for Melanoma Immunotherapy. *J Immunol* 163: 4058-4063.

2. Maraskovsky, E., S. Sjolander, D. P. Drane, M. Schnurr, T. T. T. Le, L. Mateo, T. Luft, K.-A. Masterman, T.-Y. Tai, Q. Chen, S. Green, A. Sjolander, M. J. Pearse, F. A. Lemonnier, W. Chen, J. Cebon, and A. Suhrbier. 2004. NY-ESO-1 Protein Formulated in ISCOMATRIX Adjuvant Is a Potent Anticancer Vaccine Inducing Both Humoral and CD8+ T-Cell-Mediated Immunity and Protection against NY-ESO-1+ Tumors. *Clin Cancer Res* 10: 2879-2890.

3. Held, G., M. Matsuo, M. Epel, S. Gnjatic, G. Ritter, S. Y. Lee, T. Y. Tai, C. J. Cohen, L. J. Old, M. Pfreundschuh, Y. Reiter, H. R. Hoogenboom, and C. Renner. 2004. Dissecting cytotoxic T cell responses towards the NY-ESO-1 protein by peptide/MHC-specific antibody fragments. *Eur J Immunol* 34: 2919-2929.

4. Bender, A., M. Sapp, G. Schuler, R. M. Steinman, and N. Bhardwaj. 1996. Improved methods for the generation of dendritic cells from nonproliferating progenitors in human blood. *J Immunol Methods* 196: 121-135.

5. Stubbs, A. C., K. S. Martin, C. Coeshott, S. V. Skaates, D. R. Kuritzkes, D. Bellgrau, A. Franzusoff, R. C. Duke, and C. C. Wilson. 2001. Whole recombinant yeast vaccine activates dendritic cells and elicits protective cell-mediated immunity. *Nat Med* 7: 625-629.

6. d'Ostiani, C. F., G. Del Sero, A. Bacci, C. Montagnoli, A. Spreca, A. Mencacci, P. Ricciardi-Castagnoli, and L. Romani. 2000. Dendritic cells discriminate between yeasts and hyphae of the fungus Candida albicans. Implications for initiation of T helper cell immunity in vitro and in vivo. *J Exp Med* 191: 1661-1674.

7. Newman, S. L., and A. Holly. 2001. Candida albicans is phagocytosed, killed, and processed for antigen presentation by human dendritic cells. *Infect Immun* 69: 6813-6822.

8. Torosantucci, A., G. Romagnoli, P. Chiani, A. Stringaro, P. Crateri, S. Mariotti, R. Teloni, G. Arancia, A. Cassone, and R. Nisini. 2004. Candida albicans yeast and germ tube forms interfere differently with human monocyte differentiation into dendritic cells: a novel dimorphism-dependent mechanism to escape the host's immune response. *Infect Immun* 72: 833-843.

9. Mischo, A., A. Wadle, K. Watzig, D. Jager, E. Stockert, D. Santiago, G. Ritter, E. Regitz, E. Jager, A. Knuth, L. Old, M. Pfreundschuh, and C. Renner. 2003. Recombinant antigen expression on yeast surface (RAYS) for the detection of serological immune responses in cancer patients. *Cancer Immun* 3: 5.

10. Piatesi, A., S. W. Howland, J. A. Rakestraw, C. Renner, N. Robson, J. Cebon, E. Maraskovsky, G. Ritter, L. Old, and K. D. Wittrup. 2006. Directed evolution for improved secretion of cancer-testis antigen NY-ESO-1 from yeast. *Protein Expression and Purification* 48: 232-242.

11. Kageyama, S., T. Tsomides, Y. Sykulev, and H. Eisen. 1995. Variations in the number of peptide-MHC class I complexes required to activate cytotoxic T cell responses. *J Immunol* 154: 567-576.

12. Sykulev, Y., M. Joo, I. Vturina, T. J. Tsomides, and H. N. Eisen. 1996. Evidence that a single peptide-MHC complex on a target cell can elicit a cytolytic T cell response. *Immunity* 4: 565-571.

13. Wills, M. R., A. J. Carmichael, K. Mynard, X. Jin, M. P. Weekes, B. Plachter, and J. G. Sissons. 1996. The human cytotoxic T-lymphocyte (CTL) response to cytomegalovirus is dominated by structural protein pp65: frequency, specificity, and T-cell receptor usage of pp65-specific CTL. *J Virol* 70: 7569-7579.

14. Trivedi, D., R. Y. Williams, R. J. O'Reilly, and G. Koehne. 2005. Generation of CMV-specific T lymphocytes using protein-spanning pools of pp65-derived overlapping pentadecapeptides for adoptive immunotherapy. *Blood* 105: 2793-2801.

15. Murphy, R., S. Green, G. Ritter, L. Cohen, D. Ryan, W. Woods, M. Rubira, J. Cebon, I. D. Davis, A. Sjolander, A. Kypridis, H. Kalnins, M. McNamara, M. B. Moloney, J. Ackland, G. Cartwright, J. Rood, G. Dumsday, K. Healey, D. Maher, E. Maraskovsky, Y. T. Chen, E. W. Hoffman, L. J. Old, and A. M. Scott. 2005. Recombinant NY-ESO-1 cancer antigen: production and purification under cGMP conditions. *Prep Biochem Biotechnol* 35: 119-134.

16. Davis, I. D., W. Chen, H. Jackson, P. Parente, M. Shackleton, W. Hopkins, Q. Chen, N. Dimopoulos, T. Luke, R. Murphy, A. M. Scott, E. Maraskovsky, G. McArthur, D. MacGregor, S. Sturrock, T. Y. Tai, S. Green, A. Cuthbertson, D. Maher, L. Miloradovic, S. V. Mitchell, G. Ritter, A. A. Jungbluth, Y.-T. Chen, S. Gnjatic, E. W. Hoffman, L. J. Old, and J. S. Cebon. 2004. Recombinant NY-ESO-1 protein with ISCOMATRIX adjuvant induces broad integrated antibody and CD4+ and CD8+ T cell responses in humans. *Proc Natl Acad Sci U S A* 101: 10697-10702.

17. Cappellaro, C., K. Hauser, V. Mrsa, M. Watzele, G. Watzele, C. Gruber, and W. Tanner. 1991. Saccharomyces-Cerevisiae a-Agglutinin and Alpha-Agglutinin - Characterization of Their Molecular Interaction. *Embo Journal* 10: 4081-4088.

18. Zhao, H., Z. M. Shen, P. C. Kahn, and P. N. Lipke. 2001. Interaction of alpha-agglutinin and a-agglutinin, Saccharomyces cerevisiae sexual cell adhesion molecules. *Journal of Bacteriology* 183: 2874-2880.

19. Schnurr, M., Q. Y. Chen, A. Shin, W. S. Chen, T. Toy, C. Jenderek, S. Green, L. Miloradovic, D. Drane, I. D. Davis, J. Villadangos, K. Shortman, E. Maraskovsky, and J. Cebon. 2005. Tumor antigen processing and presentation depend critically on dendritic cell type and the mode of antigen delivery. *Blood* 105: 2465-2472.

Chapter 3

Antigen Release Kinetics in the Phagosome are Critical to Cross-presentation Efficiency[1]

3.1 Abstract

Cross-presentation of exogenous antigens in MHC class I molecules by dendritic cells is the underlying basis for many developing immunotherapies and vaccines. In the phagosome-to-cytosol pathway, antigens in phagocytosed particles must become freely soluble before being exported to the cytosol, but the kinetics of this process has yet to be fully appreciated. We demonstrate with a yeast vaccine model that the rate of antigen release in the phagosome directly affects cross-presentation efficiency, with an apparent time limit of about 25 min post-phagocytosis for antigen release to be productive. Antigen expressed on the yeast surface is cross-presented much more efficiently than antigen trapped in the yeast cytosol by the cell wall. The cross-presentation efficiency of yeast surface-displayed antigen can be increased by the insertion of linkers susceptible to cleavage in the early phagosome. Antigens indirectly attached to yeast through antibody fragments are less efficiently cross-presented when the antibody dissociation rate is extremely slow.

[1] Major portions of this chapter were previously published in:
Howland, S. W., and K. D. Wittrup. 2008. Antigen Release Kinetics in the Phagosome Are Critical to Cross-Presentation Efficiency. J Immunol 180: 1576-1583.

3.2 Introduction

Vaccines that stimulate antibody production have enjoyed success for the past century, but the development of vaccines that generate effective cellular immune responses, in particular, $CD8^+$ cytotoxic lymphocytes, remains a challenge. Such vaccines provide hope for the prevention and treatment of cancer (1-3) as well as viral diseases like HIV (4), Hepatitis C (5) and herpes simplex virus (6).

Part of this challenge arises from the fact that peptide-MHC class I complexes required to prime $CD8^+$ T cells are generally produced from the endogenous proteins of antigen-presenting cells, principally dendritic cells (DCs)[3]. While alternative strategies such as adoptive transfer of lymphocytes (7), DNA vaccines (8), and vaccination with exact peptide epitopes exist (9), cross-presentation—the process by which peptides derived from exogenous antigens are displayed with MHC class I molecules—remains central to most immunotherapy strategies. Early reports of cross-presentation presented conflicting results as to whether this process required TAP and was sensitive to proteasome inhibitors (10), or was TAP-independent and sensitive to protease inhibitors (11, 12). At least two distinct mechanisms for cross-presentation emerged: the phagosome-to-cytosol pathway and the vacuolar pathway (13). In the vacuolar pathway, peptides are generated from internalized antigens by the action of endolysosomal proteases; the peptides may then meet up with recycling MHC class I molecules. In the phagosome-to-cytosol route, phagocytosed antigens escape to the cytosol to be processed by proteasomes and are loaded onto nascent MHC class I molecules with the aid of TAP.

Quantitative mechanistic details about these pathways for cross-presentation are still missing from the picture, which if discovered could lead to the development of more effective vaccines. We hypothesize that with particulate antigens that are cross-presented via the

phagosome-to-cytosol pathway, antigen release from the particles may be a rate-limiting step. To our knowledge, antigen release rates within the phagosome have not been comprehensively studied. In this work, we explore the effects of altering antigen release kinetics on cross-presentation efficiency using a yeast vaccine model.

Recombinant yeasts show promise as vaccine candidates in mouse models (14, 15) and in human blood cell assays (16-18). In particular, *S. cerevisiae* is attractive because it is non-pathogenic, well-characterized, and is a strong adjuvant—Zymosan, a cell wall preparation of this yeast, has been a valuable tool in immunology for over 50 years (19). *S. cerevisiae* potently induced the maturation of murine bone marrow-derived DCs and secretion of interleukin-12 (14). In our hands (unpublished) and others (16), human monocyte-derived DCs were similarly activated. When the recombinant antigen is expressed intracellularly in yeast, the rate of antigen release is primarily dictated by the rate of yeast cell wall degradation. With yeast surface display technology (20), on the other hand, antigen is expressed on the cell wall exterior, permitting the release kinetics to be manipulated.

3.3 Materials and Methods

3.3.1 Cells

Human HLA-A*0201 monocytes were obtained from two sources, purified either by counter-flow centrifugal elutriation (Advanced Biotechnologies Inc, Columbia, MD) or negative magnetic cell sorting (Biological Specialty Corporation, Colmar, PA). Similar results were obtained with both sources. The monocytes were aliquoted into vials and cryopreserved in 90% FBS, 10% DMSO. For each experiment, one or more vials were thawed and washed in C10 medium: RPMI 1640 with 10% FBS, 2 mM L-glutamine, 10 mM HEPES, 1 mM sodium pyruvate, 1× non-essential amino acids, 50 μM β-mercaptoethanol and Primocin (InvivoGen, San Diego, CA). Unless otherwise indicated, media components were from Hyclone (Logan, UT); low endotoxin products were chosen where available. 4-5×10^6 monocytes were cultured per well of a 6-well plate in 2.5 ml C10 medium supplemented with 1000 U/ml each of IL-4 and GM-CSF (C10GF; cytokines from R & D Systems, Minneapolis, MN). After 2 and 4 days of culture, each well was topped up with 0.5 ml C10GF; after 6 days of culture, floating and loosely adherent immature monocyte-derived DCs were harvested by gentle resuspension.

Vials of a human $CD8^+$ T cell line specifically recognizing the peptide NLVPMVATV in the context of HLA-A*0201 were purchased from ProImmune (Oxford, UK). Each vial was thawed and cultured overnight in RPMI 1640 with 10% FBS and 5 ng/ml IL-2 and used the next day.

3.3.2 Yeast Surface Display

Plasmids for yeast surface display were based on pCT-CON (21) and were transformed into EBY100 (20), a strain that expresses Aga1p under galactose induction, using the Frozen EZ Yeast Transformation II Kit (Zymo Research, Orange, CA). Yeast colonies were cultured to mid-

log phase at 30°C in selective SD-CAA medium (2% dextrose, 0.67% yeast nitrogen base, 0.5% casamino acids, 0.1 M sodium phosphate, pH 6.0) and then induced in SG-CAA (SD-CAA with galactose replacing dextrose) for 48 h at 20°C. Single copies of some expression cassettes were integrated into the EBY100 yeast chromosome using the integrating shuttle vector pRS304 (22). The resulting yeast strains were grown up in rich YPD medium (1% yeast extract, 2% peptone, 2% dextrose) and induced in YPG (1% yeast extract, 2% peptone, 2% galactose) for 36 h at 20°C. Yeast media nitrogen sources were obtained from BD (Franklin Lakes, NJ). Surface display levels were measured by flow cytometry with chicken α-c-myc (Invitrogen, Carlsbad, CA) or 9e10 monoclonal antibody (Covance, Princeton, NJ). The number of copies per yeast cell was estimated by comparison with Quantum Simply Cellular beads (Bangs Labs, Fishers IN).

3.3.3 Cross-presentation Assay

After 6 days of differentiation, immature monocyte-derived DCs were seeded in 96-well round bottom plates at 1 or 2 × 10^5 cells in 200 µl C10GF per well. Appropriate numbers of yeast cells (measured by optical density at 600 nm with 1 OD ≈ 10^7/ml) were rendered non-viable by UV-irradiation (2 × 1000 J/m^2 in a Stratalinker, Stratagene, La Jolla, CA), pelleted by centrifugation and added to the DCs. For inhibition experiments, DCs were pre-incubated with Z-FL-COCHO (10 µM; Calbiochem, San Diego, CA), lactacystin (5 µM; Calbiochem) or chloroquine (25 µM) for one hour before yeast samples were introduced. 24 h later, half the medium was replaced with a T cell suspension, with 0.7-1 × 10^5 T cells per well. Following 4 h of co-culture, the contents of each well were transferred to tubes for labeling with Miltenyi's IFNγ secretion assay kit (Bergisch Gladbach, Germany) according to the recommended protocol. Briefly, cells were labeled with a bispecific antibody that captures secreted IFNγ on the cell surface during a 45 min incubation period in medium at 37°C, and then labeled on ice for 30 min

with α-CD8-FITC (BD) and α-IFNγ-PE (Miltenyi). In experiments involving FITC-conjugated yeast, α-CD8-Alexa Fluor 647 (BD) was substituted. The percentage of $CD8^+$ cells that were $IFN\gamma^+$ was determined by flow cytometry (Coulter Epics XL, Fullerton, CA or BD FACSCalibur). The cut-off PE fluorescence was set for each experiment such that about 0.5% of T cells were $IFN\gamma^+$ in a negative control sample (no yeast or peptide). The positive control with 1 μM of the extended peptide ARNLVPMVATVQGQN (synthesized by GenScript, Piscataway, NJ) resulted in 45-70% $IFN\gamma^+$ T cells.

3.3.4 Yeast Intracellular Expression

Intracellular expression of the same fusion protein as is expressed by surface display was achieved by deleting the signal peptide of Aga2p, followed by transformation into BJ5464α (Yeast Genetic Stock Center, Berkeley, CA). BJ5464α is isogenic to the parent strain of EBY100 and lacks the galactose-inducible *Aga1p* gene. The resulting colonies were grown up in SD-CAA and induced in SG-CAA for 12 h at 30°C.

3.3.5 Slot Blot Comparison of Antigen Levels

6 OD.ml of each yeast culture was washed with PBS, resuspended in 300 μl 25 mM Tris(2-carboxyethyl)phosphine hydrochloride (TCEP, Soltec Ventures, Beverly, MA) in PBS, and incubated for on ice for 30 min. The proteins released into solution by the reducing agent were pooled with those from a second 30 min extraction with 25 mM TCEP. The yeast pellets were then washed with spheroplast buffer (50 mM Tris-HCl, pH 7.5, 1.4 M sorbitol, 40 mM β-mercaptoethanol), incubated with 2.4 U Zymolyase (Zymo Research) in 120 μl spheroplast buffer containing a protease inhibitor cocktail (Roche, Indianapolis, IN) for 15 min at 37°C, and boiled in 2% SDS for 5 min. The protein extracts were blotted onto nitrocellulose membrane

with a slot-blotting apparatus (Bio-rad, Hercules, CA). The membrane was blocked with 5% milk powder, incubated with 9e10 ascites fluid (Covance) followed by goat α-mouse-horse radish peroxidase (Pierce, Rockford, IL), developed with SuperSignal West Dura substrate (Pierce), and imaged on a FluorS Imager (Bio-rad).

3.3.6 Surface Display Antigen Dose Normalization

In experiments where different linkers were used to surface-display antigen, several cultures of each yeast sample were induced, and cultures with mean antigen levels within 10% of each other were selected to minimize the effect of variable antigen dose on cross-presentation. However, the variability in expression level across the panel of initial constructs (deleted linker, unchanged, and C1-5) was too high for this approach to be satisfactory. Therefore, each yeast sample was mixed with the appropriate amount of EBY100 yeast to normalize the antigen dose while maintaining the 20:1 ratio of yeast to DCs.

3.3.7 Measuring Linker Susceptibility to Cathepsin S

0.2 OD.ml of each yeast sample was washed and incubated with the indicated amounts of recombinant human Cathepsin S (CatS, Calbiochem) in 100 μl PBS at 37°C. The yeast samples were washed and labeled with 12CA5 monoclonal antibody (α-HA; Roche) and chicken α-c-myc, followed by goat α-mouse-PE (Sigma-Aldrich, St. Louis, MO) and goat α-chicken-Alexa Fluor 488 (Invitrogen). The mean c-myc fluorescence of the HA^+ population was compared against that of yeast samples that had not been treated with CatS.

3.3.8 Post-phagocytosis Analysis

DCs (2×10^5/well) were seeded in 96-well round bottom plates, with separate plates for each time point. After adding the yeast samples (5×10^5/well), the plates were immediately

centrifuged briefly (200 × g, 1 min) to settle the yeast and were returned to the incubator. At each time point, a plate was placed on ice and 90% of the medium in each well was replaced with cold RIPA buffer (Sigma-Aldrich). The well contents were moved to tubes, vortexed to promote cell lysis, and centrifuged to pellet the released yeast. The yeast was washed with RIPA buffer and PBS with 0.1% bovine serum albumin (BSA) before being labeled for HA and c-myc epitopes as described above.

3.3.9 Fluorescein-binding ScFvs

The fluorescein-binding scFvs used here were products of directed evolution for decreased dissociation rate using yeast surface display (23). These scFvs were subcloned into pRS316-based plasmids with an improved alpha mating factor pre-pro sequence (Rakestraw et al., unpublished). Codons encoding the extended peptide ARNLVPMVATVQGQN were inserted between the scFv C-terminus and the c-myc epitope. The resulting constructs were transformed into the protein disulfide isomerase-overexpressing yeast strain YVH10 (24) together with a dummy plasmid bearing the *trp* nutritional marker. Transformants were grown up in SD-CAA and induced in YPG containing 0.1 M sodium phosphate, pH 6.0 for 3 days at 20°C. The culture supernatants containing approximately 10 mg/L of scFv-antigen were adjusted to pH 7.4 and dialyzed against PBS.

3.3.10 Fluorescein-conjugated Yeast

UV-irradiated BJ5654α yeast cells were washed three times in 0.4 M sodium carbonate, pH 8.4 and resuspended in 10 μl/OD.ml of a freshly prepared 1.5 mg/μl solution of fluorescein-PEG-NHS (MW 5000; Nektar, Huntsville, AL) in sodium carbonate buffer. The reaction was allowed to proceed for 30 min at room temperature, after which the yeast was washed six times

with PBS containing 0.1% BSA. Fluorescein-conjugated yeast was loaded with antigen by incubation with scFv-antigen culture supernatants (1 ml per 10^7 yeast) for 1 hour on ice. Flow cytometry analysis (c-myc labeling) of the loaded yeast showed that the antigen levels mediated by 4M2.3, 4M3.12 and 4M4.5 were within ~5% of each other, but the level of 4M5.3-antigen was about 15% higher. Labeling fluorescein-conjugated yeast with 4M5.3 fusion protein for 30 min followed by 30 min, 37°C incubation in pH 5.4 PBS containing 0.1% BSA and 1 μM fluorescein-biotin resulted in a final antigen level comparable to that mediated by the other scFvs. This method of antigen level normalization was performed for the cross-presentation assay. In addition, to reduce antigen loss before phagocytosis, the plate was centrifuged (200×g, 1 min) immediately after addition of the yeast to the DCs.

3.3.11 Model Simulation

The mathematical model consisted of the following equations describing the amounts of yeast-bound antigen (A_b), free antigen within the phagosome (A_f) and cytoplasmic antigen (A_c) relative to the initial amount:

For $0 < t \leq t_{pre}$, where t_{pre} is the time prior to phagocytosis

$$\frac{dA_b}{dt} = -c_1 k_{off} A_b$$

For $t_{pre} < t \leq t_{pre} + t_{mat}$, where t_{mat} is the time taken for a phagolysosome formation

$$\frac{dA_b}{dt} = -c_2 k_{off} A_b \qquad \frac{dA_f}{dt} = c_2 k_{off} A_b - k_{esc} A_f \qquad \frac{dA_c}{dt} = k_{esc} A_f$$

For $t_{pre} + t_{mat} < t \leq 24$ h

$$\frac{dA_b}{dt} = -c_3 k_{off} A_b - k_{deg} A_b \qquad \frac{dA_f}{dt} = c_3 k_{off} A_b - k_{esc} A_f - k_{deg} A_f \qquad \frac{dA_c}{dt} = k_{esc} A_f$$

These equations were solved in Matlab with the initial conditions $A_b = 1$, $A_f = A_c = 0$. For a given set of parameter values, the final value of A_c (at 24 h) was determined for a wide range of k_{off} values. Ten logarithmically spaced values spanning three orders of magnitude were tested for each of the following parameters: c_1 (0.1 – 10), c_2 (10 – 1000), c_3 (10 – 1000), k_{esc} (0.01 – 1 min^{-1}), and k_{deg} (0.01 – 1 min^{-1}). An optimal $t_{1/2} = \ln(2)/k_{off}$ was found to exist between 10 and 10^5 min for all 10^5 possible combinations of parameter values, which should span all reasonable biological values. The time parameters, t_{pre} and t_{mat}, were fixed at 30 min and 20 min respectively. The former value is an estimate but is not a critical value since it is always multiplied by c_1, which was varied widely. The latter value was deemed reasonable based on the post-phagocytosis time course analysis we performed.

3.4 Results

3.4.1 Yeast Surface-displayed Antigen is Cross-presented to CD8$^+$ T cells

We selected the well-characterized HLA-A*0201-restricted peptide NLVPMVATV (N9V), derived from CMV phosphoprotein pp65 as our model antigen, for which cognate CD8$^+$ T cells are available commercially. To ensure proper antigen processing, we included its native flanking sequences in the yeast surface display construct, in the form of the 15-mer ARNLVPMVATVQGQN that was consistently immunogenic in HLA-A*0201, CMV-positive individuals (25). The yeast surface display construct consisted of a fusion of this extended peptide to the yeast mating adhesion receptor subunit Aga2p via a $(G_4S)_3$ linker, with HA and c-myc epitope tags for detection purposes (Fig. 3.1A). We created the yeast strain EBYN9V with co-inducible chromosomal copies of this construct and *Aga1p*, with expression resulting in ~120,000 copies/cell of the Aga2p-N9V fusion anchored to the yeast cell wall by disulfide bonds.

To test for cross-presentation, EBYN9V yeast were added to HLA-A*0201 monocyte-derived DCs at various ratios. The DCs avidly phagocytosed the yeast with an average maximum "capacity" of about 20 yeast per DC (numbers of unphagocytosed yeast rose sharply at higher ratios). Twenty four hours later, the DCs were co-cultured for four hours with a CD8$^+$ T cell line specifically recognizing the N9V/HLA-A*0201 complex. An IFNγ secretion cell capture FACS assay was performed on the T cells to quantify the percentage of cells that had been activated as a result of cross-presentation by the DCs. As shown in Fig. 3.1B, EBYN9V yeast resulted in dose-dependent cross-presentation at levels much higher than the background caused by EBY100 yeast lacking the N9V surface display construct. We decided to use the 20:1 yeast:DC

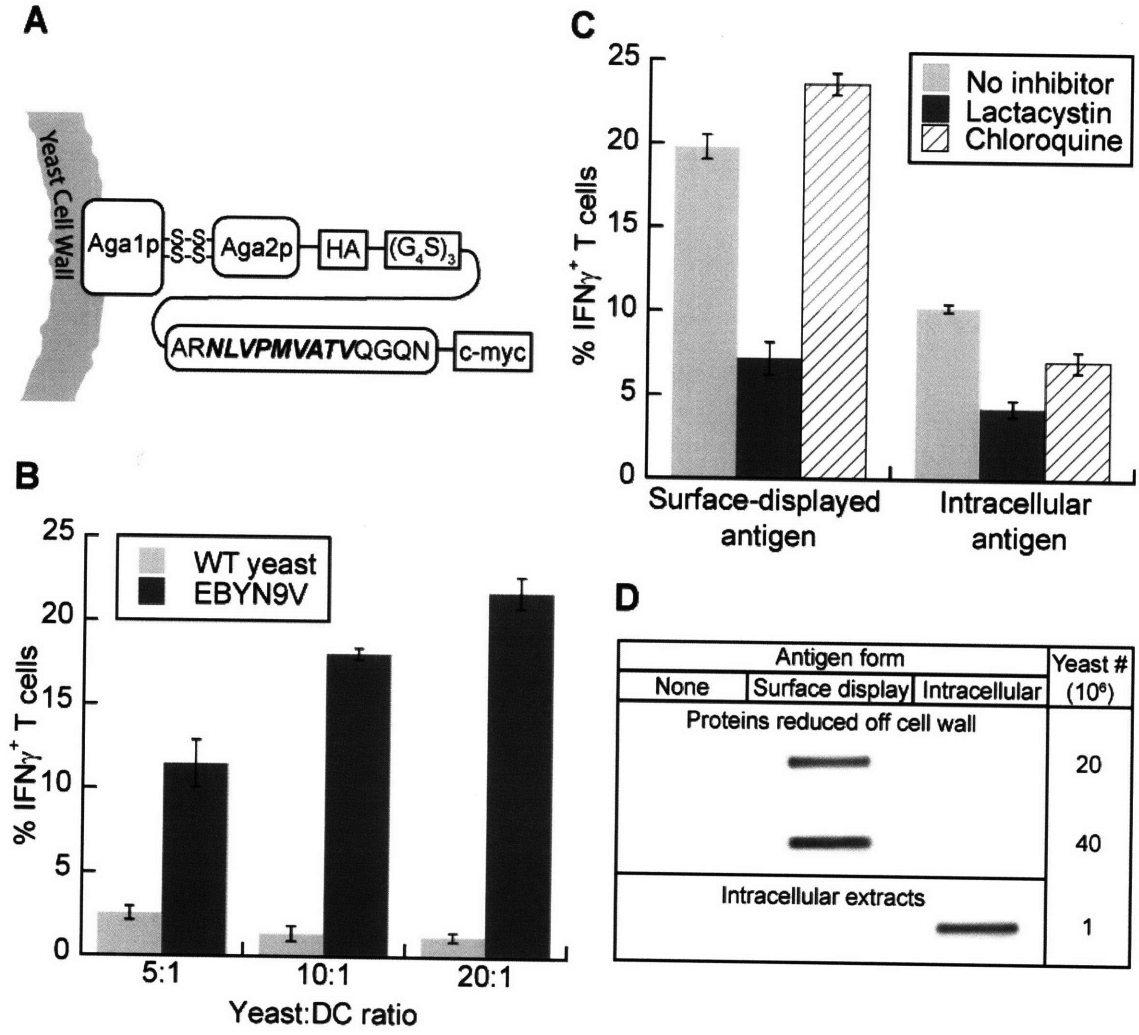

Figure 3.1, Antigen displayed on the surface of yeast is cross-presented more efficiently than antigen expressed intracellularly in yeast.

A, Diagram of the yeast surface display system of strain EBYN9V. The N9V epitope is in bold.

B, Dose response of EBYN9V on cross-presentation. EBYN9V and wild type EBY100 yeast were added to DCs at the indicated ratios. After 24 h, the DCs were assayed for the ability to stimulate IFNγ secretion in co-cultured N9V-specific T cells. Error bars represent the standard deviations of duplicate wells.

C, EBYN9V yeast and yeast expressing the same Aga2p-N9V fusion protein intracellularly were added to DCs at a 20:1 ratio and tested for the ability to stimulate IFNγ secretion in co-cultured N9V-specific T cells. Lactacystin (5 μM) or chloroquine (25 μM) were added to some wells an hour before the yeast were introduced. Error bars represent the standard deviations of duplicate wells.

D, Samples of the two yeast cultures and wt yeast were subjected to extensive reduction to release proteins disulfide-bonded to the cell wall. Subsequently, the yeast were treated with Zymolyase and lysed. The proteins reduced off the cell wall and the lysed cell extracts were slot-blotted onto the same nitrocellulose membrane and labeled for c-myc.

ratio for future cross-presentation experiments to minimize the signal-to-noise ratio; note that the concentration of peptide equivalents at this dose is only 4 nM.

3.4.2 Surface-displayed Antigen is Cross-presented Much More Efficiently than Intracellular Antigen

We next compared cross-presentation of yeast surface-displayed antigen to antigen expressed inside the cytosol of yeast. By deleting the signal peptide, the same Aga2p-N9V fusion protein was expressed intracellularly in yeast. At the same 20:1 yeast:DC ratio, cross-presentation resulting from intracellular antigen was only half that from surface-displayed antigen (Fig. 3.1C). This result was obtained even though the expression level of intracellular antigen was 20-30× the surface display level. In the slot blot in Fig. 3.1D, the amount of antigen in an intracellular extract of 1×10^6 cytosolically expressing yeast is equivalent to the amount of antigen reduced off the cell walls of $2\text{-}4 \times 10^7$ surface-displaying yeast. The blot also demonstrates that with both yeast cultures, antigen expression was restricted to the intended location.

To try to understand the marked difference in cross-presentation efficiency between surface-displayed and intracellular antigens, we studied the effects of inhibitors of either the phagosome-to-cytosol route or the vacuolar route. Cross-presentation of surface-displayed antigen was strongly inhibited by lactacystin, a proteasome inhibitor, whereas chloroquine, which raises the endolysosomal pH, had no inhibitory effect and was actually slightly beneficial (Fig. 3.1C). We deduced that the phagosome-to-cytosol pathway is the major mechanism of cross-presentation with yeast surface-displayed antigen. Chloroquine has been observed to increase the cross-presentation efficiency of soluble antigens, possibly because it increases membrane permeability and hence antigen escape into the cytosol (26), and may be having a

similar subtle effect here. Cross-presentation of intracellular antigen was inhibited by both lactacystin and chloroquine (Fig. 3.1C). It is unclear whether cross-presentation of intracellular antigen proceeds by a combination of the phagosome-to-cytosol and vacuolar routes, or whether only the phagosome-to-cytosol route is involved, with chloroquine reducing the rate at which the yeast cell wall was breached, thus slowing antigen export into the DC cytosol. In any case, it is clear to us that having antigen exposed on the yeast surface provides a significant advantage for cross-presentation due to greater accessibility to the DC cytosol compared to having antigen trapped by the thick yeast cell wall.

3.4.3 Manipulating the Kinetics of Antigen Release with Different Linkers

We hypothesized that the rate at which antigen is released from a phagocytosed particle influences the efficiency of cross-presentation, since antigen release is a necessary step before export into the cytosol can occur. The yeast surface display model provided an excellent means to test this hypothesis. We conjectured that with EBYN9V yeast, the N9V antigenic peptide could be released from the yeast cell wall by proteolysis in the phagosome or by reduction of the disulfide bonds tethering Aga2p to Aga1p. The rate of the former mechanism could potentially be manipulated by including protease recognition sites N-terminal to the antigenic peptide. We targeted Cathepsin S (CatS) because unlike most other cathepsins that are active only in acidic conditions found later in phagosomal maturation, its operating range extends from pH 5.0 to 7.5 (27). Furthermore, phagosomes in macrophages and DCs fuse preferentially with endocytic compartments enriched in CatS, with CatS activity detected in ten-minute-old phagosomes (28).

Five potential CatS recognition sites culled from the literature are listed in Table 3.1. In some cases, four amino acid residues on either side of a known CatS cleavage point were used. These sequences, termed C1 to C5, were each inserted individually between the $(G_4S)_3$ linker

and the extended antigenic peptide. An additional construct was created where the $(G_4S)_3$ linker, a suspected CatS cleavage site, was deleted. To test whether these sequences were recognized in their new context, yeast expressing the modified plasmid constructs were incubated with recombinant CatS and analyzed for loss of the c-myc epitope. CatS had negligible effect on HA epitope levels, indicating that the polypeptide chains linking together HA, Aga2p, Aga1p and the cell wall remained intact. While the addition of C1, C2, and C5 increased CatS cleavage, C3 and C4 had the opposite effect and were apparently not recognized and/or disrupted a pre-existing recognition site (Fig. 3.2A). Deleting the $(G_4S)_3$ linker altogether conferred the greatest resistance to CatS cleavage. When yeast with these different linker sequences were phagocytosed by DCs, the resulting pattern of cross-presentation was strikingly similar to the pattern of CatS cleavage (Fig. 3.2B). Performing Spearman's rank correlation on the rankings listed in Table 3.1, CatS susceptibility and cross-presentation efficiency were found to be positively correlated at the significance level of $P < 0.05$, supporting our hypothesis that faster antigen release within the phagosome results in more efficient cross-presentation. Note that one would not expect the rank order correspondence to be perfect because it is likely that other cathepsins, which may share some degree of substrate specificity with CatS, also play a role in antigen release towards cross-presentation.

Table 3.1. Linker modifications and resulting effects on cross-presentation

Name	Modification	Reference	CatS cleavage rank order	Cross-presentation rank order
Deleted	$(G_4S)_3$ deleted	-	7	7
Unchanged	-	-	4	4
C1	EKARVLAEAA inserted	(42)	2	1
C2	SSAESLK inserted	(43)	3	2
C3	NWVCAAKF inserted	(34)	6	5
C4	GILQINSR inserted	(34)	5	6
C5	QWLGAPVP inserted	(44)	1	3

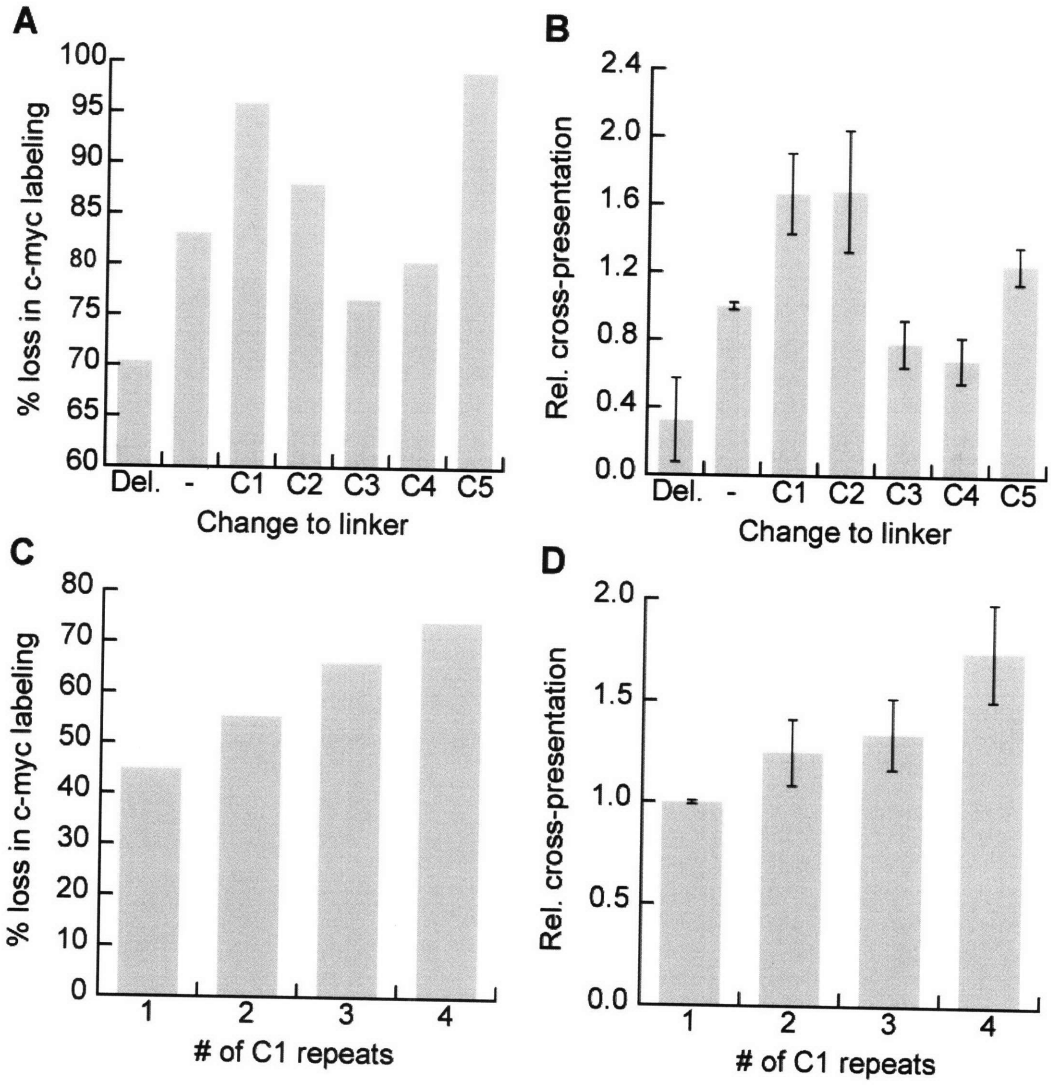

Figure 3.2, Correlation between linker susceptibility to CatS cleavage and cross-presentation efficiency.

A and C, Yeast surface-displaying N9V with different linkers (described in Table 3.1) were incubated with 50 ng (A) or 20 ng (C) of recombinant CatS for 15 min at 37°C. The percentage decrease in c-myc levels in comparison to yeast before CatS treatment was determined by flow cytometry.

B and D, The yeast samples with different linkers were added to DCs and assayed for the ability to stimulate IFNγ secretion in co-cultured T cells 24 h later. The results were normalized by the percentage of $IFN\gamma^+$ T cells stimulated by yeast with the unmodified linker (B) or a single insert of the C1 sequence (D). In (B), there were significant differences in surface display levels between constructs (as detected by flow cytometry, the mean expression levels in arbitrary units were 1677, 1258, 1526, 1323, 1430, 1853 & 1279 from left to right). Each yeast culture sample was mixed with wt yeast to normalize the delivered antigen dose to that of the lowest-expressing construct. This was unnecessary in (D) as the surface display levels were within 10% of each other. Error bars represent standard deviations between duplicate (B) or triplicate (D) wells.

In an attempt to further increase antigen release rates by CatS, we created constructs with tandem repeats of C1 and C2 sequences. Tandem repeats of C2 did not further enhance CatS susceptibility (not shown), but the rate of CatS cleavage increased with the number of tandem copies of C1 (Fig. 3.2C). Consistent with our hypothesis, there was a corresponding increase in cross-presentation efficiency (Fig. 3.2D).

3.4.4 Antigen released by CatS is Processed by Proteasomes

Yeast strains were created with chromosomally integrated expression cassettes for the constructs with the deleted $(G_4S)_3$ linker, with a single C1 insertion, and with four tandem C1 repeats, selected for being representative of the entire range of CatS susceptibilities. These yeast strains displayed the expected rank order of cross-presentation efficiency across a range of yeast to DC ratios: $(C1)_4$ > C1 > deleted (Fig. 3.3A). The differences in cross-presentation efficiency were largely diminished when the DCs were pretreated with a specific CatS inhibitor (10 μM Z-FL-COCHO) (Fig. 3.3A), showing that CatS cleavage was indeed primarily responsible for these differences. Since the disparities in cross-presentation efficiency were not completely eliminated, it is possible that other proteases may have played minor roles in antigen release; alternatively, CatS was not completely inhibited. The gains in cross-presentation efficiency with increased CatS susceptibility were not due to the vacuolar route becoming dominant; instead, cross-presentation of all three strains remained inhibited by lactacystin and unaffected or slightly improved by chloroquine (Fig. 3.3B), suggesting that the antigen released by CatS moved from the phagosome to the cytosol.

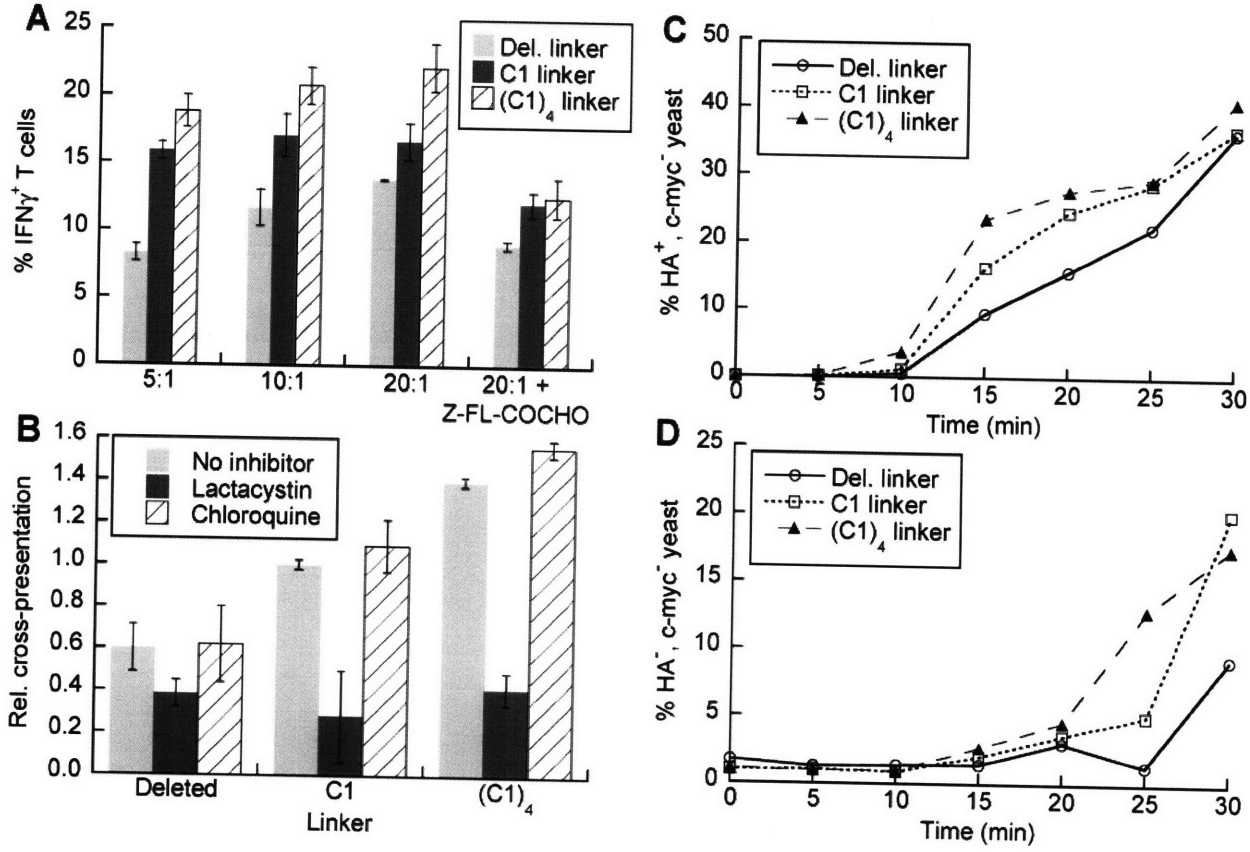

Figure 3.3, Comparison of different linkers suggest a time window for antigen release and implicate the phagosome-to-cytosol route.

A and B, Yeast strains surface-displaying N9V with different linkers were added to DCs at the indicated ratios (A) or at 20:1 (B) and assayed for the ability to stimulate IFNγ secretion in co-cultured T cells 24 h later. The antigen display levels varied by less than 10%. Z-FL-COCHO (10 μM, a concentration that did not significantly affect the peptide positive control), lactacystin (5 μM) or chloroquine (25 μM) were added to some wells an hour before the yeast were introduced. Error bars represent the standard deviations of duplicate wells.

C and D, At various time points after the yeast were added at a 2.5:1 ratio, the DCs were placed on ice and lysed with RIPA buffer. The yeast thus extracted were labeled for the presence of HA and c-myc epitopes and analyzed by flow cytometry after gating on forward and side scatter.

3.4.5 Evidence of a Time Window for Productive Antigen Release

With these integrated expression yeast strains, at least 98% of the yeast cells expressed the surface-displayed antigen (compared to ~75% for transformed yeast subject to plasmid loss), so antigen loss that occurred after phagocytosis could be clearly distinguished. We developed an assay for monitoring *in vivo* antigen processing involving lysing the DCs at various time points after phagocytosis was initiated, followed by labeling the released yeast with α-HA and α-c-myc antibodies. Antigen release by proteolytic cleavage of the linker C-terminal to the HA epitope (or less likely, cleavage of the antigenic peptide or the c-myc epitope) results in HA^+, $c\text{-}myc^-$ yeast. We observed that between 5 and 25 min post-phagocytosis, this population was largest with the $(C1)_4$ linker and smallest with the deleted linker (Fig. 3.3C). This is consistent with CatS attacking the linkers at different rates during this early stage of phagosomal maturation, and supports the notion that early proteolytic release was responsible for the variation in cross-presentation efficiency. During the first 20 min or so, very little antigen was released in a way that would cause the loss of both epitopes (Fig. 3.3D), such as disulfide bond reduction or enzymatic attack of the yeast cell wall, Aga1p or Aga2p. Between 25-30 min post-phagocytosis, the double-negative population started rising rapidly, suggesting that the phagosomes had fused with late endosomes or lysosomes that provided a more acidic environment and a larger complement of active proteases. The differences in antigen loss levels between the three strains diminished at these later time points, and presumably, all the yeast cells would eventually lose their attached antigen. This suggests that antigen release rates early in phagosomal maturation are key to cross-presentation efficiency; antigen released after the 25 min time point may be mostly degraded by lysosomal proteases rather than cross-presented.

3.4.6 Manipulating the Kinetics of Antigen Release Using Fluorescein-binding ScFvs

One of the earliest applications of yeast surface display was to perform directed evolution of a fluorescein-binding single chain variable fragment (scFv) of an antibody to select for mutants with increased affinity (23). The existence of a pool of mutants spanning over four orders of magnitude in dissociation rate provided the opportunity to manipulate antigen release kinetics in a manner distinct from proteolytic release. We first loaded yeast expressing these scFv mutants with fluorescein-tagged extended peptides, but the surface display levels of these scFvs were low and variable. We selected one scFv (4M3.12) to perform directed evolution, finding a combination of five mutations that increased the surface display level by 4-5 fold (HEAF3.12, see Appendix A.11). However, when these same mutations were made in other highly homologous scFvs, the surface display levels only increased 1-2 fold (not shown). Finally, we inverted the topology and loaded fluorescein-conjugated yeast with scFv-ARNLVPMVATVQGQN-c-myc fusion proteins, with the attendant advantage that the delivered antigen dose would be independent of the protein expression level. Four scFvs, with attributes listed in Table 3.2, were selected from the mutant pool to be produced as scFv-antigen fusions.

Table 3.2. Properties of fluorescein-binding scFvs

Name	Dissociation half-time at	
	pH 7.4, 25°C*	pH 5.4, 37°C
4M2.3	22 min	< 1 min
4M3.12	4.0 h	4.8 min
4M4.5	26 h	9.8 min
4M5.3	5.7 days	1.9 h

*From (23)

We developed a mathematical model based on the schematic in Fig. 3.4A to predict the cross-presentation outcome. In this model, the scFv-antigen fusion dissociates from yeast cells in

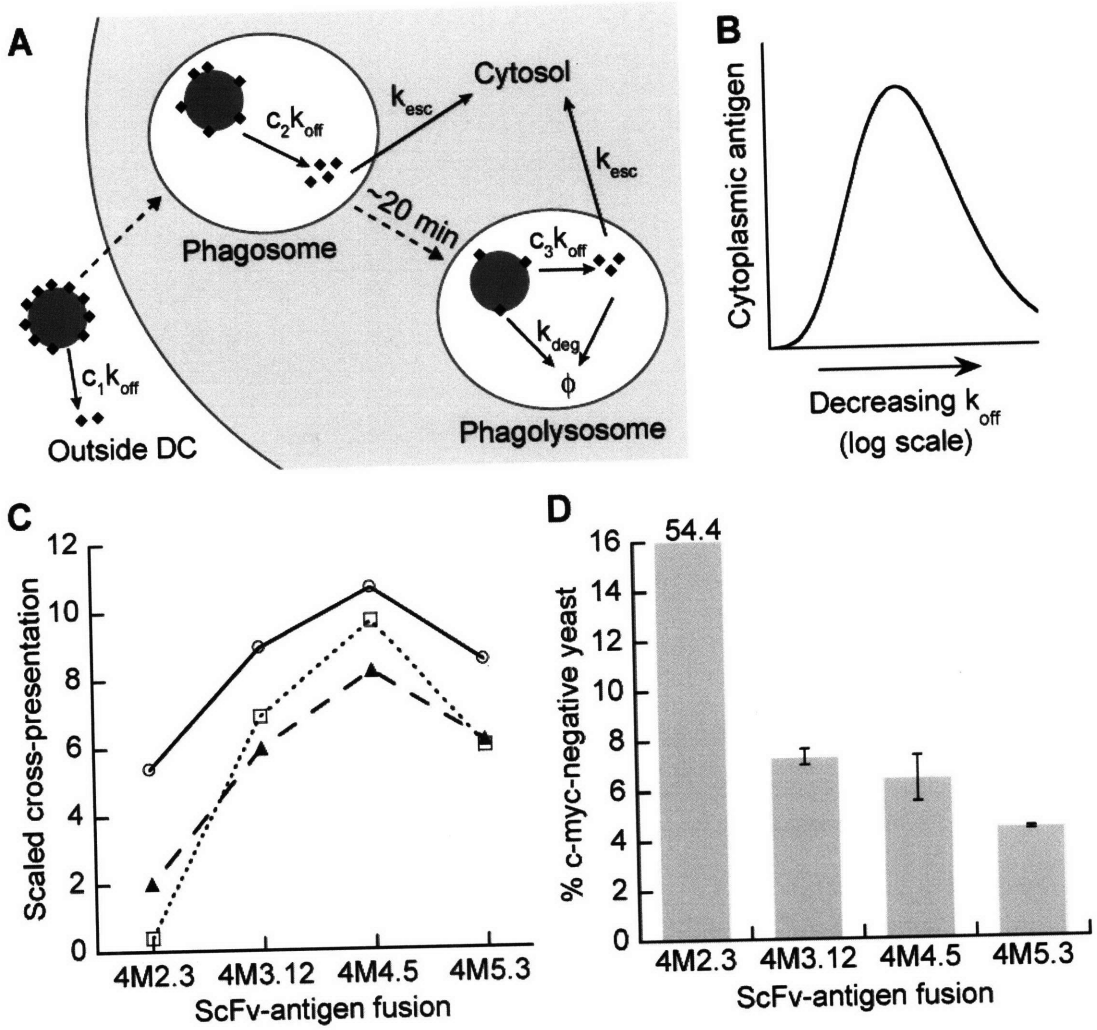

Figure 3.4, Mathematical modeling and experimental results for cross-presentation of antigen attached to yeast cells by scFv binding.

A, Schematic of a simple model describing antigen release, export and degradation before and after phagocytosis. The unbroken arrows represent first-order processes with associated rate constants that make up an ordinary differential equation-based model.

B, A representative plot of cytoplasmic antigen versus k_{off} when the equations were solved with reasonable parameter values (pre-phagocytosis time of 30 min, $c_1 = 4$, $c_2 = 50$, $c_3 = 100$, $k_{esc} = 0.02\ min^{-1}$, $k_{deg} = 0.1\ min^{-1}$).

C, Fluorescein-conjugated yeast were incubated with culture supernatants containing secreted scFv-antigen fusion proteins, washed, and added to DCs to perform cross-presentation assays. The results of three separate experiments (represented by the three line/marker combinations) were scaled such that unloaded fluorescein-conjugated yeast gave a result of 1 whereas a 1 μM extended peptide positive control gave a result of 100.

D, Fluorescein-conjugated yeast loaded with scFv-antigen were incubated with DCs for 15 min, after which the DCs were placed on ice and lysed with RIPA buffer. The released yeast cells were analyzed for the presence of the c-myc epitope tag by flow cytometry.

three stages, the first encompassing the handling steps and time lag before phagocytosis by DCs, the second being the estimated 20 min window in phagosome maturation before the transition into a phagosolysosome, the third stage. We made the simplifying approximation that for all scFvs, the dissociation rates during these three stages could each be expressed as a proportionality constant multiplied by the measured dissociation rate at neutral pH and 25°C (k_{off}). ScFv-antigen released prior to phagocytosis is assumed to be lost, whereas scFv-antigen released in the phagosome escapes to the cytosol at a rate k_{esc}. When the phagosome matures into a phagolysosome, proteases degrade both yeast-bound and free antigen with the rate constant k_{deg}. Protease activity that could cause antigen release rather than destruction of the epitope was neglected. We assumed that the final level of cross-presentation is proportional to the amount of antigen that escapes to the DC cytosol. The solution to the ordinary differential equations comprising this model describes a bell-shaped curve for cytosolic antigen versus k_{off} (Fig. 3.4B). The existence of a k_{off} value optimal for cross-presentation was a property of the model that was robust to simultaneous parameter variations spanning three orders of magnitude. At very high k_{off} values, most of the antigen is lost prior to phagocytosis, whereas at very low k_{off} values, little antigen is freed in the phagosome and the majority is degraded in the phagolysosome.

If antigen release rates in the phagosome did not affect cross-presentation, we would expect to see cross-presentation efficiencies rising monotonically with decreasing k_{off} due to the increased dose taken up by the DCs. Instead, the results of three independent cross-presentation experiments confirmed the existence of the model-predicted optimum, with the femtomolar fluorescein binder 4M5.3 resulting in less cross-presentation than the lower affinity 4M4.5 (Fig. 3.4C). When the yeast were extracted from lysed DCs 15 min post-phagocytosis, antigen loss was shown to decrease with increasing affinity (Fig. 3.4D). Although the dissociation half-time

of 4M5.3 is almost two hours *in vitro* even at pH 5.4, 37°C, proteolysis by CatS or other early phagosomal proteases contributed to a baseline level of antigen release not accounted for in the model; hence, the 4M5.3-antigen fusion gave rise to higher than expected levels of cross-presentation.

3.5 Discussion

We have shown by three distinct types of experiments that antigen release kinetics from phagoctosed yeast cells influences the efficiency of cross-presentation occurring via the phagosome-to-cytosol route. First, protease-accessible antigen exposed on the yeast external surface is cross-presented much more efficiently than antigen trapped inside the tough cell wall. Second, increasing the susceptibility to CatS cleavage of the linker between the antigen and its cell wall anchor resulted in increased cross-presentation efficiency. Third, there exists an optimal affinity for antibody fragments used to attach antigen to the yeast surface, with extremely low dissociation rates being detrimental for cross-presentation efficiency.

Although this evidence was obtained with yeast, we believe that the hypothesis applies to other particulate vaccines, since antigen release in the phagosome logically precedes phagosome-to-cytosol translocation. Indeed, in one of the earliest demonstrations of cross-presentation, it was observed that ovalbumin passively adsorbed to latex beads was more efficiently cross-presented than ovalbumin conjugated to the same beads, although no explanation was put forth at that time (29). Particulate vaccines have advantages over soluble vaccines in that they are not diluted by diffusion, and are targeted to phagocytic professional antigen-presenting cells. It behooves particulate vaccine developers to take antigen release kinetics into consideration and to perform research into methods of optimizing these kinetics for their vaccine systems. An alternative strategy is to bypass the requirement for freeing antigen in the phagosome, as illustrated by microparticles that released antigen directly in the cytosol (30).

Our analysis of antigen loss occurring post-phagocytosis suggests that there exists a limited time window for productive antigen release. In the case of yeast surface display, it appears that antigen freed after the 25 min time point did not contribute significantly to cross-

presentation. The 25 min time point coincided with a sudden rise in antigen loss by means other than cleavage of the linker, possibly indicating phagosome fusion with late endosomes or lysosomes. With macrophages that had phagocytosed yeast, the phagosomal pH took 20-25 minutes to decrease to a minimum of about 5.0 (31). A time course analysis of protease activity in murine DC phagosomes showed that Cathepsins B, L and Z jumped in activity between 20 and 30 min after phagocytosis (28). On the other hand, Savina et al. recently showed that phagosomes in murine DCs do not acidify significantly for 3 h (32). The connection between phagosome acidification and acquisition of proteolytic activity remains unclear, as well as how these may be affected by DC status and the nature of the particle.

The three constructs with different linkers that we compared displayed the greatest variation in antigen loss during the 10-20 min window, so it is likely that the major source of N9V peptide ultimately cross-presented was antigen freed during this time frame. With endocytosed antigen, it has been suggested that antigen destined for cross-presentation exited early from the endosomal pathway; the bulk of the antigen was colocalized with late endosomal/lysosomal markers after 25 min but did not contribute to cross-presentation (33). In the same study by Palliser et al., aggregated protein antigen was observed to be cross-presented almost ten times less efficiently than the monomeric form. A possible explanation for this result is that aggregates that were not dispersed soon after uptake could not egress to the cytosol and were not cross-presented.

The narrow time window available for antigen release suggests that CatS, unusual among cathepsins for being active at up to neutral pHs, may play a special role in phagosome-to-cytosol cross-presentation. Roles for CatS in the vacuolar route of cross-presentation (30) and class II presentation (34) have previously been identified.

In our mathematical model, after 20 min of phagosome maturation, proteolytic degradation of antigen competed with antigen export into the cytosol. Thus, only a small fraction of antigen released after 25 min or so contributed to cross-presentation. However, we further speculate that phagolysosome formation may in some way close off the means for antigen egress to the cytosol, thus imposing another limit on the time window for productive antigen release. Teleologically, it would make sense for the class II epitopes generated in phagolysosomes to be retained rather than exported to the cytosol. The nature of this phagosomal "pore" remains a mystery, although it appears to have a size limit, with 40 K but not 500 K dextran being translocated (35). Several years ago, at least three studies provided evidence that membranes of the endoplasmic reticulum (ER) contribute to the nascent phagosome (36-38), leading to speculation that ER-resident proteins like the Sec61 translocon or Derlp (39) may be responsible. ER-phagosome fusion has since been disputed (40), but Cresswell et. al recently demonstrated the involvement of ER retrotranslocation mechanisms in cross-presentation (41). Solving this mystery would represent a significant advance in the state-of-the-art and may permit the development of techniques to either increase the rate of antigen export to the cytosol or extend the time window for which this mechanism is active. Increasing the transport of antigen to the cytosol in this manner, combined with more complete antigen release during the critical time window, could lead to the development of more effective vaccines designed to raise cellular immunity against virus-infected cells and cancer cells.

3.6 References

1. Morse, M. A., S. Chui, A. Hobeika, H. K. Lyerly, and T. Clay. 2005. Recent developments in therapeutic cancer vaccines. *Nat Clin Pract Oncol* 2: 108-113.
2. Lollini, P.-L., F. Cavallo, P. Nanni, and G. Forni. 2006. Vaccines for tumour prevention. *Nat Rev Cancer* 6: 204-216.
3. Srivastava, P. K. 2006. Therapeutic cancer vaccines. *Current Opinion in Immunology Lymphocyte development / Tumour immunology* 18: 201-205.
4. McMichael, A. J. 2006. HIV VACCINES. *Annual Review of Immunology* 24: 227-255.
5. Shiina, M., and B. Rehermann. 2006. Hepatitis C vaccines: Inducing and challenging memory T cells. *Hepatology* 43: 1395-1398.
6. Koelle, D. M. 2006. Vaccines for herpes simplex virus infections. *Curr Opin Investig Drugs* 7: 136-141.
7. Gattinoni, L., D. J. Powell, S. A. Rosenberg, and N. P. Restifo. 2006. Adoptive immunotherapy for cancer: building on success. 6: 383-393.
8. Devin B. Lowe, M. H. S., Ronald C. Kennedy,. 2006. DNA vaccines: Successes and limitations in cancer and infectious disease. *Journal of Cellular Biochemistry* 98: 235-242.
9. Brinkman, J. A., S. C. Fausch, J. S. Weber, and W. M. Kast. 2004. Peptide-based vaccines for cancer immunotherapy. *Expert Opinion on Biological Therapy* 4: 181-198.
10. Kovacsovics-Bankowski, M., and K. L. Rock. 1995. A phagosome-to-cytosol pathway for exogenous antigens presented on MHC class I molecules. *Science* 267: 243-246.
11. Pfeifer, J. D., M. J. Wick, R. L. Roberts, K. Findlay, S. J. Normark, and C. V. Harding. 1993. Phagocytic processing of bacterial antigens for class I MHC presentation to T cells. *Nature* 361: 359-362.
12. Bachmann, M. F., A. Oxenius, H. Pircher, H. Hengartner, P. A. Ashton-Richardt, S. Tonegawa, and R. M. Zinkernagel. 1995. TAP1-independent loading of class I molecules by exogenous viral proteins. *Eur J Immunol* 25: 1739-1743.
13. Rock, K. L., and L. Shen. 2005. Cross-presentation: underlying mechanisms and role in immune surveillance. *Immunological Reviews* 207: 166-183.
14. Stubbs, A. C., K. S. Martin, C. Coeshott, S. V. Skaates, D. R. Kuritzkes, D. Bellgrau, A. Franzusoff, R. C. Duke, and C. C. Wilson. 2001. Whole recombinant yeast vaccine activates dendritic cells and elicits protective cell-mediated immunity. *Nat Med* 7: 625-629.
15. Lu, Y., D. Bellgrau, L. D. Dwyer-Nield, A. M. Malkinson, R. C. Duke, T. C. Rodell, and A. Franzusoff. 2004. Mutation-selective tumor remission with Ras-targeted, whole yeast-based immunotherapy. *Cancer Res* 64: 5084-5088.
16. Barron, M. A., N. Blyveis, S. C. Pan, and C. C. Wilson. 2006. Human Dendritic Cell Interactions with Whole Recombinant Yeast: Implications for HIV-1 Vaccine Development. *J Clin Immunol* 26: 251-264.

17. Breinig, F., T. Heintel, A. Schumacher, A. Meyerhans, and M. J. Schmitt. 2003. Specific activation of CMV-primed human T lymphocytes by cytomegalovirus pp65 expressed in fission yeast. *FEMS Immunology and Medical Microbiology* 38: 231-239.

18. Wadle, A., G. Held, F. Neumann, S. Kleber, B. Wuellner, A. M. Asemissen, B. Kubuschok, C. Scheibenbogen, T. Breinig, A. Meyerhans, and C. Renner. 2006. Cross-presentation of HLA class I epitopes from influenza matrix protein produced in Saccharomyces cerevisiae. *Vaccine* 24: 6272-6281.

19. Underhill, D. M. 2003. Macrophage recognition of zymosan particles. *J Endotoxin Res* 9: 176-180.

20. Boder, E. T., and K. D. Wittrup. 1997. Yeast surface display for screening combinatorial polypeptide libraries. *Nat Biotechnol* 15: 553-557.

21. Colby, D. W., B. A. Kellogg, C. P. Graff, Y. A. Yeung, J. S. Swers, and K. D. Wittrup. 2004. Engineering Antibody Affinity by Yeast Surface Display. *Methods Enzymol.*: 348-358.

22. Sikorski, R. S., and P. Hieter. 1989. A System of Shuttle Vectors and Yeast Host Strains Designed for Efficient Manipulation of DNA in Saccharomyces cerevisiae. *Genetics* 122: 19-27.

23. Boder, E. T., K. S. Midelfort, and K. D. Wittrup. 2000. Directed evolution of antibody fragments with monovalent femtomolar antigen-binding affinity. *Proc Natl Acad Sci U S A* 97: 10701-10705.

24. Robinson, A. S., V. Hines, and K. D. Wittrup. 1994. Protein disulfide isomerase overexpression increases secretion of foreign proteins in Saccharomyces cerevisiae. *Biotechnology (N Y)* 12: 381-384.

25. Trivedi, D., R. Y. Williams, R. J. O'Reilly, and G. Koehne. 2005. Generation of CMV-specific T lymphocytes using protein-spanning pools of pp65-derived overlapping pentadecapeptides for adoptive immunotherapy. *Blood* 105: 2793-2801.

26. Accapezzato, D., V. Visco, V. Francavilla, C. Molette, T. Donato, M. Paroli, M. U. Mondelli, M. Doria, M. R. Torrisi, and V. Barnaba. 2005. Chloroquine enhances human CD8+ T cell responses against soluble antigens in vivo. *J. Exp. Med.* 202: 817-828.

27. Pillay, C. S., E. Elliott, and C. Dennison. 2002. Endolysosomal proteolysis and its regulation. *Biochem J* 363: 417-429.

28. Lennon-Dumenil, A.-M., A. H. Bakker, R. Maehr, E. Fiebiger, H. S. Overkleeft, M. Rosemblatt, H. L. Ploegh, and C. Lagaudriere-Gesbert. 2002. Analysis of Protease Activity in Live Antigen-presenting Cells Shows Regulation of the Phagosomal Proteolytic Contents During Dendritic Cell Activation. *J. Exp. Med.* 196: 529-540.

29. Kovacsovics-Bankowski, M., K. Clark, B. Benacerraf, and K. Rock. 1993. Efficient Major Histocompatibility Complex Class I Presentation of Exogenous Antigen Upon Phagocytosis by Macrophages. *Proc Natl Acad Sci U S A* 90: 4942-4946.

30. Shen, L., L. J. Sigal, M. Boes, and K. L. Rock. 2004. Important Role of Cathepsin S in Generating Peptides for TAP-Independent MHC Class I Crosspresentation In Vivo. *Immunity* 21: 155-165.

31. Geisow, M., P. D'Arcy Hart, and M. Young. 1981. Temporal changes of lysosome and phagosome pH during phagolysosome formation in macrophages: studies by fluorescence spectroscopy. *J. Cell Biol.* 89: 645-652.

32. Savina, A., C. Jancic, S. Hugues, P. Guermonprez, P. Vargas, I. C. Moura, A.-M. Lennon-Dumenil, M. C. Seabra, G. Raposo, and S. Amigorena. 2006. NOX2 Controls Phagosomal pH to Regulate Antigen Processing during Crosspresentation by Dendritic Cells. *Cell* 126: 205-218.

33. Palliser, D., E. Guillen, M. Ju, and H. N. Eisen. 2005. Multiple Intracellular Routes in the Cross-Presentation of a Soluble Protein by Murine Dendritic Cells. *J Immunol* 174: 1879-1887.

34. Pluger, E. B., M. Boes, C. Alfonso, C. J. Schroter, H. Kalbacher, H. L. Ploegh, and C. Driessen. 2002. Specific role for cathepsin S in the generation of antigenic peptides in vivo. *Eur J Immunol* 32: 467-476.

35. Rodriguez, A., A. Regnault, M. Kleijmeer, P. Ricciardi-Castagnoli, and S. Amigorena. 1999. Selective transport of internalized antigens to the cytosol for MHC class I presentation in dendritic cells. *Nat Cell Biol* 1: 362-368.

36. Gagnon, E., S. Duclos, C. Rondeau, E. Chevet, P. H. Cameron, O. Steele-Mortimer, J. Paiement, J. J. Bergeron, and M. Desjardins. 2002. Endoplasmic reticulum-mediated phagocytosis is a mechanism of entry into macrophages. *Cell* 110: 119-131.

37. Guermonprez, P., L. Saveanu, M. Kleijmeer, J. Davoust, P. Van Endert, and S. Amigorena. 2003. ER-phagosome fusion defines an MHC class I cross-presentation compartment in dendritic cells. *Nature* 425: 397-402.

38. Ackerman, A. L., C. Kyritsis, R. Tampe, and P. Cresswell. 2003. Early phagosomes in dendritic cells form a cellular compartment sufficient for cross presentation of exogenous antigens. *Proc Natl Acad Sci U S A* 100: 12889-12894.

39. Guermonprez, P., and S. Amigorena. 2005. Pathways for antigen cross presentation. *Springer Semin Immunopathol* 26: 257-271.

40. Touret, N., P. Paroutis, M. Terebiznik, R. E. Harrison, S. Trombetta, M. Pypaert, A. Chow, A. Jiang, J. Shaw, and C. Yip. 2005. Quantitative and Dynamic Assessment of the Contribution of the ER to Phagosome Formation. *Cell* 123: 157-170.

41. Ackerman, A. L., A. Giodini, and P. Cresswell. 2006. A Role for the Endoplasmic Reticulum Protein Retrotranslocation Machinery during Crosspresentation by Dendritic Cells. *Immunity* 25: 607-617.

42. Thurmond, R. L., S. Sun, C. A. Sehon, S. M. Baker, H. Cai, Y. Gu, W. Jiang, J. P. Riley, K. N. Williams, J. P. Edwards, and L. Karlsson. 2004. Identification of a Potent and Selective Noncovalent Cathepsin S Inhibitor. *J Pharmacol Exp Ther* 308: 268-276.

43. Zaliauskiene, L., S. Kang, K. Sparks, K. R. Zinn, L. M. Schwiebert, C. T. Weaver, and J. F. Collawn. 2002. Enhancement of MHC Class II-Restricted Responses by Receptor-Mediated Uptake of Peptide Antigens. *J Immunol* 169: 2337-2345.

44. Baumgrass, R., M. K. Williamson, and P. A. Price. 1997. Identification of peptide fragments generated by digestion of bovine and human osteocalcin with the lysosomal proteinases cathepsin B, D, L, H, and S. *J Bone Miner Res* 12: 447-455.

Chapter 4

Inducing Efficient Cross-Priming using Antigen-Coated Yeast Particles[2]

4.1 Abstract

Saccharomyces cerevisiae stimulates dendritic cells and represents a promising candidate for cancer vaccine development. Effective cross-presentation of antigen delivered to dendritic cells is necessary for successful induction of cellular immunity. Here, we present a yeast-based vaccine approach that is independent of yeast's ability to express the chosen antigen, which is instead produced separately and conjugated to the yeast cell wall. The conjugation method is site-specific (based on the SNAP-tag) and designed to facilitate antigen release in the dendritic cell phagosome and subsequent translocation for cross-presentation. We demonstrate that non-site-specific chemical conjugation of the same protein hinders cross-presentation. Phagosomal antigen release was further expedited through the insertion of the invariant chain ectodomain as a linker, which is rapidly cleaved by Cathepsin S. The dose of delivered antigen was increased in several ways: by using yeast strains with higher surface amine densities, by using yeast hulls (cell wall fragments) instead of whole cells, and by conjugating multiple layers of antigen. The novel multi-layer conjugation scheme takes advantage of Sfp phosphopantetheinyl transferase and remains site-specific; it enables the antigen dose to grow linearly with the number of layers. We show that whole yeast cells coated with one layer of the cancer-testis antigen NY-ESO-1 and yeast hulls bearing three layers were able to cross-prime naïve $CD8^+$ T cells *in vitro*, with the latter resulting in higher frequencies of antigen-specific cells after ten days. This cross-

[2] Major portions of this chapter will shortly be published in:
Howland, S. W., Tsuji, T., Gnjatic, S., Ritter, G., Old, L. J. and K. D. Wittrup, 2008. Inducing Efficient Cross-Priming using Antigen-Coated Yeast Particles. J Immunother 31.

presentation-efficient antigen conjugation scheme is not limited to yeast and can readily be applied towards the development of other particulate vaccines.

4.2 Introduction

The goal of cancer vaccination is to elicit a tumor-protective immune response against cancer-associated antigens, in order to defeat cancer in much the same way as we have defeated many infectious diseases. However, despite the leaps made in understanding of cellular immune function and tumor immunology, objective response rates in cancer vaccine clinical trials have been disappointingly low (1). Many early generation cancer vaccines were simply peptide or protein injections, sometimes paired with a cytokine adjuvant. With respect to infectious diseases, it has been pointed out that modern peptide or protein vaccines are problematic in that they are often considerably less immunogenic than primitive vaccines made from live or dead organisms (2). New, more immunogenic vaccine approaches, including ones that more closely mimic pathogens, are required in the field of cancer immunotherapy.

One such promising new approach is the use of recombinant *S. cerevisiae* yeast expressing antigen in the cytosol (3-10) or on the cell wall (11, 12). With its fungal cell wall, yeast cells are avidly phagocytosed and induce maturation of dendritic cells (DCs) and the secretion of Th1-type cytokines (3, 5-10) *S. cerevisiae* is not pathogenic and despite its potent effect on the innate immune system, subcutaneous administration of heat-killed yeast did not exhibit dose-limiting toxicity in phase I clinical trials (10). The adjuvant properties of yeast are only half the story, as successful vaccine development also requires that a sufficient dose of antigen be delivered to the DCs in a way that facilitates processing and MHC class I presentation (i.e. cross-presentation).

We have previously shown that timely antigen release from the yeast cell upon phagocytosis by DCs is critical for efficient cross-presentation (12). In that study, the extended peptide antigen was recombinantly expressed on the cell wall as a fusion to the mating adhesion

receptor subunit Aga2p, in a technique termed yeast surface display (13). Yeast surface-displayed antigen was cross-presented much more efficiently than antigen expressed in the yeast cytosol, and cross-presentation could be further enhanced by inserting linkers susceptible to Cathepsin S (CatS) cleavage between the antigen and Aga2p (12). While this model system was useful for studying the impact of phagosomal antigen release kinetics upon cross-presentation, its utility as an immunotherapy vaccine candidate is limited by the reliance on yeast expression levels for antigen delivery. For many reasons, it is often desirable to immunize with a full-length protein as opposed to a known peptide epitope, and yeast surface display levels of the former may not be adequate or optimal. We therefore set out to develop a system for attaching soluble protein antigens to the yeast cell wall, so as to decouple antigen dose from yeast expression levels while retaining a desirable antigen release profile upon DC phagocytosis.

We focused our attentions on the highly immunogenic cancer-testis antigen, NY-ESO-1, which has been widely tested in cancer vaccine clinical trials (reviewed in (14) and (15)). NY-ESO-1 is surface-displayed very poorly by yeast, and although a combination of rational design and directed evolution approaches identified a mutant that has a 100-fold improved display level (16), the number of copies per yeast cell still did not reach peptide display levels. In contrast, NY-ESO-1 can be expressed solubly and at high yield in *E. coli* when fused to maltose-binding protein (MBP, unpublished observation by A. Piatesi).

Our challenge was to conjugate bacterially expressed NY-ESO-1 to the yeast cell wall, in a manner facilitating release of the antigenic domain in the DC phagosome. Insertion of a CatS-susceptible linker, which worked admirably with yeast surface display, would likely be foiled by conventional chemical conjugation methods where the reaction can occur at multiple amino acid positions along the fusion protein. For example, a reaction scheme based on primary amines

might bind a lysine residue of NY-ESO-1 directly to the cell wall, thus preventing release when the CatS-susceptible linker is cleaved. Consequently, we turned to site-specific conjugation methods where the reaction is mediated by a protein and is restricted to a known amino acid residue.

4.3 Materials and Methods

4.3.1 Reagents

Recombinant human cytokines were obtained from R & D Systems (Minneapolis, MN). Monoclonal α-NY-ESO-1 antibody, clone E978, was obtained from Sigma-Aldrich (St. Louis, MO). Dye-conjugated monoclonal antibodies against CD8 and DC markers were from BD Biosciences (San Jose, CA) except for α-CD40 (Calbiochem, Gibbstown, NJ), α-CD86 (Chemicon, Billerica, MA) and α-HLA-DR (Leinco, St. Louis, MO).

4.3.2 Cells

Human HLA-A*0201 monocytes purified by negative magnetic cell sorting from leukapheresis packs were purchased from Biological Specialty Corporation (Colmar, PA). The monocytes were cryopreserved in 90% fetal bovine serum (FBS), 10% DMSO and aliquots were thawed as needed. The monocytes were cultured in C10 medium—RPMI-1640 with 10% FBS, 2 mM L-glutamine, 10 mM HEPES, 1 mM sodium pyruvate, 1× non-essential amino acids, 50 μM β-mercaptoethanol and Primocin (InvivoGen, San Diego, CA)—supplemented with 1000 U/ml each of IL-4 and GM-CSF in 6-well plates (4-5 × 10^6 monocytes in 2.5 ml medium per well). Each well was fed with 0.5 ml cytokine-supplemented C10 on days 2 and 4; on day 5 or 6, the floating and loosely adherent immature monocyte-derived DCs were harvested by gentle resuspension.

A human $CD8^+$ T cell line specifically recognizing the cytomegalovirus-derived peptide NLVPMVATV (N9V) in the context of HLA-A*0201 was obtained from ProImmune (Oxford, UK). The vials of frozen cells were thawed and cultured overnight in RPMI-1640 with 10% FBS, 5 ng/ml IL-2 and Primocin before use.

PBMCs were isolated by Ficoll-Paque density gradient centrifugation from HLA-A2 buffy coats (Research Blood Components, Brighton, MA). A portion of the PBMCs from each donor were cryopreserved in 90% FBS, 10% DMSO while the rest were subjected to magnetic cell separation by an autoMACS Separator (Miltenyi Biotec, Auburn, CA). CD8 and CD45RO microbeads (Miltenyi) were used sequentially in positive and negative selection modes according to the manufacturer's protocol to isolate $CD8^+$ $CD45RO^-$ cells.

4.3.3 Yeast

S. cerevisiae strain BJ5464α (ATCC, Manassas, VA) was grown in YPD medium (1% yeast extract, 2% peptone and 2% dextrose) in a 30°C shaker. Plasmids for yeast surface display were constructed based on pCTCON2 (17), and the shuttle vector pRS304 (18) was used to integrate expression cassettes into EBY100 (13), a yeast strain that expresses Aga1p under galactose induction. In particular, the strain SWH100 was created from EBY100 by integrating an Aga2p-HA expression cassette, constructed by substituting two stop codons between the *Pst*I and *Bam*HI sites in pCTCON2. SWH100 was grown to mid-log phase in SD-CAA medium (2% dextrose, 0.67% yeast nitrogen base, 0.5% casamino acids, 0.1 M sodium phosphate, pH 6.0) at 30°C and induced for 12 h at 30°C in YPG (1% yeast extract, 2% peptone and 2% galactose). Yeast cell densities were estimated by measuring the absorbance at 600 nm, with an OD of 1 taken to be 1×10^7 cells/ml.

4.3.4 MBP fusion proteins

Plasmids for *E. coli* expression of MBP fusion proteins were constructed using pMAL-c2x (New England Biolabs, Ipswich, MA) as the vector backbone. The plasmid for expressing MSCE was constructed by inserting sequences encoding the SNAP tag (*Ava*I/*Eco*RI; from

pSS26b, Covalys, Witterswil, Switzerland), the CatS-susceptible linker $(C1)_4$ and the CMV-derived peptide ARNLVPMVATVQGQN (*Eco*RI/*Bam*HI; from pCT-$(C1)_4$-N9V (12)), and the CS variant of NY-ESO-1, with C to S mutations at positions 75, 76 and 78 (*Bam*HI/*Hind*III; from pCT-NY-ESO-CS (16)). To express MS74NEY2, further modifications included replacing the $(C1)_4$ coding sequence with that of aa 73-207 of human CD74 (*Eco*RI/*Nhe*I; from cDNA clone LIFESEQ1001730, Open Biosystems, Huntsville, AL) and C-terminal insertion of a sequence encoding TVQL-$(G_4S)_3$-DSLEFIASKLA-H_6 (ybbR tag (19) is underlined).

Plasmid-bearing BL21(DE3)-RIPL bacteria (Stratagene, La Jolla, CA) in 1 L LB broth were induced at an OD_{600} of 0.7 with 0.3 mM isopropyl-β-D-thiogalactoside for 4-6 h at 20°C. The cell pellet was frozen, thawed, resuspended in 25 ml of the appropriate column buffer containing Complete Protease Inhibitor Cocktail (Roche Applied Science, Indianapolis, IN) and lysed by sonication. For fusion proteins lacking a His_6 tag, the cell lysate was clarified by centrifugation (20000 × g, 30 min, 4°C) and loaded onto an amylose resin (New England Biolabs) column equilibrated with amylose resin buffer (AR buffer; 20 mM Tris-HCl pH 7.4, 200 mM NaCl, 1 mM DTT, 1 mM EDTA). The column was washed with 50 column volumes (CV) of AR buffer containing 0.1% Triton X-114 (Sigma-Aldrich; to reduce endotoxin content (20)), followed by 5 CV of AR buffer and eluted with 5 CV of AR buffer containing 10 mM maltose. The eluate was further subjected to size exclusion chromatography (Superdex 200 10/300 GL, GE Healthcare, Piscataway, NJ) to purify full-length protein. For fusion proteins containing a C-terminal His_6 tag, the clarified cell lysate was loaded onto a TALON resin (Clontech, Mountain View, CA) column equilibrated with Talon buffer (20 mM Tris-HCl pH 7.4, 20 mM NaCl, 5 mM β-mercaptoethanol). The column was washed with 10 CV Talon buffer and eluted with 5 CV Talon buffer with 150 mM imidazole. The eluate was then subjected to

amylose resin affinity chromatography as described above. For more thorough endotoxin removal, the purified protein used in the *in vitro* immunization and DC maturation experiments (see below) was treated with Polymyxin B-agarose (Sigma-Aldrich).

4.3.5 SNAP-tag conjugation to yeast

Yeast cells were UV-irradiated (2 × 1000 J/m^2 in a Stratagene Stratalinker), washed 5× with PBS + 0.01% CHAPS (the detergent reduces yeast adherence to tube walls) and once with dimethylformamide (DMF). A pellet of 1 OD.ml or 10^7 yeast (or the equivalent amount of yeast hulls) was resuspended in 10 µl DMF containing 0.2 mg BG-GLA-NHS (Covalys), shaken at 30°C for 2 h and washed 3× with PBS + 0.1% bovine serum albumin (BSA). The BG-modified yeast was then resuspended in 0.4 ml PBS and 0.1 ml of 60 µM SNAP-tagged fusion protein (dissolved in AR buffer with 10 mM maltose) and rotated at 30°C for 5 h. The yeast was washed at least twice with PBS + 0.1% BSA before use. Conjugation levels were monitored by flow cytometry (e.g. labeling with α-NY-ESO-1 followed by Alexa Fluor 488-conjugated goat α-mouse antibody).

4.3.6 Conjugation to yeast by reductive amination

2.5 OD.ml of UV-irradiated BJ5464α yeast was washed thrice and resuspended in 450 µl 0.1 M sodium acetate pH 5.5 buffer. After the addition of 50 µl 100 mM $NaIO_4$ dissolved in the same buffer, the yeast was incubated on ice for 20 min and then washed twice with 1 ml sodium acetate buffer. The yeast was resuspended in 200 µl 50 µM MSCE protein that had been buffer-exchanged into PBS + 1 mM DTT. $NaCNBH_3$ (2 µl of a 1 M solution in 10 mM NaOH) was added and the tube was rotated at 4°C for three days.

4.3.7 N9V cross-presentation assay

Immature monocyte-derived DCs were seeded in 96-well round bottom plates with 2×10^5 DCs in 200 µl cytokine-supplemented C10 medium per well. Yeast cells or yeast hulls were added to the DCs at the indicated ratios; after 24 h, half the medium was replaced by 100 µl of 0.7 - 1×10^6 cells/ml suspension of N9V/HLA-A*0201-specific T cells. Four hours later, the cells in each well were transferred to tubes to perform an IFNγ secretion assay (Miltenyi) according to the manufacturer's protocol. Briefly, the cells were labeled for 5 min with a bispecific antibody that captures secreted IFNγ, incubated in medium for 45 min at 37°C, and labeled with α-CD8-FITC and α-IFNγ-PE. The fraction of $CD8^+$ cells that were also $IFN\gamma^+$ was determined by flow cytometry, with the gate for IFNγ fluorescence set such that the negative control test (no stimulus added to the DCs) gave a result of 0.5% or lower.

4.3.8 ELISpot assay

Monocytes were isolated by CD14 magnetic cell sorting (Miltenyi) from the PBMCs of a healthy HLA-Cw3 donor and differentiated into DCs by culturing for 6 days in the presence of GM-CSF and IL-4. DCs were pulsed overnight with NY-ESO-$1_{92\text{-}100}$ peptide or antigen-coated yeast (20 yeast per DC). The DCs were washed and seeded at 5×10^4 cells/well in a mixed cellulose ester membrane filter plate (Millipore, Billerica, MA) pre-coated with α-IFNγ (1-D1K, Mabtech, Mariemont, OH) together with the indicated number of C5 cells. C5 is an HLA-Cw3-restricted $CD8^+$ T cell clone recognizing NY-ESO-$1_{92\text{-}100}$ (21). After 24 h of co-culture, the plate was developed with biotinylated α-IFNγ (7-B6-1, Mabtech), streptavidin-alkaline phosphatase conjugate (Roche) and BCIP/NBT substrate (Sigma) for evaluation with a CTL ImmunoSpot Analyzer.

4.3.9 CatS cleavage time course

For each time point, 0.2 OD.ml of antigen-conjugated yeast was resuspended in 100 µl AR buffer. Recombinant CatS solution (Calbiochem; 20 ng in 100 µl AR buffer) was added and each tube was incubated at 37°C for the indicated time before the yeast was washed with cold PBS + 0.1% BSA. The yeast was labeled with α-NY-ESO-1 followed by Alexa Fluor 488-conjugated goat α-mouse IgG prior to analysis by flow cytometry.

4.3.10 Multi-layer conjugation

Sfp phosphopantetheinyl transferase was produced as described by Yin et. al (19) except that BL21(DE3)-RIPL was used as the expression strain and the bacteria were lysed by sonication. BG-CoA was synthesized by reacting 1 mg (2.0 µmoles) of BG-maleimide (Covalys) dissolved in 0.5 ml DMF with an equal volume of PBS containing 1.5 µmoles of Coenzyme A trilithium salt (Sigma-Aldrich). After incubating at 30°C for 24 h, the presence of the product was confirmed by mass spectrometry. 1 mM DTT was added to quench the excess BG-maleimide and the BG-CoA solution was used without purification. The initial layer of fusion protein containing both the SNAP and ybbR tags was conjugated to BG-modified yeast (or yeast hulls) as described above. 1 OD.ml of coated yeast was resuspended in 200 µl PBS + 0.1% BSA containing 10 mM $MgCl_2$, 75 µM BG-CoA and 12.5 µM Sfp. The yeast was incubated at 37°C for 1.5 h with occasional vortexing and washed twice with PBS + 0.1% BSA. The next layer was conjugated by mixing the yeast with 0.4 ml PBS and 0.1 ml 60 µM fusion protein for 2 h at 30°C. The Sfp/BG-CoA reaction and the SNAP-tag conjugation reaction were alternated to add more layers.

4.3.11 Yeast hulls

A 1 L culture of induced SWH100 yeast was pelleted, washed, and resuspended in 200 ml PBS to give an OD value of 25. The yeast suspension was passed twice through an M-110EH-30 Microfluidizer processor (Microfluidics, Newton, MA) at 30,000 psi using the G10Z (87 μm) interaction chamber. 40 ml of lysed yeast suspension was pelleted by centrifugation at 2000 × g for 5 min and then washed once with 100 ml PBS + 0.1% CHAPS, once with 100 ml 20% ethanol, and four times with 100 ml PBS + 0.01% CHAPS. The yeast fragments were resuspended in 100 ml PBS + 0.01% CHAPS and were stored in aliquots at -70°C. We assumed that there was no change in the cell wall material concentration during processing and washing, and treated the final yeast hull suspension as being equivalent to 10 OD of yeast.

4.3.12 In vitro immunization experiment

Nine wells of a 24-well plate were each seeded with 5×10^5 immature human monocyte-derived DCs in 1 ml C10 medium containing IL-4 and GM-CSF. Either unmodified yeast hulls, SWH100 whole yeast conjugated with one layer of MS74NEY2, or yeast hulls coated three times were added to the wells in triplicate, at a dose equivalent to 10 yeast per DC. The next day, $CD8^+$ $CD45RO^-$ T cells were isolated from the PBMCs of three HLA-A2 donors as described and resuspended in CTL medium (RPMI-1640 with 10% FCS, 50 μM β-mercaptoethanol, 12.5 mM HEPES, pH 7.3 and Primocin). The *in vitro* immunization assay conditions were adapted from a protocol for generating $CD8^+$ T cell clones (22). For each donor, 5×10^6 naïve T cells in 1 ml CTL medium were added directly to three DC wells with the three test conditions. In addition, 2×10^6 naïve T cells from each donor were labeled with 20 μl α-CD8-FITC and 10 μl SLLMWITQV/HLA-A*0201 peptide-MHC pentamer (ProImmune) in a total volume of 100 μl for 30 min on ice prior to analysis by flow cytometry (day 0 results). On day 3, 75% of the

medium was replaced by fresh CTL medium containing IL-2 and IL-7 to give final concentrations of 2.5 ng/ml and 5 ng/ml, respectively. The medium was refreshed in this manner every 2-3 days, and on day 7, the cells were transferred to a 12-well plate with the well volume doubling to 4 ml. On day 10, 2×10^6 cells from each well were labeled for CD8 and peptide-MHC pentamer binding as described above. To restimulate the T cells, 3×10^7 PBMCs from each donor were thawed, gamma-irradiated (35 Gy), and resuspended in 3 ml CTL medium containing 40 μM SLLMWITQV peptide (synthesized by AnaSpec, San Jose, CA). The PBMCs were seeded at 1 ml per well of a 12-well plate, and 3 h later, 5×10^6 day 10 T cells from each test condition were added in 3 ml CTL medium to donor-matched PBMC wells. On day 12 and every 2-3 days later, the cells were fed with fresh medium containing IL-2 and IL-7 and split when overcrowded. Flow cytometry analysis was again performed on day 20.

4.3.13 DC maturation experiment

Wells of a 24-well plate were each seeded with 4×10^5 immature monocyte-derived DCs in 0.8 ml C10 medium containing IL-4 and GM-CSF. The stimuli (either 1 μg/ml *E. coli* 055 lipopolysaccharide, LPS, from GE Healthcare, 0.5 μM MS74NEY2 or 10 yeast per DC doses of naked or antigen-coated whole yeast or yeast hulls) were added in duplicate to the wells. After 48 h, the culture supernatant from each well was set aside to be tested for IL-12p70 content using the OptEIA ELISA kit (BD Biosciences). The manufacturer's protocol was followed and both 2× and 20× dilutions of each sample in PBS were tested to cover a wide range of IL-12 concentrations. The DCs from duplicate wells were pooled and then divided into 5 portions; each aliquot was labeled with α-DC-SIGN-FITC and a phycoerythrin-conjugated antibody against one of 5 markers of DC maturation (CD40, CD80, CD83, CD86 and HLA-DR). The flow cytometry data were gated by DC-SIGN expression to exclude non-DC events.

4.4 Results

4.4.1 Antigen Conjugated to Yeast via the SNAP-tag is Cross-presented

The SNAP-tag is a 20 kDa protein domain derived from human O(6)-alkylguanine-DNA alkyltransferase, which reacts with benzyl guanine (BG) moieties resulting in the formation of a covalent thioether bond (23). We anticipated that SNAP-tagged NY-ESO-1 fusion protein could be site-specifically conjugated to yeast cell surfaces modified with BG. Due to the limited availability of NY-ESO-1-specific T cell clones, we decided to use a peptide derived from cytomegalovirus (CMV) pp65 as a surrogate antigen: ARNLVPMVATVQGQN (HLA-A*0201 epitope N9V is underlined). Cross-presentation of this epitope by DCs stimulated with yeast surface-displaying the peptide can be detected using commercially available cognate $CD8^+$ T cells (12).

We designed two fusion proteins, MSCcmyc and MSCE, both containing (in order from N terminus to C): MBP for yield, solubility and ease of purification, SNAP-tag for site-specific conjugation, four tandem repeats of the CatS-susceptible linker EKARVLAEAAS (12), and the CMV peptide. MSCE further included NY-ESO-1 as the C-terminal component, whereas MSCcmyc had only a final c-myc tag for detection purposes. Both fusion proteins were expressed in *E. coli* and purified by amylose affinity chromatography (including extensive washes with 0.1% Triton X-114 to greatly reduce endotoxin content (20)) and size exclusion chromatography. Wild type BJ5464α yeast cells (BJ5α for short) were reacted with an amine-reactive BG derivative (BG-GLA-NHS) and subsequently incubated with either MSCcmyc or MSCE protein. The SNAP-tag mediated conjugation was successful as determined by flow cytometry for c-myc and NY-ESO-1, respectively (not shown).

To test for cross-presentation, the antigen-conjugated yeast as well as the control BG-only yeast were added to immature HLA-A*0201 monocyte-derived DCs. Twenty four hours later, the DCs were co-cultured for four hours with an N9V-specific $CD8^+$ T cell clone. Cross-presentation of the N9V epitope could be assessed by quantifying the percentage of $CD8^+$ cells that had responded by secreting interferon gamma (IFNγ). As shown in Fig. 4.1A, yeast coated with either fusion protein induced cross-presentation at levels significantly above the background caused by BG-BJ5α yeast alone. The presence of NY-ESO-1 in the fusion protein did not interfere with cross-presentation of the surrogate CMV epitope, so we continued using MSCE for subsequent experiments.

4.4.2 Site-specificity of Conjugation is Crucial for Cross-presentation

We had investigated SNAP-tag-mediated conjugation on the premise that conventional chemical conjugation methods create covalent bonds at random sites in the protein and can interfere with antigen release in the DC phagosome and subsequent transport to the cytosol. To test this premise, we conjugated the same fusion protein, MSCE, to the yeast cell wall using either the SNAP-tag to BG reaction or by reductive amination. In the latter chemical conjugation scheme, the sugars on the yeast cell wall were partially oxidized with sodium meta-periodate to generate aldehyde groups, which form covalent bonds with lysine side chains in MSCE in the presence of sodium cyanoborohydride as a reducing agent. To enable a fair comparison, the concentration of MSCE used during SNAP-tag-mediated conjugation was reduced so as to match the conjugation level achieved by reductive amination (resulting in a mere 2% difference as determined by flow cytometry). Fig. 4.1B shows that antigen conjugated by reductive amination was not cross-presented at significant levels, unlike antigen attached via the SNAP-tag.

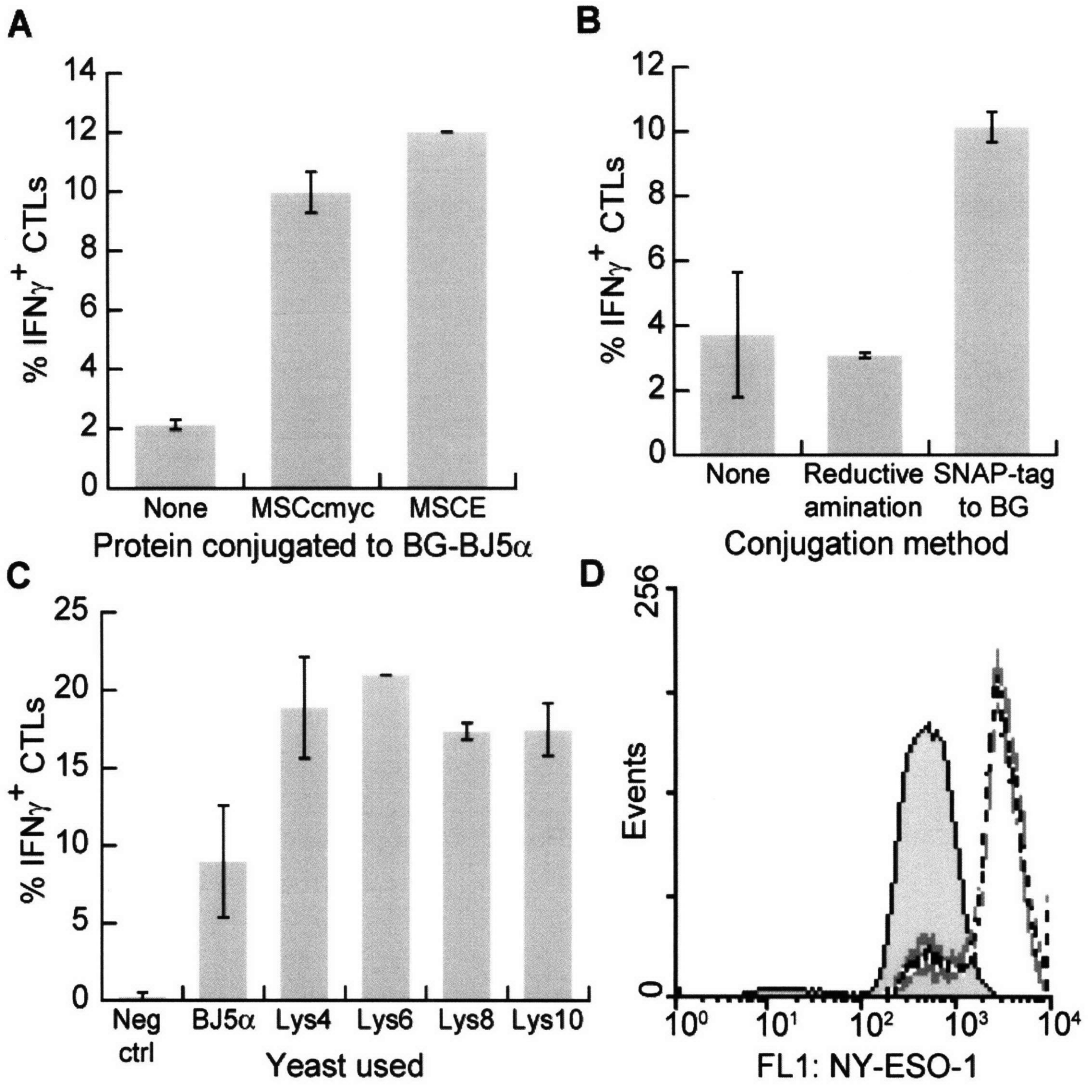

Figure 4.1, Antigen site-specifically conjugated to yeast via the SNAP-tag is cross-presented, with yeast expressing Aga1p and Aga2p giving rise to higher conjugation and cross-presentation levels.

A-C, Yeast with or without conjugated antigen were added to DCs at a 20:1 ratio. After 24 h, the DCs were assayed for the ability to stimulate N9V-specific $CD8^+$ T cells to secrete IFNγ. Error bars indicate SDs of duplicate wells. A, BJ5α yeast cells modified with BG were coated via the SNAP-tag reaction with either no protein, MSCcmyc or MSCE. B, MSCE was conjugated to BJ5α yeast either chemically by reductive amination or site-specifically via the SNAP-tag/BG reaction. The conjugation level of the latter method was matched to the former (within 5%) by reducing the MSCE concentration. C, MSCE was conjugated to either BJ5α yeast or yeast surface-displaying 4-10 tandem repeats of the sequence GGGGKGS (with X in LysX indicating the repeat number). The negative control was BG-BJ5α lacking MSCE.

D, BG and MSCE were conjugated to either BJ5α (grey fill), LysX yeast (where X = 4, 6, 8, or 10; grey lines), or yeast surface-displaying a short peptide lacking lysines (black dashed line). The yeast cells were labeled for flow cytometry with α-NY-ESO-1 followed by an Alexa Fluor 488-conjugated secondary antibody. The four histograms corresponding to the LysX yeast strains were not distinguished by color as they essentially overlaid each other.

4.4.3 Increasing Amine Density and Conjugation Levels on Yeast

Since BG-GLA-NHS reacts with primary amines on the yeast cell wall, we hypothesized that the antigen dose per yeast cell could be increased by surface-displaying lysine-rich polypeptides. To this end, we constructed yeast strains expressing 4-10 tandem repeats of the sequence GGGGKGS fused to Aga2p on the cell wall. These yeast strains, termed LysX where X indicates the number of added lysines, were reacted with BG-GLA-NHS followed by MSCE and tested for cross-presentation. The results revealed that all the modified yeast strains induced about twice as many $CD8^+$ T cells to secrete IFNγ as compared to wild type BJ5α, but the number of extra lysine residues appeared to be inconsequential (Fig. 4.1C). By analyzing the NY-ESO-1 conjugation levels by antibody labeling and flow cytometry, we discovered that a yeast strain surface-displaying a lysine-less peptide resulted in the same NY-ESO-1 density as the LysX strains, which was about 6-fold that on BJ5α (Fig. 4.1D). Similar results were obtained when fluorescently tagged MSCE was conjugated, eliminating antibody access limits as a confounding factor (not shown). It appears that the expression of Aga1p and Aga2p in the yeast surface display system fully accounts for the increase in numbers of amines available for conjugation. Steric hindrance may impose an upper limit on the number of bulky MSCE molecules that can be attached surrounding a single Aga1p-Aga2p complex. The yeast strain SWH100 with inducible expression of Aga1p and HA-tagged Aga2p was created and used henceforth instead of BJ5α.

4.4.4 An NY-ESO-1 Epitope is Cross-presented

Before investigating further improvements in the antigen conjugation strategy, we wanted to ensure that cross-presentation was not limited to the surrogate epitope. Using an HLA-Cw3-restricted $CD8^+$ T cell clone specifically recognizing the NY-ESO-1 epitope LAMPFATPM (21),

we performed an ELISpot assay to detect IFNγ secretion in response to DCs that had phagocytosed antigen-conjugated yeast. When MSCE fusion protein was conjugated, a significant number of spots were formed, in contrast to when MSCcmyc (with c-myc replacing the NY-ESO-1 domain) was conjugated (Fig. 4.2).

4.4.5 CD74 as a CatS-mediated Antigen Release Mechanism

The decision to include $(C1)_4$, a CatS-susceptible linker consisting of 4 repeats of the sequence EKARVLAEAAS, in MSCE was driven by its effectiveness in boosting cross-presentation efficiency with yeast surface-displaying the CMV peptide (12). However, when we deleted $(C1)_4$ from MSCE and conjugated it to SWH100 yeast via the SNAP-tag, the cross-presentation efficiency did not decrease significantly. To shed light on this observation, we digested both proteins in solution with CatS and studied the fragmentation patterns. N-terminal sequencing of one of the earliest fragments revealed that the CMV epitope itself, NLVPMVA|TV, can be cleaved by CatS at the indicated position. As competition between antigen release and epitope destruction may be a confounding factor, we sought to eliminate the CatS cleavage site. According to Rückrich et. al, only V, L, M, C, and F are found in the P2 position of effective CatS cleavage sites (24). Mutating the epitope to NLVPMIATV prevented CatS cleavage while maintaining recognition by the $CD8^+$ T cell clone used in our cross-presentation assays. This mutated CMV epitope was used henceforth, but there remained no clear benefit in cross-presentation when $(C1)_4$ was included versus deleted.

We hypothesized that $(C1)_4$ in the context of MSCE may be inaccessible to phagosomal CatS, perhaps because it assumes a compact instead of extended conformation when sandwiched between two sizeable protein domains (SNAP-tag and NY-ESO-1). In contrast, in the yeast surface display model, the linker was more exposed and had only a short peptide C-terminal to it.

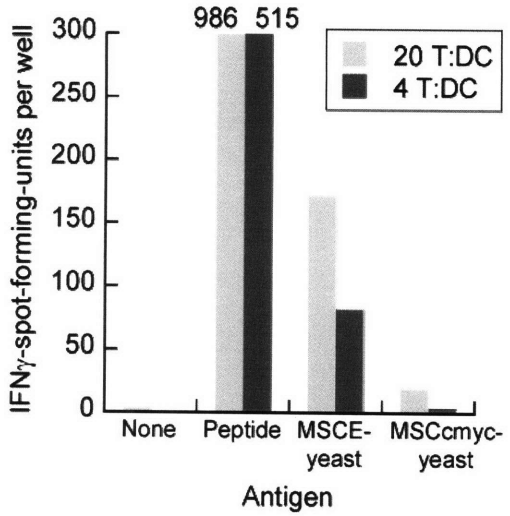

Figure 4.2, Cross-presentation on an NY-ESO-1 epitope as detected by ELISpot. HLA-Cw3 DCs were pulsed overnight with antigen and then cultured at 5×10^4 cells/well with the indicated ratio of a HLA-Cw3-restricted $CD8^+$ T cell clone recognizing NY-ESO-$1_{92\text{-}100}$. Lys6 yeast conjugated with MSCE (containing NY-ESO-1) or MSCcmyc (lacking NY-ESO-1) were each added to the DCs at a 20:1 ratio. This experiment was performed by T. Tsuji, Ludwig Institute for Cancer Research, New York Branch.

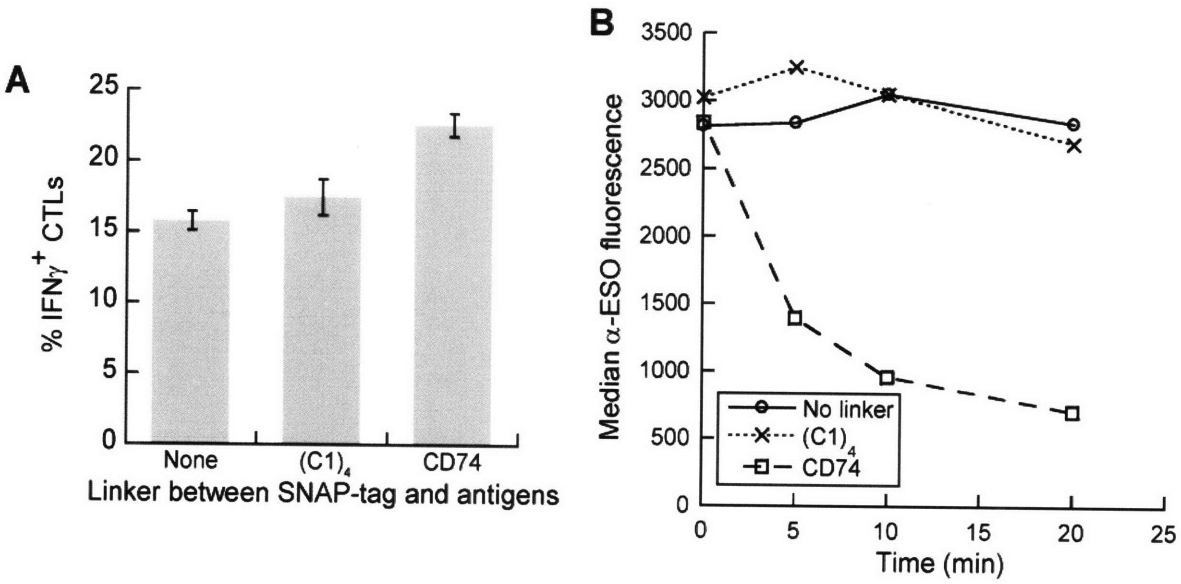

Figure 4.3, The extracellular domain of CD74 is highly susceptible to CatS cleavage and improves cross-presentation efficiency when used as a linker. Fusion protein variants containing either no linker, $(C1)_4$ or CD74 (aa 73-207) between the SNAP-tag and the CMV and NY-ESO-1 antigens were conjugated to SWH100 yeast in parallel.

A, The conjugated yeast were added at a 15:1 ratio to DCs, which a day later were tested for their ability to activate antigen-specific $CD8^+$ T cells. Error bars indicate SDs of triplicate wells.

B, The conjugated yeast (2×10^6 per test) were incubated with 20 ng CatS and incubated at 37°C for different time periods. The loss of the NY-ESO-1 domain was monitored by antibody labeling and flow cytometry.

Seeking an alternative polypeptide sequence that would not be obscured by the flanking domains and would be rapidly cleaved by CatS, the human invariant chain was considered. CatS-mediated degradation of the invariant chain, also called CD74, is known to be a prerequisite before MHC class II molecules can acquire peptides (25). More than a dozen CatS cleavage sites have been identified in the CD74 sequence (24). We therefore produced a new fusion protein replacing $(C1)_4$ with the ectodomain of CD74 (aa 73-207). SWH100 yeast coated with fusion protein containing CD74 as a linker induced more efficient cross-presentation than when either no linker or $(C1)_4$ was used (Fig. 4.3A). As expected, when yeast cells coated with each of the three fusion proteins were incubated with a limiting concentration of CatS, the loss of the NY-ESO-1 domain was dramatically faster when CD74 was used as the linker (Fig. 4.3B).

4.4.6 A Reaction Scheme for Producing Multiple Coats of Antigen

Although SNAP-tag-mediated conjugation to SWH100 resulted in an average of 5-7.5 × 10^5 molecules of antigen per yeast cell, or about 4-6× the typical yeast surface display level for a short peptide, we believed that vaccine potency could be enhanced by further increasing the conjugation level. The experiments with the LysX yeast strains (Fig. 4.1C & D) suggested that the addition of more primary amine groups to the yeast cell wall would be futile, so we instead pursued the strategy of building up multiple layers of conjugated antigen. To retain rapid phagosomal antigen release by CatS cleavage of the CD74 ectodomain, any new reactions would also need to be site-specific.

Yin et al. have developed a system for site-specific protein labeling using the enzyme Sfp phosphopantetheinyl transferase (Sfp for short), which covalently transfers small molecule tags linked to Coenzyme A (CoA) to the serine residue of a peptide tag called ybbR (sequence: DSLEFIASKLA) (19). We conjugated BG-maleimide to the free sulfhydryl group of CoA

(forming BG-CoA) with the intention of using Sfp to add a fresh layer of BG to yeast coated with ybbR-tagged fusion protein, thus allowing a second coat to be conjugated via the SNAP-tag reaction. Our initial experiments inserting the ybbR tag either between MBP and the SNAP-tag or as a C-terminal fusion to NY-ESO-1 failed to generate a significant second layer. Steric hindrance appeared to be an obstacle, which was solved by the addition of a glycine/serine linker between NY-ESO-1 and the ybbR tag. The final version of the fusion protein, named MS74NEY2, comprised (in order from N terminus to C): MBP, SNAP-tag, CD74 ectodomain, the mutated CMV peptide ASARNLVPMIATV, NY-ESO-1, TVQL (a CatS-sensitive peptide (24)), $(GGGGS)_3$ linker, ybbR tag, and His_6 tag (for easy purification of the full-length protein).

Under the appropriate reaction conditions, SNAP-tag conjugation and Sfp-mediated BG labeling could be alternated to build up multiple coats of fusion protein. Four coats of MS74NEY2 protein sparsely labeled with FITC (F/P ratio of 0.5) were layered onto SWH100 yeast, and samples from each reaction cycle were analyzed by flow cytometry (Fig. 4.4A). The increase in fluorescence was essentially linear, suggesting that there was no significant loss in conjugation efficiency as the number of cycles increased. Yeast coated with 0-4 layers of unlabeled MS74NEY2 were added to DCs at the low dose of only 2:1. At this dose, yeast coated with a single coat of antigen elicited cross-presentation at nearly background levels, whereas each subsequent antigen layer resulted in an increase in cross-presentation level (Fig. 4.4B).

4.4.7 Antigen can be Coated onto Yeast Hulls for Cross-presentation

With this vaccine model, both the functions of antigen delivery and adjuvancy are fulfilled by the cell wall of yeast; presumably, the yeast cytoplasm is dispensable. We anticipated that using yeast cell wall fragments instead of whole yeast cells may hold potential advantages. The antigen density would be increased on a per-volume basis, possibly permitting a higher dose

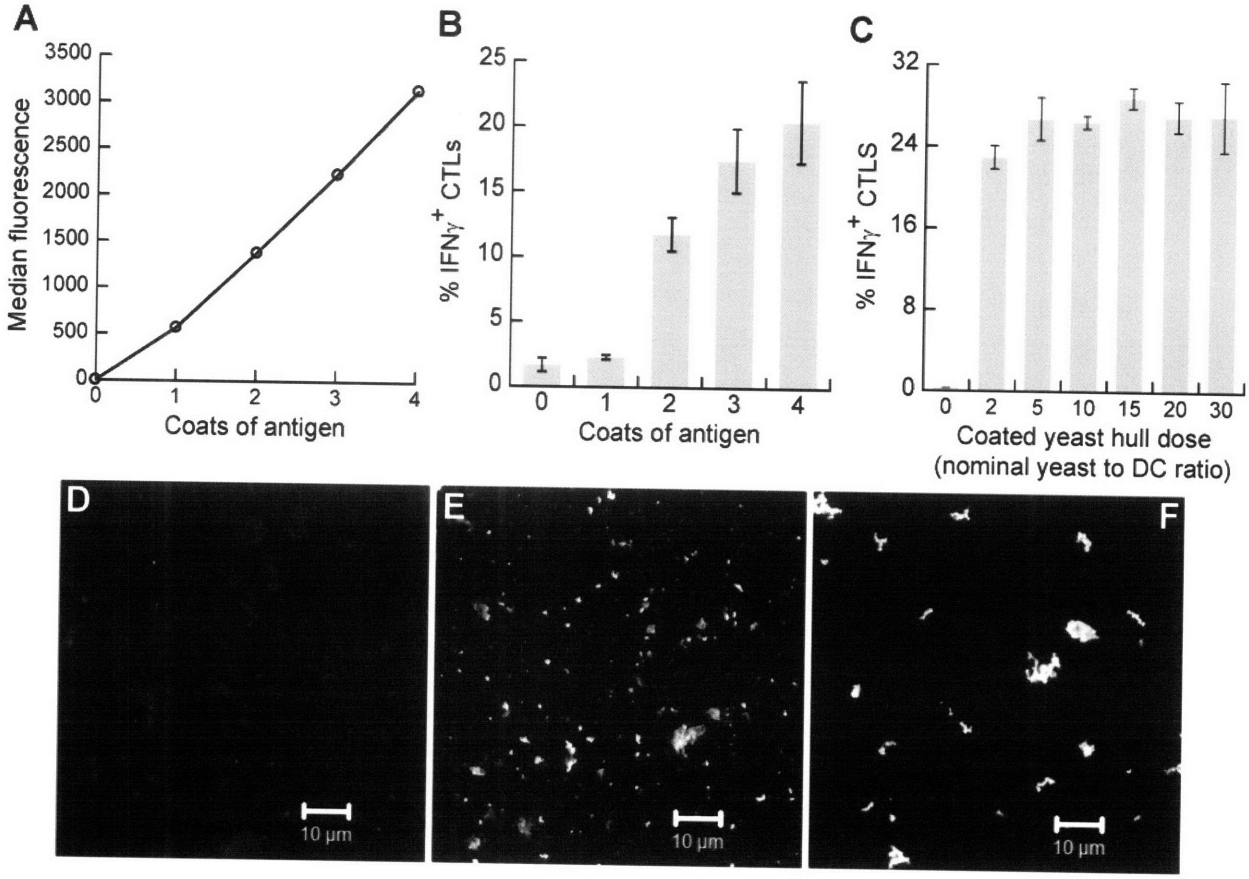

Figure 4.4, Antigen dose and cross-presentation efficiency can be increased by conjugating multiple coats of antigen and by using yeast hulls.

A, MS74NEY2 was lightly labeled with FITC and conjugated to SWH100 yeast in multiple layers by alternately performing SNAP-tag/BG and Sfp/BG-CoA reactions. The yeast cells with different numbers of antigen coats were directly analyzed by flow cytometry.

B, SWH100 whole yeast cells with 0-4 coats of MS74NEY2 (unlabeled) were added to DCs at a 2:1 ratio. After 24 h, the DCs were co-cultured with N9V-specific T cells and assess for their ability to stimulate IFNγ secretion. Error bars indicate SDs of duplicate wells.

C, SWH100 yeast hulls were conjugated with a single layer of MS74NEY2 and added to DCs at varying doses. The same cross-presentation assay was performed.

D-F, Confocal microscopy images of yeast hulls coated with one (D), two (E), or three (F) layers of MS74NEY2 lightly tagged with FITC.

to be delivered to each DC, whereas the variety and quantity of native yeast proteins that are also cross-presented would be reduced. Induced SWH100 yeast cells were disrupted at very high shear rates with a Microfluidizer® processor. After two passes, the resulting fragments had mean and median diameters of 1.7 μm and 0.9 μm respectively, as determined by static light scattering. After several washes, the fragments, henceforth termed yeast hulls, were subjected to conjugation with BG-GLA-NHS followed by MS74NEY2, using the same reaction conditions as were developed for whole yeast cells. We quantified the yeast hulls in terms of the numbers of originating whole yeast (estimated by measuring OD600), assuming negligible loss during processing and washing.

A dose-response cross-presentation assay was performed by adding antigen-coated yeast hulls to DCs. The coated yeast hulls were surprisingly potent: the lowest dose tested, nominally equivalent to 2 yeast per DC, resulted in a near-maximal response. In contrast, singly coated whole yeast elicited barely detectable levels of cross-presentation at the equivalent dose (Fig. 4.4B). Increasing the dose of yeast hulls from 5 to 30 yeast equivalents per DC did not result in higher percentages of IFNγ^+ T cells (Fig. 4.4C). The total number of recovered CD8$^+$ T cells dropped with increasing dose (not shown), suggesting a role for TCR-triggered activation-induced cell death (AICD) in limiting the assay response. We could not accurately quantify the level of antigen conjugation to yeast hulls by flow cytometry (the low forward and side scatter profile of the hulls overlapped with artifactual events), but the levels appeared to be qualitatively higher than achieved with whole yeast despite their smaller size distribution. We speculate that cell wall disruption may have revealed additional primary amine groups for conjugation, perhaps located on the inner face of the cell wall or at fissure sites. The alternating reaction scheme for conjugating multiple layers of antigen was also effective on yeast hulls. Figures 4.4D-F are

confocal microscopy images of yeast hulls coated with 1-3 layers of MS74NEY2 lightly labeled with FITC (F/P ratio of 0.1). In addition to the increased fluorescence, the yeast hulls displayed a greater tendency to aggregate with three coats of antigen.

4.4.8 NY-ESO-1-specific In Vitro Immunization of Naïve CD8$^+$ T Cells

The multiple refinements that we have made to improve our antigen-coated yeast-based vaccine strategy have thus far been tested primarily by detecting cross-presentation of the surrogate CMV epitope using a T cell clone. We now wished to investigate if the vaccine candidates are capable of priming naïve CD8$^+$ T cells to elicit NY-ESO-1-specific immunity. CD8$^+$ CD45RO$^-$ T cells were isolated from the PBMCs of three HLA-A*0201 donors by magnetic cell sorting. The naïve CD8$^+$ T cells were added at a 10:1 ratio to DCs (from a fourth donor) that had been stimulated the previous day with either unconjugated yeast hulls, whole yeast cells carrying one coat of MS74NEY2, or yeast hulls with three coats of antigen. Before and after 10 days of co-culture, the cells were labeled with a SLLMWITQV/HLA-A*0201 peptide-MHC pentamer, with the peptide being the well-characterized NY-ESO-$1_{157\text{-}165}$ epitope with the final Cys residue mutated to Val to avoid oxidation-related issues (26).

As shown in Fig. 5, the naïve precursor frequencies were around 0.02% with all three donors, and the frequency of higher avidity T cells (arbitrarily defined as those falling within the rectangular gate) were in the 0.003-0.005% range. Ten days after stimulation by the DCs, the frequencies of pentamer-positive CD8$^+$ T cells increased under all nine test conditions. The proliferation of pentamer-positive T cells after "immunization" with yeast hulls lacking NY-ESO-1 may be a result of extensive TCR degeneracy observed in many experiments (27-33), with theoretical analysis suggesting a TCR ligand repertoire size of 10^6-10^7 peptide epitopes (34). With all three donors, the yeast hulls coated with three layers of antigen elicited the highest

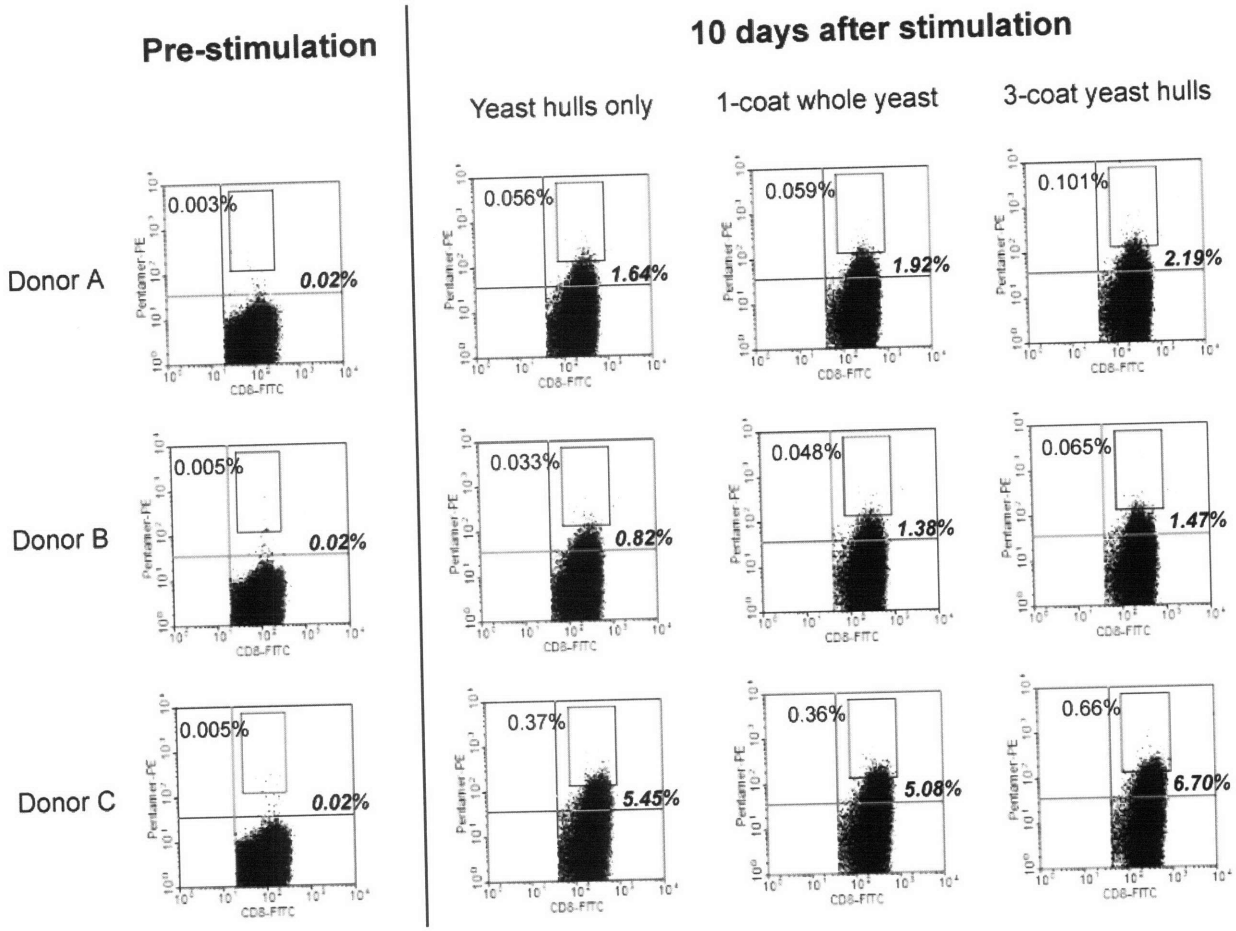

Figure 4.5, DCs fed MS74NEY2-coated yeast and yeast hulls stimulated the expansion of cells recognizing an NY-ESO-1 peptide/MHC complex from a naïve CD8$^+$ pool. CD8$^+$ CD45RO$^-$ cells from three HLA-A2 donors were added to immature DCs fed either yeast hulls alone, whole yeast coated with one layer of MS74NEY2 or yeast hulls with three coats (each at a dose equivalent to 10 yeast per DC). The T cells before co-culture and after 10 days (IL-2 and IL-7 were added from day 3 onwards) were labeled with α-CD8-FITC and PE-conjugated SLLMWITQV/HLA-A*0201 pentamer. 2×10^6 cells were labeled per test and 2×10^5 CD8$^+$ events are shown in each dot plot. The proportions of events (out of CD8$^+$ events) falling in the top right quadrant (in bold italics) and in the rectangular gate are shown.

proportion of pentamer-stained cells, with almost double the frequency of high avidity T cells as compared to the yeast-hull-only controls. The singly coated whole yeast cells, which delivered a smaller dose of antigen as compared to the 3-coat yeast hulls, gave rise to intermediate pentamer-positive T cell frequencies with two out of the three donors. Although the double-positive events are rare and not clearly distinct from the pentamer-negative cells, we believe that they represent genuine NY-ESO-1-specific T cells because restimulation with peptide-pulsed autologous PBMCs on day 10 expanded the double-positive populations to 5-20% by day 20 (Fig. 4.6). We conclude that DCs fed either whole yeast cells coated with one layer of MS74NEY2 or yeast hulls coated three times were able to prime naïve, NY-ESO-1-recognizing $CD8^+$ T cells, with the latter formulation being initially more potent.

4.4.9 DC Maturation by Yeast Particles

The ability of *S. cerevisiae* yeast to stimulate inflammatory cytokine secretion by murine splenocytes (7, 8) and DCs (3, 9) and to induce maturation of human (6) and murine (3, 9) DCs is well-established. In our preliminary experiments, yeast cells upregulated various markers of maturation in human monocyte-derived DCs to an extent comparable with 1 μg/ml LPS and induced even more IL-12 secretion than LPS. We now investigated whether the processes of antigen conjugation and cell disruption would alter the immunostimulatory properties of yeast. SWH100 yeast and yeast hulls, each with and without a single layer of conjugated antigen, were added to immature DCs at the nominal dose of 10 yeast per DC. After 48 h, the DCs were analyzed for the expression levels of CD40, CD80, CD83, CD86 and HLA-DR (all markers of DC maturation), whereas the cell culture supernatants were subjected to an IL-12p70 ELISA assay. As we had observed previously, whole unconjugated yeast upregulated the maturation markers to levels similar to those caused by LPS (Fig. 4.7A) and massively induced IL-12

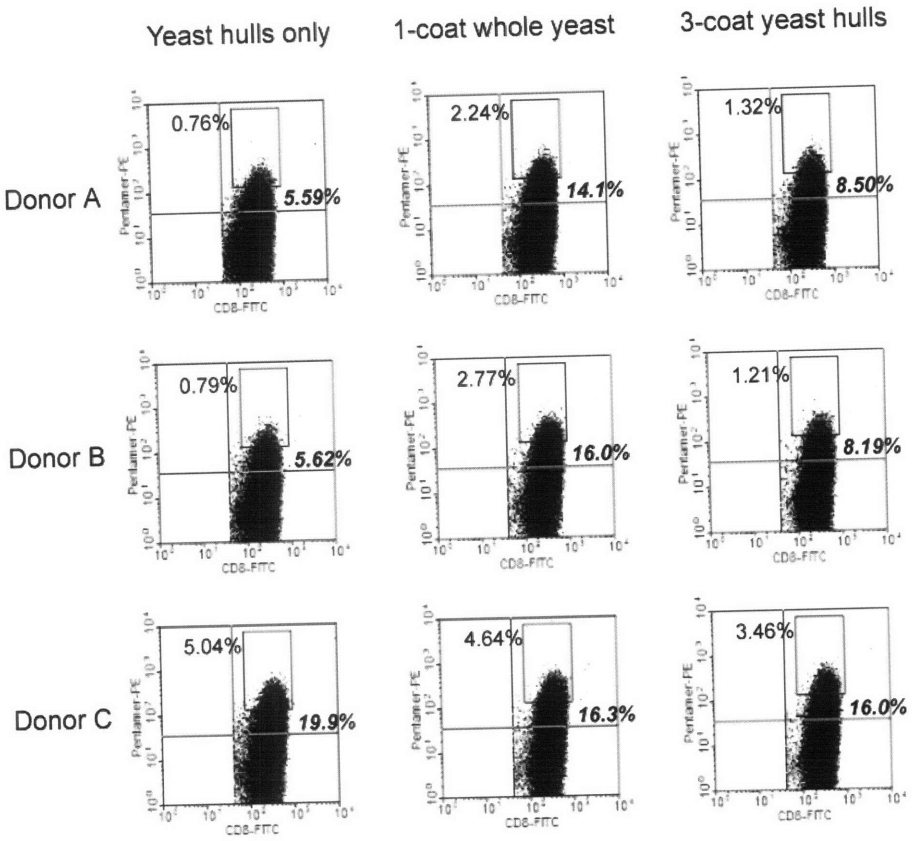

Figure 4.6, Peptide/MHC pentamer-positive T cells primed by yeast particles continue to multiply after re-stimulation with peptide-pulsed autologous PBMCs. On day 10 of the experiment described in Fig. 4, PBMCs from each donor were thawed, gamma-irradiated, and pulsed with 40 μM SLLMWITQV peptide for 3 h. Day 10 T cells from each test condition (5×10^6 per well) were co-cultured with 10^7 donor-matched PBMCs in 4 ml CTL medium (with 10 μM peptide) in a 12-well plate. The cells were fed and split as necessary. Flow cytometry analysis after labeling with α-CD8-FITC and PE-conjugated SLLMWITQV/HLA-A*0201 pentamer was performed on day 20.

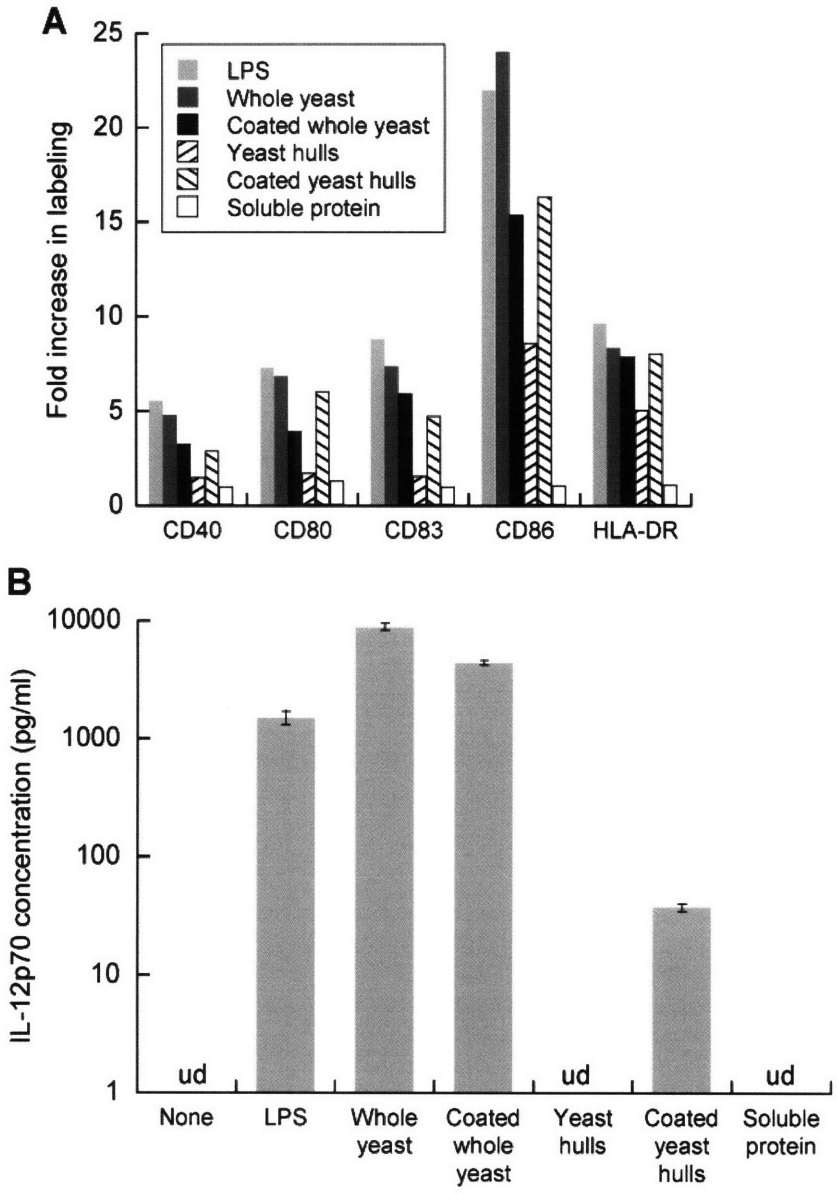

Figure 4.7, DC maturation in response to yeast is influenced by cell integrity and antigen conjugation. Immature DCs were stimulated with either LPS (1 μg/ml) or soluble fusion protein (0.5 μM) or whole SWH100 yeast or yeast hulls either unmodified or conjugated with one layer of antigen (each at a dose equivalent to 10 yeast per DC).

A, Two days later, the DCs were labeled with α-DC-SIGN-FITC and a PE-conjugated antibody against one of the five selected markers of DC maturation. The flow cytometry results were gated by DC-SIGN positivity and the median PE fluorescence in each test was compared against the result with unstimulated DCs.

B, The cell culture supernatants after two days were tested for IL-12p70 by ELISA. Readings calculated to be lower than 5 pg/ml were considered undetectable (ud). Error bars indicate SDs of duplicate wells.

secretion (Fig. 4.7B). To our surprise, uncoated yeast hulls behaved very differently compared to whole yeast, causing strikingly less marker upregulation and no detectable IL-12 secretion. Antigen conjugation had opposite effects on whole yeast and yeast hulls, slightly reducing DC maturation and IL-12 secretion by whole yeast while increasing these metrics with yeast hulls. Although some IL-12 was secreted by DCs exposed to antigen-coated yeast hulls, the quantity was two orders of magnitude lower than that caused by coated or uncoated whole yeast (Fig. 4.7B). The effects of antigen conjugation were not simply caused by endotoxin contamination or some intrinsic property of the protein, since soluble fusion protein alone (at 0.5 μM, roughly 100× the level of yeast-conjugated antigen present in a well) had little effect on the DCs (Fig. 4.7).

4.5 Discussion

We present here a flexible vaccine-oriented scheme for conjugating antigen to yeast particles that has undergone multiple refinements with the aim of maximizing cross-presentation. The fusion protein MS74NEY2 represents the latest embodiment, consisting of the following functional elements: MBP, SNAP-tag, CD74 ectodomain, 15-mer CMV-derived surrogate antigen, NY-ESO-1 cancer-testis antigen, glycine/serine linker, ybbR tag and His_6 tag. We have demonstrated cross-presentation of both the surrogate antigen and an NY-ESO-1 HLA-A2 epitope; these antigens can readily be exchanged to suit different immunotherapy applications. The highly hydrophobic NY-ESO-1 protein used in clinical trials is purified from *E. coli* inclusion bodies (35), but insertion of MBP as the N-terminal domain enabled our fusion proteins to be expressed solubly and also facilitated purification. For other antigens, MBP may be omitted or replaced if desired. A key feature of our conjugation scheme is its site-specific nature, which ensures that antigen can be released in the DC phagosome to translocate to the cytosol for entry into the MHC class I processing pathway. The initial layer of fusion protein is conjugated to BG-derivatized particles through the formation of a stable thioether bond with the SNAP-tag domain. We showed that cross-presentation is highly inefficient when a non-site-specific chemical conjugation method was used to attach the same protein to yeast. The lack of efficacy is especially noteworthy considering that there were no reactive lysine residues within the CMV peptide and only one in the C-terminal direction. This suggests that merely "tethering" an epitope on both ends with no intervening phagosomal protease sites can impede cross-presentation. To expedite phagosomal antigen release in our scheme, we inserted the extremely CatS-susceptible CD74 ectodomain between the SNAP-tag tether and the antigens, resulting in improved cross-presentation efficiency.

In addition to developing the conjugation scheme with antigen release kinetics in mind, we have also made several improvements to increase antigen dose delivery. The first refinement was to use a yeast strain expressing Aga1p and Aga2p, which provided more free amines on the cell wall for BG and fusion protein conjugation compared to the wild type. Fusing lysine-containing polypeptides to Aga2p did not further increase the antigen density in this first layer, so we devised a novel multi-layer conjugation strategy that is retains site-specificity. Sfp enzyme is used to attach BG-linked CoA to the ybbR tags of one antigen layer, thus permitting the next layer to be added via the SNAP-tag/BG reaction. We experienced no loss in conjugation efficiency in building up to four antigen layers (suggesting that further coats can be added almost indefinitely) and demonstrated that cross-presentation levels rose with the number of layers. Finally, breaking up the cell wall into fragments prior to conjugation further increased the amount of antigen delivered per yeast cell equivalent, probably because the surfaces that were revealed provided additional free amines for BG attachment.

While the use of yeast hulls instead of whole yeast improves antigen delivery and reduces native yeast protein content, it is at present unclear whether yeast hulls will ultimately be more effective in the setting of immunotherapy. A major reason behind the attractiveness of yeast-based vaccines is their ability to mature DCs and stimulate the secretion of pro-inflammatory cytokines, obviating the need for additional adjuvants (5). To our surprise, yeast hulls were significantly inferior to whole yeast cells in inducing DC maturation, and more importantly, they elicited little or no IL-12 secretion. In retrospect, this observation is not without precedent as several groups have reported that Zymosan, a preparation of *S. cerevisiae* cell wall particles, is a poor inducer of DC IL-12 secretion despite its long-standing reputation as a pro-inflammatory agent (36-38). IL-12 secretion is likely to be important to vaccine efficacy because it plays a role

in enhancing the clonal expansion of primed $CD8^+$ T cells (39, 40), perhaps by increasing resistance to AICD (41).

The disparity in DC reactions to whole yeast cells and yeast cell wall fragments is puzzling and warrants further investigation. One possibility is that an immunostimulatory component is lacking in yeast hulls, which was either removed with the yeast cytoplasm or washed away from the cell wall fragments. Re-evaluation of the wash steps may be helpful in the latter case. In the former case, a possible candidate is double-stranded RNA from viruses that ubiquitously infect yeast cells (42). It has been observed that a combination of Zymosan and poly I:C (a synthetic double-stranded RNA analog) stimulates far greater levels of IL-12 secretion than either agent alone (38), raising the intriguing possibility that whole yeast cells induce massive IL-12 secretion through a similar synergism. If this is the case, conjugating poly I:C to yeast hulls may present a simple solution. An alternative explanation stems from the complex structure of the yeast cell wall, with fragmentation resulting in the exposure of different molecular patterns leading to altered signaling cascades in DCs. To elaborate, the outer layer of the *S. cerevisiae* cell wall is composed primarily of mannan (hypermannosylated proteins), which in undamaged yeast cells largely masks the inner layer of β1,3-glucan, β1,6-glucan and chitin (43). Our observation that antigen conjugation (and thus partial disruption of the molecular patterns) had opposite effects on whole yeast cells and yeast hulls could be an indication that DC recognition of the inner cell wall layer partially counteracts the maturation signals derived from ligands in the outer layer.

Vaccination experiments *in vivo* will be required to discover the effects of yeast particle choice on T cell memory and protective immunity and to develop an optimal formulation (possibly a mixture of uncoated whole yeast and coated yeast hulls). At the same time, the

conjugation scheme presented here is not restricted to yeast and can easily be applied to any particle that is or can be amine-functionalized, including heat-killed bacteria and bacterial ghosts, polymer and inorganic microspheres, ribosomes and liposomes. Although the ability of antigen-coated particles to induce protective tumor immunity was demonstrated almost 15 years ago (44), particulate antigen delivery vehicles (with the exception of virus-like particles) have received little attention in the field of cancer immunotherapy. Co-delivery of adjuvant and antigen in particles holds several advantages over injection of soluble agents, including a high local concentration that does not quickly dissipate, assurance that both adjuvant and a minimum bolus of antigen are delivered to the same cell, and inherent targeting for uptake by phagocytic cells (besides DCs, macrophages (45) and neutrophils (46) are also capable of cross-priming). Poor phagosomal escape of antigen represents one barrier to the development of particulate vaccines, and the conjugation strategy described here presents a novel way to break this barrier.

4.6 References

1. Rosenberg, S. A., J. C. Yang, and N. P. Restifo. 2004. Cancer immunotherapy: moving beyond current vaccines. *Nat Med* 10: 909-915.
2. Petrovsky, N., and J. C. Aguilar. 2004. Vaccine adjuvants: Current state and future trends. *Immunol Cell Biol* 82: 488-496.
3. Stubbs, A. C., K. S. Martin, C. Coeshott, S. V. Skaates, D. R. Kuritzkes, D. Bellgrau, A. Franzusoff, R. C. Duke, and C. C. Wilson. 2001. Whole recombinant yeast vaccine activates dendritic cells and elicits protective cell-mediated immunity. *Nat Med* 7: 625-629.
4. Lu, Y., D. Bellgrau, L. D. Dwyer-Nield, A. M. Malkinson, R. C. Duke, T. C. Rodell, and A. Franzusoff. 2004. Mutation-selective tumor remission with Ras-targeted, whole yeast-based immunotherapy. *Cancer Res* 64: 5084-5088.
5. Franzusoff, A., R. C. Duke, T. H. King, Y. Lu, and T. C. Rodell. 2005. Yeasts encoding tumour antigens in cancer immunotherapy. *Expert Opinion on Biological Therapy* 5: 565-575.
6. Barron, M. A., N. Blyveis, S. C. Pan, and C. C. Wilson. 2006. Human Dendritic Cell Interactions with Whole Recombinant Yeast: Implications for HIV-1 Vaccine Development. *J Clin Immunol* 26: 251-264.
7. Haller, A. A., G. M. Lauer, T. H. King, C. Kemmler, V. Fiolkoski, Y. Lu, D. Bellgrau, T. C. Rodell, D. Apelian, A. Franzusoff, and R. C. Duke. 2007. Whole recombinant yeast-based immunotherapy induces potent T cell responses targeting HCV NS3 and Core proteins. *Vaccine* 25: 1452-1463.
8. Riemann, H., J. Takao, Y. G. Shellman, W. A. Hines, C. K. Edwards, D. A. Norris, and M. Fujita. 2007. Generation of a prophylactic melanoma vaccine using whole recombinant yeast expressing MART-1. *Experimental Dermatology* 16: 814-822.
9. Bernstein, M. B., M. Chakraborty, E. K. Wansley, Z. Guo, A. Franzusoff, S. Mostbock, H. Sabzevari, J. Schlom, and J. W. Hodge. 2008. Recombinant Saccharomyces cerevisiae (yeast-CEA) as a potent activator of murine dendritic cells. *Vaccine* 26: 509-521.
10. Munson, S., J. Parker, T. H. King, Y. Lio, V. Kelley, Z. Guo, V. Borges, and A. Franzusoff. 2008. Coupling innate and adaptive immunity with yeast-based cancer immunotherapy. In *Cancer Vaccines and Tumor Immunity*. R. Orentas, J. W. Hodge, and B. D. Johnson, eds. Wiley-Liss, New York, p. 131-149.
11. Wadle, A., G. Held, F. Neumann, S. Kleber, B. Wuellner, A. M. Asemissen, B. Kubuschok, C. Scheibenbogen, T. Breinig, A. Meyerhans, and C. Renner. 2006. Cross-presentation of HLA class I epitopes from influenza matrix protein produced in Saccharomyces cerevisiae. *Vaccine* 24: 6272-6281.
12. Howland, S. W., and K. D. Wittrup. 2008. Antigen Release Kinetics in the Phagosome Are Critical to Cross-Presentation Efficiency. *J Immunol* 180: 1576-1583.
13. Boder, E. T., and K. D. Wittrup. 1997. Yeast surface display for screening combinatorial polypeptide libraries. *Nat Biotechnol* 15: 553-557.

14. Gnjatic, S., H. Nishikawa, A. A. Jungbluth, A. O. Gure, G. Ritter, E. Jager, A. Knuth, Y. T. Chen, and L. J. Old. 2006. NY-ESO-1: review of an immunogenic tumor antigen. *Adv Cancer Res* 95: 1-30.

15. Nicholaou, T., L. Ebert, I. D. Davis, N. Robson, O. Klein, E. Maraskovsky, W. Chen, and J. Cebon. 2006. Directions in the immune targeting of cancer: Lessons learned from the cancer-testis Ag NY-ESO-1. *Immunol Cell Biol* 84: 303-317.

16. Piatesi, A., S. W. Howland, J. A. Rakestraw, C. Renner, N. Robson, J. Cebon, E. Maraskovsky, G. Ritter, L. Old, and K. D. Wittrup. 2006. Directed evolution for improved secretion of cancer-testis antigen NY-ESO-1 from yeast. *Protein Expression and Purification* 48: 232-242.

17. Chao, G., W. L. Lau, B. J. Hackel, S. L. Sazinsky, S. M. Lippow, and K. D. Wittrup. 2006. Isolating and engineering human antibodies using yeast surface display. *Nat Protoc* 1: 755-768.

18. Sikorski, R. S., and P. Hieter. 1989. A System of Shuttle Vectors and Yeast Host Strains Designed for Efficient Manipulation of DNA in Saccharomyces cerevisiae. *Genetics* 122: 19-27.

19. Yin, J., A. J. Lin, D. E. Golan, and C. T. Walsh. 2006. Site-specific protein labeling by Sfp phosphopantetheinyl transferase. *Nat Protoc* 1: 280-285.

20. Reichelt, P., C. Schwarz, and M. Donzeau. 2006. Single step protocol to purify recombinant proteins with low endotoxin contents. *Protein Expression and Purification* 46: 483-488.

21. Gnjatic, S., Y. Nagata, E. Jager, E. Stockert, S. Shankara, B. L. Roberts, G. P. Mazzara, S. Y. Lee, P. R. Dunbar, B. Dupont, V. Cerundolo, G. Ritter, Y.-T. Chen, A. Knuth, and L. J. Old. 2000. Strategy for monitoring T cell responses to NY-ESO-1 in patients with any HLA class I allele. *Proceedings of the National Academy of Sciences* 97: 10917-10922.

22. Ho, W. Y., H. N. Nguyen, M. Wolfl, J. Kuball, and P. D. Greenberg. 2006. In vitro methods for generating CD8+ T-cell clones for immunotherapy from the naive repertoire. *Journal of Immunological Methods* 310: 40-52.

23. Keppler, A., M. Kindermann, S. Gendreizig, H. Pick, H. Vogel, and K. Johnsson. 2004. Labeling of fusion proteins of O6-alkylguanine-DNA alkyltransferase with small molecules in vivo and in vitro. *Methods* 32: 437-444.

24. Ruckrich, T., J. Brandenburg, A. Cansier, M. Muller, S. Stevanovic, K. Schilling, B. Wiederanders, A. Beck, A. Melms, M. Reich, C. Driessen, and H. Kalbacher. 2006. Specificity of human cathepsin S determined by processing of peptide substrates and MHC class II-associated invariant chain. *Biol Chem* 387: 1503-1511.

25. Riese, R. J., P. R. Wolf, D. Bromme, L. R. Natkin, J. A. Villadangos, H. L. Ploegh, and H. A. Chapman. 1996. Essential Role for Cathepsin S in MHC Class II-Associated Invariant Chain Processing and Peptide Loading. *Immunity* 4: 357-366.

26. Chen, J.-L., P. R. Dunbar, U. Gileadi, E. Jager, S. Gnjatic, Y. Nagata, E. Stockert, D. L. Panicali, Y.-T. Chen, A. Knuth, L. J. Old, and V. Cerundolo. 2000. Identification of NY-ESO-1 Peptide Analogues Capable of Improved Stimulation of Tumor-Reactive CTL. *J Immunol* 165: 948-955.

27. Wucherpfennig, K. W., and J. L. Strominger. 1995. Molecular mimicry in T cell-mediated autoimmunity: Viral peptides activate human T cell clones specific for myelin basic protein. *Cell* 80: 695-705.

28. Kersh, G., and P. Allen. 1996. Structural basis for T cell recognition of altered peptide ligands: a single T cell receptor can productively recognize a large continuum of related ligands. *J. Exp. Med.* 184: 1259-1268.

29. Hemmer, B., M. Vergelli, B. Gran, N. Ling, P. Conlon, C. Pinilla, R. Houghten, H. F. McFarland, and R. Martin. 1998. Cutting Edge: Predictable TCR Antigen Recognition Based on Peptide Scans Leads to the Identification of Agonist Ligands with No Sequence Homology. *J Immunol* 160: 3631-3636.

30. Hemmer, B., M. Vergelli, C. Pinilla, R. Houghten, and R. Martin. 1998. Probing degeneracy in T-cell recognition using peptide combinatorial libraries. *Immunology Today* 19: 163-168.

31. Misko, I. S., S. M. Cross, R. Khanna, S. L. Elliott, C. Schmidt, S. J. Pye, and S. L. Silins. 1999. Crossreactive recognition of viral, self, and bacterial peptide ligands by human class I-restricted cytotoxic T lymphocyte clonotypes: Implications for molecular mimicry in autoimmune disease. *Proceedings of the National Academy of Sciences* 96: 2279-2284.

32. Chen, J., H. N. Eisen, and D. M. Kranz. 2003. A model T-cell receptor system for studying memory T-cell development. *Microbes and Infection* 5: 233-240.

33. Wucherpfennig, K. W. 2004. T cell receptor crossreactivity as a general property of T cell recognition. *Mol Immunol* 40: 1009-1017.

34. Mason, D. 1998. A very high level of crossreactivity is an essential feature of the T-cell receptor. *Immunology Today* 19: 395-404.

35. Murphy, R., S. Green, G. Ritter, L. Cohen, D. Ryan, W. Woods, M. Rubira, J. Cebon, I. D. Davis, A. Sjolander, A. Kypridis, H. Kalnins, M. McNamara, M. B. Moloney, J. Ackland, G. Cartwright, J. Rood, G. Dumsday, K. Healey, D. Maher, E. Maraskovsky, Y. T. Chen, E. W. Hoffman, L. J. Old, and A. M. Scott. 2005. Recombinant NY-ESO-1 cancer antigen: production and purification under cGMP conditions. *Prep Biochem Biotechnol* 35: 119-134.

36. Edwards, A. D., S. P. Manickasingham, R. Sporri, S. S. Diebold, O. Schulz, A. Sher, T. Kaisho, S. Akira, and C. Reis e Sousa. 2002. Microbial Recognition Via Toll-Like Receptor-Dependent and -Independent Pathways Determines the Cytokine Response of Murine Dendritic Cell Subsets to CD40 Triggering. *J Immunol* 169: 3652-3660.

37. Dillon, S., S. Agrawal, K. Banerjee, J. Letterio, T. L. Denning, K. Oswald-Richter, D. J. Kasprowicz, K. Kellar, J. Pare, T. van Dyke, S. Ziegler, D. Unutmaz, and B. Pulendran. 2006. Yeast zymosan, a stimulus for TLR2 and dectin-1, induces regulatory antigen-presenting cells and immunological tolerance. *J Clin Invest* 116: 916-928.

38. Bohnenkamp, H. R., K. T. Papazisis, J. M. Burchell, and J. Taylor-Papadimitriou. 2007. Synergism of Toll-like receptor-induced interleukin-12p70 secretion by monocyte-derived dendritic cells is mediated through p38 MAPK and lowers the threshold of T-helper cell type I responses. *Cellular Immunology* 247: 72-84.

39. Valenzuela, J., C. Schmidt, and M. Mescher. 2002. The Roles of IL-12 in Providing a Third Signal for Clonal Expansion of Naive CD8 T Cells. *J Immunol* 169: 6842-6849.

40. Chang, J., J.-H. Cho, S.-W. Lee, S.-Y. Choi, S.-J. Ha, and Y.-C. Sung. 2004. IL-12 Priming during In Vitro Antigenic Stimulation Changes Properties of CD8 T Cells and Increases Generation of Effector and Memory Cells. *J Immunol* 172: 2818-2826.

41. Díaz-Montero, C., S. El Naggar, A. Al Khami, R. El Naggar, A. Montero, D. Cole, and M. Salem. 2008. Priming of naive CD8+ T cells in the presence of IL-12 selectively enhances the survival of CD8+CD62Lhi cells and results in superior anti-tumor activity in a tolerogenic murine model. *Cancer Immunology, Immunotherapy* 57: 563-572.

42. Wickner, R. B. 1996. Prions and RNA viruses of Saccharomyces cerevisiae. *Annual Review of Genetics* 30: 109-139.

43. Wheeler, R. T., and G. R. Fink. 2006. A Drug-Sensitive Genetic Network Masks Fungi from the Immune System. *PLoS Pathogens* 2: e35.

44. Falo, L. D., M. Kovacsovics-Bankowski, K. Thompson, and K. L. Rock. 1995. Targeting antigen into the phagocytic pathway in vivo induces protective tumour immunity. *Nat Med* 1: 649-653.

45. Pozzi, L.-A. M., J. W. Maciaszek, and K. L. Rock. 2005. Both Dendritic Cells and Macrophages Can Stimulate Naive CD8 T Cells In Vivo to Proliferate, Develop Effector Function, and Differentiate into Memory Cells. *J Immunol* 175: 2071-2081.

46. Beauvillain, C., Y. Delneste, M. Scotet, A. Peres, H. Gascan, P. Guermonprez, V. Barnaba, and P. Jeannin. 2007. Neutrophils efficiently cross-prime naive T cells in vivo. *Blood* 110: 2965-2973.

Appendix A – Sequences of Key Plasmids

A.1 pHAH-L5

Backbone: pCT2
Description: Used for NY-ESO-L5 production by reduction off the cell wall of surface-displaying yeast. Cleavage with human rhinovirus 3C protease releases untagged NY-ESO-L5, whereas aga2p, which is flanked by two His_6 sites, remains bound to the metal affinity resin.

```
    |--> Aga2p with His6 inserted after signal peptide
  1 ATGCAGTTAC TTCGCTGTTT TTCAATATTT TCTGTTATTG CTTCAGTTTT
      |--> His6       <--|
 51 AGCACATCAC CATCATCATC ACCAGGAACT GACAACTATA TGCGAGCAAA
101 TCCCCTCACC AACTTTAGAA TCGACGCCGT ACTCTTTGTC AACGACTACT
151 ATTTTGGCCA ACGGGAAGGC AATGCAAGGA GTTTTTGAAT ATTACAAATC
201 AGTAACGTTT GTCAGTAATT GCGGTTCTCA CCCCTCAACA ACTAGCAAAG
                              <--||--> GGGGS   <--||-->
251 GCAGCCCCAT AAACACACAG TATGTTTTTG GTGGAGGAGG CTCTCATCAC
    His6     <--|NheI  |--> HRV 3C site       <--||-->
301 CATCATCACC ATGCTAGCTT GGAAGTTTTG TTTCAAGGTC CAATGCAGGC
    NY-ESO-1 (L5 mutant)
351 CGAAGGCCGG GGCACAGGGG GTTCGACGGG CGATGCTGAT GGCCCAGGAG
401 GCCCTGGCAT TCCTGATGGC CCAGGGGGCA ATGCTGGCGG CCCAGGAGAG
451 GCGGGTGCCA CGGGCGGCAG AGGTCCCCGG GGCGCAGGGG CAGCAAGGGC
501 CTCGGGGCCG GGAGGAGGCG CCCCGCGGGG TCCGCATGGC GGCGCGGCTT
551 CAGGGCTGAA TGGAGCCGCC AGAGCCGGGG CCAGGGGGCC GGAGAGCCGC
601 CTGCTTGAGT TCTACCTCGC CATGCCTTTC GCGACACCCA TGGAAGCAGA
651 GCTGGCCCGC AGGAGCCTGG CCCAGGATGC CCCACCGCTT CCTGTGCCAG
701 GGGTGCTTCT GAAGGAGTTC ACTGTGTCCG GCAACATACT GACTATCCGA
751 CTGACTGCTG CAGACCACCG CCAACTGCAG CTCTCCATCA GCTCCTGTCA
801 CCAGCAGCTT TCCCTGTTGA TGTGGATCAC GCAGTGCTTT CTGCCCGTGT
                                    <--|*  XhoI
851 TTTTGGCTCA GCCTCCCTCA GGGCAGAGGC GCTAACTCGA G
```

A.2 pCT-N9V

Backbone: pCT2
Description: Basic N9V surface-display construct, with the epitope in the context of the extended 15-mer CMV-derived peptide.

```
    |--> Aga2p
  1 ATGCAGTTAC TTCGCTGTTT TTCAATATTT TCTGTTATTG CTTCAGTTTT
 51 AGCACAGGAA CTGACAACTA TATGCGAGCA AATCCCCTCA CCAACTTTAG
101 AATCGACGCC GTACTCTTTG TCAACGACTA CTATTTTGGC CAACGGGAAG
151 GCAATGCAAG GAGTTTTTGA ATATTACAAA TCAGTAACGT TTGTCAGTAA
201 TTGCGGTTCT CACCCCTCAA CAACTAGCAA AGGCAGCCCC ATAAACACAC
          <--|                                    |-->
251 AGTATGTTTT TAAGGACAAT AGCTCGACGA TTGAAGGTAG ATACCCATAC
    HA tag         <--|PstI           |--> (G4S)3 linker
301 GACGTTCCAG ACTACGCTCT GCAGGCTAGT GGTGGAGGAG GCTCTGGTGG
                          <--|NheI    |--> ARNLVPMVATVQGQN
351 AGGCGGTAGC GGAGGCGGAG GGTCGGCTAG CGCTAGAAAT TTGGTTCCAA
```

```
                              <--|BamHI  |--> c-myc tag
401 TGGTTGCTAC TGTTCAAGGT CAAAACGGAT CCGAACAAAA GCTTATTTCT
            <--|*  *  XhoI
451 GAAGAGGACT TGTAATAGCT CGAG
```

A.3 pCTc-N9V

Backbone: pCT-N9V
Description: Modified from the pCT-N9V plasmid by replacing the signal peptide of aga2p with just an initial methionine. When transformed into a yeast strain lacking aga1p, the aga2p fusion protein is expressed intracellularly upon induction instead of being surface-displayed.

```
    Met|--> Aga2p without signal peptide
  1 ATGCAGGAAC TGACAACTAT ATGCGAGCAA ATCCCCTCAC CAACTTTAGA
 51 ATCGACGCCG TACTCTTTGT CAACGACTAC TATTTTGGCC AACGGGAAGG
101 CAATGCAAGG AGTTTTTGAA TATTACAAAT CAGTAACGTT TGTCAGTAAT
151 TGCGGTTCTC ACCCCTCAAC AACTAGCAAA GGCAGCCCCA TAAACACACA
       <--|                                      |--> HA
201 GTATGTTTTT AAGGACAATA GCTCGACGAT TGAAGGTAGA TACCCATACG
    tag           <--|PstI          |--> (G4S)3 linker
251 ACGTTCCAGA CTACGCTCTG CAGGCTAGTG GTGGAGGAGG CTCTGGTGGA
                        <--|NheI    |--> ARNLVPMVATVQGQN
301 GGCGGTAGCG GAGGCGGAGG GTCGGCTAGC GCTAGAAATT TGGTTCCAAT
                         <--|BamHI  |--> c-myc tag
351 GGTTGCTACT GTTCAAGGTC AAAACGGATC CGAACAAAAG CTTATTTCTG
          <--|*  *  XhoI
401 AAGAGGACTT GTAATAGCTC GAG
```

A.4 pCT-C1-N9V

Backbone: pCT-N9V
Description: The C1 linker, EKARVLAEAA, was inserted between the $(G_4S)_3$ linker and the A15N peptide in pCT-N9V. The final Ala is encoded by the *Nhe*I site. Only the sequence between the *Pst*I and *Nhe*I sites are shown; the rest is identical to pCT-N9V.

```
    PstI          |--> (G4S)3 linker
  1 CTGCAGGCTA GTGGTGGAGG AGGCTCTGGT GGAGGCGGTA GCGGAGGCGG
     <--|         |--> EKARVLAEAA              <--|NheI
 51 AGGGTCGGCT AGTGAAAAAG CTAGAGTTTT GGCTGAAGCT GCTAGC
```

A.5 pCT-C2-N9V

Backbone: pCT-N9V
Description: The C2 linker, SSAESLK, was inserted between the $(G_4S)_3$ linker and the A15N peptide in pCT-N9V. Only the sequence between the *Pst*I and *Nhe*I sites are shown; the rest is identical to pCT-N9V.

```
    PstI          |--> (G4S)3 linker
  1 CTGCAGGCTA GTGGTGGAGG AGGCTCTGGT GGAGGCGGTA GCGGAGGCGG
     <--|         |--> SSAESLK        <--|NheI
 51 AGGGTCGGCT AGTTCTTCTG CTGAATCTTT GAAAGCTAGC
```

A.6 pCT-C3-N9V

Backbone: pCT-N9V
Description: The C3 linker, NWVCAAKF, was inserted between the $(G_4S)_3$ linker and the A15N peptide in pCT-N9V. Only the sequence between the *Pst*I and *Nhe*I sites are shown; the rest is identical to pCT-N9V.

```
   PstI          |--> (G4S)3 linker
 1 CTGCAGGCTA GTGGTGGAGG AGGCTCTGGT GGAGGCGGTA GCGGAGGCGG
     <--|        |--> NWVCAAKF          <--|NheI
51 AGGGTCGGCT AGTAATTGGG TTTGTGCTGC TAAATTTGCT AGC
```

A.7 pCT-C4-N9V

Backbone: pCT-N9V
Description: The C4 linker, GILQINSR, was inserted between the $(G_4S)_3$ linker and the A15N peptide in pCT-N9V. Only the sequence between the *Pst*I and *Nhe*I sites are shown; the rest is identical to pCT-N9V.

```
   PstI          |--> (G4S)3 linker
 1 CTGCAGGCTA GTGGTGGAGG AGGCTCTGGT GGAGGCGGTA GCGGAGGCGG
     <--|        |--> GILQINSR          <--|NheI
51 AGGGTCGGCT AGTGGTATTT TGCAGATTAA TTCTAGAGCT AGC
```

A.8 pCT-C5-N9V

Backbone: pCT-N9V
Description: The C5 linker, QWLGAPVP, was inserted between the $(G_4S)_3$ linker and the A15N peptide in pCT-N9V. Only the sequence between the *Pst*I and *Nhe*I sites are shown; the rest is identical to pCT-N9V.

```
   PstI          |--> (G4S)3 linker
 1 CTGCAGGCTA GTGGTGGAGG AGGCTCTGGT GGAGGCGGTA GCGGAGGCGG
     <--|        |--> QWLGAPVP          <--|NheI
51 AGGGTCGGCT AGTCAATGGT TGGGTGCTCC AGTTCCAGCT AGC
```

A.9 pNL-N9V

Backbone: pCT-N9V
Description: The $(G_4S)_3$ linker of pCT-N9V was deleted by digesting with *Pst*I and *Nhe*I and ligating the blunt ends generated by using Klenow fragment to remove the *Pst*I 3' overhang and fill in the *Nhe*I 5' overhang.

```
   |--> Aga2p
  1 ATGCAGTTAC TTCGCTGTTT TTCAATATTT TCTGTTATTG CTTCAGTTTT
 51 AGCACAGGAA CTGACAACTA TATGCGAGCA AATCCCCTCA CCAACTTTAG
101 AATCGACGCC GTACTCTTTG TCAACGACTA CTATTTTGGC CAACGGGAAG
151 GCAATGCAAG GAGTTTTTGA ATATTACAAA TCAGTAACGT TTGTCAGTAA
201 TTGCGGTTCT CACCCCTCAA CAACTAGCAA AGGCAGCCCC ATAAACACAC
          <--|                                  |-->
251 AGTATGTTTT TAAGGACAAT AGCTCGACGA TTGAAGGTAG ATACCCATAC
```

```
    HA tag          <--|        |--> ARNLVPMVATVQGQN
301 GACGTTCCAG ACTACGCTCC TAGCGCTAGA AATTTGGTTC CAATGGTTGC
                     <--|BamHI   |--> c-myc tag
351 TACTGTTCAA GGTCAAAACG GATCCGAACA AAAGCTTATT TCTGAAGAGG
     <--|*  *   XhoI
401 ACTTGTAATA GCTCGAG
```

A.10 pCT-(C1)$_4$-N9V

Backbone: pCT-N9V
Description: Four copies of the C1 linker were inserted between the $(G_4S)_3$ linker and the NheI site of pCT-N9V. Only the sequence between the *Pst*I and *Nhe*I sites are shown; the rest is identical to pCT-N9V.

```
    PstI          |--> (G4S)3 linker
  1 CTGCAGGCTA GTGGTGGAGG AGGCTCTGGT GGAGGCGGTA GCGGAGGCGG
      <--|        |--> EKARVLAEAA              <--|    |-->
 51 AGGGTCGGCT AGTGAAAAAG CTAGAGTTTT GGCTGAAGCT GCTAGTGAAA
    EKARVLAEAA              <--|    |--> EKARVLAEAA
101 AAGCTAGAGT TTTGGCTGAA GCTGCTAGTG AAAAAGCTAG AGTTTTGGCT
         <--|     |--> EKARVLAEAA              <--|NheI
151 GAAGCTGCTA GTGAAAAAGC TAGAGTTTTG GCTGAAGCTG CTAGC
```

A.11 HEAF 3.12

Backbone: pCT
Description: "HEAF" is short for high-expressing anti-fluorescein and it is a mutant of Eric Boder's 4M3.12 fluorescein-binding scFv. Introduction of five mutations, K182N, F186S, S187P, F315S and N351D (numbered from the start of the aga2p fusion protein) increased the expression level by 4-5 fold. However, the mutations also weakened the affinity and gave rise to a bi-exponential k_{off} curve. Only the sequence between the *Nhe*I and *Xho*I sites are shown, with the mutations highlighted.

```
    NheI  |--> scFv
  1 GCTAGCGACG TCGTTATGAC TCAAACACCA CTATCACTTC CTGTTAGTCT
 51 AGGTGATCAA GCCTCCATCT CTTGCAGATC TAGTCAGAGC CTTGTACACA
101 GTAATGGAAA CACCTATTTA CGTTGGTACC TGCAGAAGCC AGGCCAGTCT
151 CCAAAGGTCC TGATCTACAA AGTTTCCAAC CGATTTCTG GAGTCCCAGA
201 CAGGTTCAGT GGCAGTGGAT CAGGGACAGA TTTCACGCTC AAGATCAGCA
251 GAGTGGAGGC TGAGGATCTG GGAGTTTATT TCTGCTCTCA AAGTACACAT
301 GTTCCGTGGA CGTTCGGTGG AGGCACCAAG CTTGAAATTA AGTCCTCTGC
351 TGATGATGCT AAGAAGGATG CTGCTAAGAA GGATGATGCT AAGAAAGATG
401 ATGCTAAGAA AGATGGTGAC GTCAAACTGG ATGAGACTGG AGGAGGCTTG
451 GTGCAACCTG GGAGGCCCAT GAAACTCTCC TGTGTTACCT CTGGATTCAC
501 TTTTAGTGAC TACTGGATGA ACTGGGTCCG CCAGTCTCCA GAGAAAGGAC
551 TGGAGTGGAT AGCACAATAT AGAAACAAAC CTTATAATTA TGAAACATAT
601 TATTCAGATT CTGTGAAAGG CAGATTCACC ATCTCAAGAG ATGATTCCAA
651 AAGTAGTGTC TATCTGCAAA TGAACAACTT AAGAGTTGAA GACACGGGTA
701 TCTATTACTG TACGGGTTCT TACTATGGTA TGGACTACTT GGGTCAAGGA
                      <--||--> c-myc tag
751 ACTTCAGTCA CCGTCTCCTC AGAACAAAAG CTTATTTCTG AAGAAGACTT
 <--|*  *  XhoI
801 GTAATAGCTC GAG
```

A.12 pMSCE

Backbone: pMal-c2x (New England Biolabs)
Description: The first construct used for bacterial expression of a fusion protein containing NY-ESO-1 (CS mutant) that can be site-specifically conjugated to yeast via the SNAP-tag.

```
    NdeI|--> Cytoplasmic maltose-binding protein
   1 CATATGAAAA TCGAAGAAGG TAAACTGGTA ATCTGGATTA ACGGCGATAA
  51 AGGCTATAAC GGTCTCGCTG AAGTCGGTAA GAAATTCGAG AAAGATACCG
 101 GAATTAAAGT CACCGTTGAG CATCCGGATA AACTGGAAGA GAAATTCCCA

 151 CAGGTTGCGG CAACTGGCGA TGGCCCTGAC ATTATCTTCT GGGCACACGA
 201 CCGCTTTGGT GGCTACGCTC AATCTGGCCT GTTGGCTGAA ATCACCCCGG
 251 ACAAAGCGTT CCAGGACAAG CTGTATCCGT TTACCTGGGA TGCCGTACGT
 301 TACAACGGCA AGCTGATTGC TTACCCGATC GCTGTTGAAG CGTTATCGCT
 351 GATTTATAAC AAAGATCTGC TGCCGAACCC GCCAAAAACC TGGGAAGAGA
 401 TCCCGGCGCT GGATAAAGAA CTGAAAGCGA AAGGTAAGAG CGCGCTGATG
 451 TTCAACCTGC AAGAACCGTA CTTCACCTGG CCGCTGATTG CTGCTGACGG
 501 GGGTTATGCG TTCAAGTATG AAAACGGCAA GTACGACATT AAAGACGTGG
 551 GCGTGGATAA CGCTGGCGCG AAAGCGGGTC TGACCTTCCT GGTTGACCTG
 601 ATTAAAAACA AACACATGAA TGCAGACACC GATTACTCCA TCGCAGAAGC
 651 TGCCTTTAAT AAAGGCGAAA CAGCGATGAC CATCAACGGC CCGTGGGCAT
 701 GGTCCAACAT CGACACCAGC AAAGTGAATT ATGGTGTAAC GGTACTGCCG
 751 ACCTTCAAGG GTCAACCATC CAAACCGTTC GTTGGCGTGC TGAGCGCAGG
 801 TATTAACGCC GCCAGTCCGA ACAAAGAGCT GGCAAAAGAG TTCCTCGAAA
 851 ACTATCTGCT GACTGATGAA GGTCTGGAAG CGGTTAATAA AGACAAACCG
 901 CTGGGTGCCG TAGCGCTGAA GTCTTACGAG GAAGAGTTGG CGAAAGATCC
 951 ACGTATTGCC GCCACTATGG AAAACGCCCA GAAAGGTGAA ATCATGCCGA
1001 ACATCCCGCA GATGTCCGCT TTCTGGTATG CCGTGCGTAC TGCGGTGATC
1051 AACGCCGCCA GCGGTCGTCA GACTGTCGAT GAAGCCCTGA AAGACGCGCA
     <--|      SacI     |--> N10 linker                <--|AvaI:used to clone
1101 GACTAATTCG AGCTCGAACA ACAACAACAA TAACAATAAC AACAACCTCG SNAP-tag but not
       |--> SNAP-tag                                      unique after NY-
1151 GGATGGACAA AGATTGCGAA ATGAAACGTA CCACCCTGGA TAGCCCGCTG ESO-CS was added
1201 GGCAAACTGG AACTGAGCGG CTGCGAACAG GGCCTGCATG AAATTAAACT
1251 GCTGGGTAAA GGCACCAGCG CGGCCGATGC GGTTGAAGTT CCGGCCCCGG
1301 CCGCCGTGCT GGGTGGTCCG GAACCGCTGA TGCAGGCGAC CGCGTGGCTG
1351 AACGCGTATT TTCATCAGCC GGAAGCGATT GAAGAATTTC CGGTTCCGGC
1401 GCTGCATCAT CCGGTGTTTC AGCAGGAGAG CTTTACCCGT CAGGTGCTGT
1451 GGAAACTGCT GAAAGTGGTT AAATTTGGCG AAGTGATTAG CTATCAGCAG
1501 CTGGCGGCCC TGGCGGGTAA TCCGGCGGCC ACCGCCGCCG TTAAAACCGC
1551 GCTGAGCGGT AACCCGGTGC CGATTCTGAT TCCGTGCCAT CGTGTGGTTA
1601 GCTCTAGCGG TGCGGTTGGC GGTTATGAAG GTGGTCTGGC GGTGAAAGAG
                                                  <--|EcoRI
1651 TGGCTGCTGG CCCATGAAGG TCATCGTCTG GGTAAACCGG GTCTGGGAGA
       |--> GGGGS  <--|       |--> (C1)4
1701 ATTCGGAGGC GGAGGGTCGG CTAGTGAAAA AGCTAGAGTT TTGGCTGAAG
1751 CTGCTAGTGA AAAAGCTAGA GTTTTGGCTG AAGCTGCTAG TGAAAAAGCT
1801 AGAGTTTTGG CTGAAGCTGC TAGTGAAAAA GCTAGAGTTT TGGCTGAAGC
    <--|NheI|--> ASARNLVPMVATVQGQN (surrogate CMV antigen)
1851 TGCTAGCGCT AGAAATTTGG TTCCAATGGT TGCTACTGTT CAAGGTCAAA
   <--|BamHI |--> NY-ESO-CS
1901 ACGGATCCAT GCAGGCCGAA GGCCGGGGCA CAGGGGGTTC GACGGGCGAT
1951 GCTGATGGCC CAGGAGGCCC TGGCATTCCT GATGGCCCAG GGGGCAATGC
```

```
2001 TGGCGGCCCA GGAGAGGCGG GTGCCACGGG CGGCAGAGGT CCCCGGGGCG
2051 CAGGGGCAGC AAGGGCCTCG GGGCCGGGAG GAGGCGCCCC GCGGGGTCCG
2101 CATGGCGGCG CGGCTTCAGG GCTGAATGGA AGCAGCAGAA GCGGGGCCAG
2151 GGGGCCGGAG AGCCGCCTGC TTGAGTTCTA CCTCGCCATG CCTTTCGCGA
2201 CACCCATGGA AGCAGAGCTG GCCCGCAGGA GCCTGGCCCA GGATGCCCCA
2251 CCGCTTCCCG TGCCAGGGGT GCTTCTGAAG GAGTTCACTG TGTCCGGCAA
2301 CATACTGACT ATCCGACTGA CTGCTGCAGA CCACCGCCAA CTGCAGCTCT
2351 CCATCAGCTC CTGTCTCCAG CAGCTTTCCC TGTTGATGTG GATCACGCAG
                                                        *
2401 TGCTTTCTGC CCGTGTTTTT GGCTCAGCCT CCCTCAGGGC AGAGGCGCTG
      HindIII
2451 AAAGCTT
```

A.13 pMSCcmyc

Backbone: pMal-c2x
Description: Used to produce a control protein lacking NY-ESO-1. Its sequence is identical to that of pMSCE except that there is only a c-myc tag between the *Bam*HI and *Hind*III sites (only this is shown below).

```
    BamHI |--> c-myc tag                    *HindIII
  1 GGATCCGAAC AAAAACTTAT TTCTGAAGAG GACTTGTAAG CTT
```

A.14 pCT-Lys10

Backbone: pCT2
Description: Used to surface display a polypeptide containing 10 lysine residues in the form of repeats of the sequence GGGGKGS. The sequences of the other pCT-LysX plasmids can be inferred by analogy.

```
     |--> Aga2p
   1 ATGCAGTTAC TTCGCTGTTT TTCAATATTT TCTGTTATTG CTTCAGTTTT
  51 AGCACAGGAA CTGACAACTA TATGCGAGCA AATCCCCTCA CCAACTTTAG
 101 AATCGACGCC GTACTCTTTG TCAACGACTA CTATTTTGGC CAACGGGAAG
 151 GCAATGCAAG GAGTTTTTGA ATATTACAAA TCAGTAACGT TTGTCAGTAA
 201 TTGCGGTTCT CACCCCTCAA CAACTAGCAA AGGCAGCCCC ATAAACACAC
           <--|                                    |-->
 251 AGTATGTTTT TAAGGACAAT AGCTCGACGA TTGAAGGTAG ATACCCATAC
     HA tag          <--|PstI    |--> KGS(GGGGKGS)9
 301 GACGTTCCAG ACTACGCTCT GCAGAAAGGA TCTGGTGGAG GCGGTAAAGG
 351 ATCTGGTGGA GGCGGTAAAG GATCTGGTGG AGGCGGTAAA GGATCTGGTG
 401 GAGGCGGTAA AGGATCTGGT GGAGGCGGTA AAGGATCTGG TGGAGGCGGT
 451 AAAGGATCTG GTGGAGGCGG TAAAGGATCT GGTGGAGGCG GTAAAGGATC
                     BamHI
                        <--||--> c-myc tag
 501 TGGTGGAGGC GGTAAAGGAT CCGAACAAAA GCTTATTTCT GAAGAGGACT
   <--|*  *  XhoI
 551 TGTAATAGCT CGAG
```

A.15 pRS304-aga2p-HA

Backbone: pRS304

Description: Integrating shuttle vector used to derive SWH100 yeast from EBY100 yeast. Upon galactose induction, HA-tagged aga2p protein (with no additional fusions) is expressed.

```
    |--> aga2p
  1 ATGCAGTTAC TTCGCTGTTT TTCAATATTT TCTGTTATTG CTTCAGTTTT
 51 AGCACAGGAA CTGACAACTA TATGCGAGCA AATCCCCTCA CCAACTTTAG
101 AATCGACGCC GTACTCTTTG TCAACGACTA CTATTTTGGC CAACGGGAAG
151 GCAATGCAAG GAGTTTTTGA ATATTACAAA TCAGTAACGT TTGTCAGTAA
201 TTGCGGTTCT CACCCCTCAA CAACTAGCAA AGGCAGCCCC ATAAACACAC
          <--|                                    |--> HA
251 AGTATGTTTT TAAGGACAAT AGCTCGACGA TTGAAGGTAG ATACCCATAC
    tag            <--|       *  *         BamHI
301 GACGTTCCAG ACTACGCTCC TAGCTAATAG GGTGGCGGAT CC
```

A.16 pMSICE

Backbone: pMSCE
Description: The $(C1)_4$ sequence in pMSCE was replaced with a pH-sensitive self-cleaving intein, ΔI-CM (DW Wood et al., 1999, Nature Biotech. **17**: 889-892). In this particular plasmid, the first codon downstream of the intein encodes Met; other versions were made where this codon was changed to alter the cleavage kinetics. Only the sequence between the *Eco*RI and *Nhe*I sites is shown, with the rest being identical to pMSCE.

```
    EcoRI |--> intein
  1 GAATTCGCCC TCGCAGAGGG CACTCGGATC TTCGATCCGG TCACCGGTAC
 51 AACGCATCGC ATCGAGGATG TTGTCGGTGG GCGCAAGCCT ATTCATGTCG
101 TGGCTGCTGC CAAGGACGGA ACGCTGCGTG CGCGGCCCGT GGTGTCCTGG
151 TTCGACCAGG GAACGCGGGA TGTGATCGGG TTGCGGATCG CCGGTGGCGC
201 CATCCTGTGG GCGACACCCG ATCACAAGGT GCTGACAGAG TACGGCTGGC
251 GTGCCGCCGG GGAACTCCGC AAGGGAGACA GGGTGGCGCA ACCGCGACGC
301 TTCGATGGAT TCGGTGACAG TGCGCCGATT CCGGCGCGCG TGCAGGCGCT
351 CGCGGATGCC CTGGATGACA AATTCCTGCA CGACATGCTG GCGGAAGAAC
401 TCCGCTATTC CGTGATCCGA GAAGTGCTGC CAACGCGGCG GGCACGGACG
451 TTCGGCCTCG AGGTCGAGGA ACTGCACACC CTCGTCGCCG AAGGGGTTGT
          <--| Met NheI
501 TGTACACAAC ATGGCTAGC
```

A.17 pMS74NEY2

Backbone: pMal-c2x
Description: This construct produces the latest generation fusion protein that permits multi-layer conjugation to yeast particles; phagosomal antigen release is mediated by the ectodomain of the invariant chain, CD74. The N9V epitope was mutated to NLVPMIATV to inhibit CatS cleavage. Purification of the full-length protein is facilitated by the C-terminal His_6 tag.

```
   NdeI|--> Cytoplasmic maltose-binding protein
  1 CATATGAAAA TCGAAGAAGG TAAACTGGTA ATCTGGATTA ACGGCGATAA
 51 AGGCTATAAC GGTCTCGCTG AAGTCGGTAA GAAATTCGAG AAAGATACCG
101 GAATTAAAGT CACCGTTGAG CATCCGGATA AACTGGAAGA GAAATTCCCA
151 CAGGTTGCGG CAACTGGCGA TGGCCCTGAC ATTATCTTCT GGGCACACGA
201 CCGCTTTGGT GGCTACGCTC AATCTGGCCT GTTGGCTGAA ATCACCCCGG
251 ACAAAGCGTT CCAGGACAAG CTGTATCCGT TTACCTGGGA TGCCGTACGT
```

```
 301 TACAACGGCA AGCTGATTGC TTACCCGATC GCTGTTGAAG CGTTATCGCT
 351 GATTTATAAC AAAGATCTGC TGCCGAACCC GCCAAAAACC TGGGAAGAGA
 401 TCCCGGCGCT GGATAAAGAA CTGAAAGCGA AAGGTAAGAG CGCGCTGATG
 451 TTCAACCTGC AAGAACCGTA CTTCACCTGG CCGCTGATTG CTGCTGACGG
 501 GGGTTATGCG TTCAAGTATG AAAACGGCAA GTACGACATT AAAGACGTGG
 551 GCGTGGATAA CGCTGGCGCG AAAGCGGGTC TGACCTTCCT GGTTGACCTG
 601 ATTAAAAACA AACACATGAA TGCAGACACC GATTACTCCA TCGCAGAAGC
 651 TGCCTTTAAT AAAGGCGAAA CAGCGATGAC CATCAACGGC CCGTGGGCAT
 701 GGTCCAACAT CGACACCAGC AAAGTGAATT ATGGTGTAAC GGTACTGCCG
 751 ACCTTCAAGG GTCAACCATC CAAACCGTTC GTTGGCGTGC TGAGCGCAGG
 801 TATTAACGCC GCCAGTCCGA ACAAAGAGCT GGCAAAAGAG TTCCTCGAAA
 851 ACTATCTGCT GACTGATGAA GGTCTGGAAG CGGTTAATAA AGACAAACCG
 901 CTGGGTGCCG TAGCGCTGAA GTCTTACGAG GAAGAGTTGG CGAAAGATCC
 951 ACGTATTGCC GCCACTATGG AAAACGCCCA GAAAGGTGAA ATCATGCCGA
1001 ACATCCCGCA GATGTCCGCT TTCTGGTATG CCGTGCGTAC TGCGGTGATC
1051 AACGCCGCCA GCGGTCGTCA GACTGTCGAT GAAGCCCTGA AAGACGCGCA
     <--|      SacI     |--> N10 linker                <--|AvaI:used to clone
1101 GACTAATTCG AGCTCGAACA ACAACAACAA TAACAATAAC AACAACCTCG SNAP-tag but not
       |--> SNAP-tag                                       unique after NY-
1151 GGATGGACAA AGATTGCGAA ATGAAACGTA CCACCCTGGA TAGCCCGCTG ESO-CS was added
1201 GGCAAACTGG AACTGAGCGG CTGCGAACAG GGCCTGCATG AAATTAAACT
1251 GCTGGGTAAA GGCACCAGCG CGGCCGATGC GGTTGAAGTT CCGGCCCCGG
1301 CCGCCGTGCT GGGTGGTCCG GAACCGCTGA TGCAGGCGAC CGCGTGGCTG
1351 AACGCGTATT TTCATCAGCC GGAAGCGATT GAAGAATTTC CGGTTCCGGC
1401 GCTGCATCAT CCGGTGTTTC AGCAGGAGAG CTTTACCCGT CAGGTGCTGT
1451 GGAAACTGCT GAAAGTGGTT AAATTTGGCG AAGTGATTAG CTATCAGCAG
1501 CTGGCGGCCC TGGCGGGTAA TCCGGCGGCC ACCGCCGCCG TTAAAACCGC
1551 GCTGAGCGGT AACCCGGTGC CGATTCTGAT TCCGTGCCAT CGTGTGGTTA
1601 GCTCTAGCGG TGCGGTTGGC GGTTATGAAG GTGGTCTGGC GGTGAAAGAG
                                                  <--|EcoRI
1651 TGGCTGCTGG CCCATGAAGG TCATCGTCTG GGTAAACCGG GTCTGGGAGA
         |--> CD74 ectodomain (aa 73-207)
1701 ATTCCAGCAG CAGGGCCGGC TGGACAAACT GACAGTCACC TCCCAGAACC
                              HindIII (makes final site not unique)
1751 TGCAGCTGGA GAACCTGCGC ATGAAGCTTC CCAAGCCTCC CAAGCCTGTG
1801 AGCAAGATGC GCATGGCCAC CCCGCTGCTG ATGCAGGCGC TGCCCATGGG
1851 AGCCCTGCCC CAGGGGCCCA TGCAGAATGC CACCAAGTAT GGCAACATGA
1901 CAGAGGACCA TGTGATGCAC CTGCTCCAGA ATGCTGACCC CCTGAAGGTG
1951 TACCCGCCAC TGAAGGGGAG CTTCCCGGAG AACCTGAGAC ACCTTAAGAA
2001 CACCATGGAG ACCATAGACT GGAAGGTCTT TGAGAGCTGG ATGCACCATT
2051 GGCTCCTGTT TGAAATGAGC AGGCACTCCT TGGAGCAAAA GCCCACTGAC
         <--|NheI    |--> ARNLVPMIATVQGQN
2101 GCTCCACCGG CTAGCGCTAG AAATTTGGTT CCAATGATTG CTACTGTTCA
          <--| BamHI |--> NY-ESO-CS
2151 AGGTCAAAAC GGATCCATGC AGGCCGAAGG CCGGGGCACA GGGGGTTCGA
2201 CGGGCGATGC TGATGGCCCA GGAGGCCCTG GCATTCCTGA TGGCCCAGGG
2251 GGCAATGCTG GCGGCCCAGG AGAGGCGGGT GCCACGGGCG GCAGAGGTCC
2301 CCGGGGCGCA GGGGCAGCAA GGGCCTCGGG GCCGGGAGGA GGCGCCCCGC
2351 GGGGTCCGCA TGGCGGCGCG GCTTCAGGGC TGAATGGAAG CAGCAGAAGC
2401 GGGGCCAGGG GGCCGGAGAG CCGCCTGCTT GAGTTCTACC TCGCCATGCC
2451 TTTCGCGACA CCCATGGAAG CAGAGCTGGC CCGCAGGAGC CTGGCCCAGG
2501 ATGCCCCACC GCTTCCCGTG CCAGGGGTGC TTCTGAAGGA GTTCACTGTG
2551 TCCGGCAACA TACTGACTAT CCGACTGACT GCTGCAGACC ACCGCCAACT
2601 GCAGCTCTCC ATCAGCTCCT GTCTCCAGCA GCTTTCCCTG TTGATGTGGA
2651 TCACGCAGTG CTTTCTGCCC GTGTTTTTGG CTCAGCCTCC CTCAGGGCAG
```

```
            BsrGI
      <--||--> TVQL<--||--> (G4S)3 linker
2701 AGGCGCACTG TACAGCTGGG TGGCGGCGGT AGCGGTGGCG GTGGCTCTGG
               <--||--> ybbR tag (DSLEFIASKLA)     <--||-->
2751 CGGTGGTGGC TCCGATTCTC TTGAATTTAT TGCTAGTAAA CTTGCGCACC
     His6 tag   <--|*  HindIII
2801 ATCACCACCA CCATTGAAAG CTT
```

A.18 IIIa5.3.7

Backbone: pCT
Description: This is one of the two fibronectin domains evolved to bind to human FcγRIIIA that was selected for further investigation. Only the sequence between the *Pst*I and *Bam*HI sites is shown (i.e. the $(G_4S)_3$ linker and the fibronectin domain).

```
     PstI
   1 CTGCAGGCTA GTGGTGGTGG TGGTTCTGGT GGCGGTGGTT CTGGTGGTGG
  51 TGGTTCTGCT AGCGTTTCCG ATGTTCCGAG GGACCTGGAA GTTGTTGTTG
 101 CGACCCCCAC CAGCCTACTG ATCAACTGGG ATTTGCCCTT TTCGGACTCT
 151 TACAGGATCA CTTACGGAGA AACAGGAGGA AATAGCCCTG TCCAGGGGTT
 201 CACTGTGCCT GGTACCGAGT CTATCGCTAC CATCAGCGGC CTTAAACCTG
 251 GAGTTGATTA TACCATCACT GTGTATGCTG TCGCTTCTAG TGGGTCTAAC
 301 TCTTATCCAA TTTCCATTAA TTACCGAACA GAAATTGACA AACCATCCCA
     BamHI
 351 GGGATCC
```

A.19 IIIa6.2.6

Backbone: pCT
Description: This is one of the two fibronectin domains evolved to bind to human FcγRIIIA that was selected for further investigation. Only the sequence between the *Pst*I and *Bam*HI sites is shown (i.e. the $(G_4S)_3$ linker and the fibronectin domain).

```
     PstI
   1 CTGCAGGCTA GTGGTGGTGG TGGTTCTGAT GGTGGTTCTG GTGGTGGTGG
  51 CTCTGCTAGC GTTTCTGATG TTCCGAGGGA CCTGGAAGTT GTTGTTGCGA
 101 CCCCCACCAG CCTACTGATC AACTGGGATA TGCCCTTTTC GGACTCTTAC
 151 AGGATCGCTT ACGGAGAAAC AGGAGGAAAT AGCCCTGTCC AGGAGTTCAC
 201 TGTGCCTGGT ACCGACTCTC TCGCTACCAT CAGCGGCCTT AAACCTGGAG
 251 TTGATTATAC CATCACTGTG TATGCTGTCA CTTCTAGTGG GTCTAACTCT
 301 TATCCAATTT CCATTAATTA CCGGACAGAA ATTGACAAAC CATCCCAGGG
    BamHI
 351 ATCC
```

A.20 IIa7.2.6

Backbone: pCT
Description: This is one of the two fibronectin domains evolved to bind selectively to human FcγRIIA but not FcγRIIB that was selected for further investigation. Only the sequence between the *Pst*I and *Bam*HI sites is shown (i.e. the $(G_4S)_3$ linker and the fibronectin domain).

```
     PstI
   1 CTGCAGGCTA GTGGTGGTGG TGGTTCTGGT GGTGGTGGTT CTGGTGGTAG
  51 TGGTTCTGCT AGCGTTTCTG ATGTTCCGGG GGACCTGGAA GTTGTTGCTG
 101 CGACCCCCAC CAGCCTACTG ATTAGCTGGT GTACCCATCT ACATTGGGAT
 151 TATTACAGGA TCTTTTACGG AGAAACAGGA GGAAATAGCC CTGTCCAGGA
 201 GTTCACTGTG CCTGCCCTCT GTCCCGGGGC TACCATTAGC GGCCTTAAAC
 251 CTGGAGTTGA TTATACCATC ACTGCGTATG CTGTCACTGT GGGGGGGGAT
 301 GATTGGCCAA TTTCCATTAA TTACCGAACA GAAATTGACG AACCATCCCA
     BamHI
 351 GGGATCC
```

A.21 IIa8.2.7

Backbone: pCT
Description: This is one of the two fibronectin domains evolved to bind selectively to human FcγRIIA but not FcγRIIB that was selected for further investigation. Only the sequence between the *Pst*I and *Bam*HI sites is shown (i.e. the $(G_4S)_3$ linker and the fibronectin domain).

```
     PstI
   1 CTGCAGGCTA GTGGTGGTGG TGGTTCTGGT GGTGGTGGTT CTGGTGGTAG
  51 TGGTTCTGCT AGCGTTTCTG ATGTTCCGGG GGACCTGGAA GTTGTTGCTG
 101 CGACCCCCAC CAGCCTACTG ATTAGCTGGT GTACCCATCT ACATTGGGAT
 151 TATTACAGGA TCTTTTACGG AGAAACAGGA GGAAATAGCC CTGTCCAGGA
 201 GTTCACTGTG CCTGCCCTCT GTCCCGGGGC TACCATTAGC GGCCTTAAAC
 251 CTGGAGTTGA TTATACCATC ACTGCGTATG CTGTCACTGT GGGGGGGGAT
 301 GATTGGCCAA GTTCCATTAA TTACCGAACA GAAATTGACG AACCATCCCA
     BamHI
 351 GGGATCC
```

Appendix B – Details of Selected Protocols

B.1 Generation of monocyte-derived DCs

Monocyte sources
Elutriated monocytes from Advanced Biotechnologies Inc (07-210-000)
or
Monocytes purified by negative magnetic cell sorting from leukapheresis packs from Biological Specialty Corporation (custom product)

The expected yield from either company is roughly 10^9 cells. At the time I made my inquiry, ABI only had one known HLA-A*0201 donor. The first batch from this donor worked well but subsequent batches gave rise to abnormal cross-presentation results.

C10 medium
500 ml RPMI-1640 with glutamine (HyClone SH30027.01)
50 ml low endotoxin fetal calf serum (FCS, HyClone SH30073.03, no need to heat inactivate)
5 ml 100× non-essential amino acids (HyClone SH30238.01)
5 ml 100 mM sodium pyruvate (Hyclone SH30239.01)
5 ml 1 M Hepes solution, pH 7.2-7.4 (HyClone discontinued, switched to Amresco J848)
1 ml Primocin (InvivoGen ant-pm-1)
1.75 µl β-mercaptoethanol (final concentration of 50 µM)
Filter sterilize after mixing.

Cytokines
Recombinant human IL-4 (R&D Systems 204-IL, treat as 2.9×10^4 U/µg)
Recombinant human GM-CSF (R&D Systems 215-GM, treat as 1.5×10^4 U/µg)
Dissolve each in PBS + 1% BSA to 1×10^5 U/ml and freeze in 0.5 ml aliquots. Keep one aliquot at 4°C.

Monocyte cryopreservation
- Before the monocytes arrive, thaw 2 aliquots of 50 ml FCS. Add 12.5 ml sterile DMSO to 50 ml FCS. Chill both the FCS and the FCS + 20% DMSO on ice. Also chill about 50 cryogenic vials. Ensure that at least 3 "Mr Frosty" containers are available and at room temperature.
- Centrifuge the monocytes at 200×g for 10 min and discard the supernatant.
- The monocyte preparation from BSC also contains platelets. To remove the platelets, wash twice with PBS (fill each 50 ml tube), centrifuging as above. These wash steps can be omitted with ABI's elutriated monocytes.
- Resuspend in 25 ml cold FCS (less if listed cell yield is fewer than 10^9 cells).
- Count the cells with trypan blue and the hematocytometer. The viability should be >90% and the cell concentration should be 4-6 × 10^7 cells/ml. Add FCS if necessary.
- Add an equal volume of cold FCS + 20% DMSO drop-wise while gentle swirling. Keep cold.

- Fill cryogenic vials on ice with 1 ml of cell suspension. It is a good idea to also make a few 0.5 ml aliquots for smaller experiments.
- Place vials in a "Mr Frosty" container and immediately move to the -70°C freezer. Transfer vials to the liquid nitrogen tank after 4-24 h.

Generation of immature moDCs
The instructions given below are for a typical experiment. My final batch of monocytes was cryopreserved at 2.6×10^7 monocytes per vial. One vial cultured in one 6-well plate typically resulted in $4\text{-}7 \times 10^6$ DCs.

Day 0
- Pre-warm the C10 medium. Thaw a vial of monocytes in the 37°C water bath, swirling gently until only a small chunk of ice (~10% by volume) remains.
- Move the vial's contents to a 15 ml conical tube. Add 9 ml C10 medium gradually while swirling the tube gently (add drop-wise at first, then slowly speed up).
- Centrifuge at 200×g for 8 min. Meanwhile, combine 25 ml of C10 with 0.25 ml each of IL-4 and GM-CSF (1000 U/ml each) to make up C10GF medium.
- Resuspend the monocytes in 15 ml C10GF and seed 2.5 ml in each well of a 6-well tissue culture plate. Place in humidified 37°C, 5% CO_2 incubator. Store the remaining C10GF at 4°C.

Day 2
- Add 0.5 ml of warm C10GF to each well. The cells should now be irregular in shape.

Day 4
- Add 0.5 ml of warm C10GF to each well. The cells should now be larger and irregularly shaped with some visible dendrites.

Day 6 (or day 5 if pressed for time)
- Harvest the floating or loosely adherent DCs by gentle resuspension. Centrifuge at 200×g for 6 min in a 50 ml tube.
- Add an equal volume of supernatant to the remaining C10GF and discard the rest of the supernatant. Resuspend the DCs in this partially recycled C10GF, count, and adjust to the desired cell density.

B.2 Cross-presentation assay with N9V-specific T cells

Materials needed
Day 6 immature HLA-A2 DCs as described in the previous protocol
A15N positive control peptide (ARNLVPMVATVQGQN, synthesized by GenScript)
A vial of frozen $CD8^+$ T cells specific against N9V/HLA-A2 (ProImmune C008-0B)
RPMI/FCS medium (RPMI-1640 with glutamine, 10% FCS, Primocin; see B.1 for suppliers)
Recombinant human IL-2 (R&D Systems 202-IL)
Labeling buffer (PBS + 0.5% BSA + 2 mM EDTA)
Human IFNγ secretion assay detection kit (Miltenyi 130-054-202) consisting of Catch Reagent and α-IFNγ-PE
α-CD8-FITC antibody (BD Biosciences 555634)

Day 6 morning
- For each desired test condition, seed 1-2 × 10^5 DCs in 200 µl C10GF in a well of a 96-well round bottom plate (e.g. BD Falcon 353077). The optimal number of DCs per well may vary between batches of monocytes.
- Allow the DCs to settle in the incubator for 30-90 min while the antigens are being prepared.
- Add the antigens to the respective wells. One well should be left unstimulated as a negative control, whereas 10 µM A15N peptide should be added to a positive control well. To add yeast cells, the yeast should be pelleted and resuspended in some medium taken from the target DC well.
- Return the plate to the incubator and note the time.

Day 6 evening
- Pre-warm the RPMI/FCS medium. Thaw a vial of N9V-specific T cells in the 37°C water bath, swirling gently until only a small chunk of ice remains.
- Move the vial's contents to a 15 ml conical tube. Slowly add 2 ml RPMI/FCS drop-wise using a 1 ml pipette tip while gently swirling the tube. Continue adding another 7 ml RPMI/FCS drop-wise using a 10 ml pipette. I have found the T cells to be quite sensitive to osmotic shock.
- Centrifuge at 200×g for 10 min and completely aspirate the supernatant.
- Resuspend the cells in 4 ml RPMI/FCS and add 5 ng/ml IL-2. Seed 1 ml each in 4 wells of a 24-well tissue culture plate and incubate overnight.

Day 7
- About 40 minutes before 24 h have elapsed since antigen addition, carefully set aside 0.5 ml of medium from each T cell well without disturbing the cells.
- Combine, resuspend, and count the T cells in the presence of trypan blue. Adjust the live T cell concentration to 0.7-1 × 10^6 cells/ml. The viability can sometimes be as low as 50%.

- Remove 100 µl of medium from each DC well without disturbing the cells. Add 100 µl of T cells and gently resuspend.
- Centrifuge the plate at 200×g for about 1 min to settle the cells, then return the plate to the incubator (this should be approximately 24 h since antigen addition).
- Four hours later, place the plate on ice and move the contents of each well to a microcentrifuge tube containing 1 ml cold labeling buffer.
- Centrifuge the tubes at 300×g, 4°C for 10 min. To reduce cell loss, centrifuge for 7 minutes, then rotate the tubes 180° (e.g. from having the lid hinge facing the center of the rotor to facing outside) to centrifuge for a further 3 min. The subsequent centrifugation steps should be performed in the same manner.
- Aspirate the supernatant and resuspend each cell pellet in 100 µl of a solution consisting of 10% Catch Reagent, 90% labeling buffer.
- Incubate for 5 min on ice, then add 1 ml warm RPMI/FCS.
- Incubate at 37°C for 45 min with gentle rotation. If a MACSmix tube rotator is not available, place the tubes in a water bath and invert them every 5-7 min.
- Place the tubes on ice and add 0.5 ml cold labeling buffer. Centrifuge and aspirate.
- Optional wash step: Add 0.5 ml cold labeling buffer, centrifuge and aspirate.
- Resuspend each cell pellet in 100 µl of a solution consisting of 20% α-CD8-FITC, 10% α-IFNγ-PE, 70% labeling buffer. Incubate for 30 min on ice.
- Add 0.5 ml cold labeling buffer to each tube. Centrifuge and aspirate.
- Analyze the cells on a flow cytometry machine. The events should be gated by forward and side scatter and by the FITC channel to identify the $CD8^+$ T cells. The assay readout is the percentage of such cells that are PE-positive. Since the PE-positive and PE-negative populations are not clearly distinct, draw the region such that ~0.5% (or fewer) of the $CD8^+$ T cells in the negative control are PE-positive.

B.3 Expression and purification of MS74NEY2

Solutions to prepare
LB + glucose:
10 g tryptone, 5 g yeast extract, 5 g NaCl, 2 g glucose. Dissolve in 1 L water and autoclave.

0.5 M IPTG:
Dissolve 1.19 g isopropyl-β-D-thiogalactopyranoside in 10 ml ddH_2O. Filter sterilize and store at 4°C protected from light.

Column buffer base:
20 mM Tris-HCl, pH 7.4, 200 mM NaCl

3 M imidazole stock:
Dissolve 10.2 g imidazole in 40 ml ddH_2O. Adjust pH to 7.5 with HCl and add ddH_2O to bring volume to 50 ml.

1 M maltose stock:
Dissolve 18.0 g maltose in ddH_2O to give a final volume of 50 ml.

Talon buffer:
Prepare just before use and keep cold. To 200 ml column base buffer, add 5 mM β-mercaptoethanol (70.1 µl).

Amylose resin buffer:
Prepare just before use and keep cold. To 150 ml column base buffer, add 1 mM EDTA (0.3 ml of a 0.5 M EDTA stock) and 23.1 mg dithiothreitol (DTT).

Amylose wash buffer:
Move 100 ml of the above amylose resin buffer to a new bottle, add 0.1 ml Triton X-114 (Sigma) and stir. The wash buffer will be cloudy at room temperature but will become clear when chilled.

Transformation, growth and induction

- Transform pMS74NEY2 plasmid into BL21(DE3)-RIPL competent cells (Stratagene) according to the manufacturer's protocol, which can be scaled down to use only 25 µl of competent cells. Plate 50 µl of the transformation mix onto an LB + ampicillin plate and incubate at 37°C overnight.
- In the evening of the next day, inoculate 2 culture tubes each with 5 ml LB + glucose + 100 µg/ml ampicillin + 34 µg/ml chloramphenicol. I split one colony between the two tubes. Shake at 30°C overnight (~16 h) or at 37°C for ~12 h.
- Add the 10 ml of culture to 1 L LB + glucose (without antibiotics) in a large Tunair flask. Shake at 37°C until the OD600 reading reaches ~0.7 (about 2.5 h).
- Add 0.3 mM IPTG (0.6 ml of 0.5 M stock) and move the flask to the 20°C shaker.

- After 6 h of induction, harvest the bacteria by centrifugation at 12,000×g for 5 min, preferably into one centrifuge bottle.
- Discard the supernatant. Freeze the pellet overnight at -20°C.

Lysis

- Thaw the bacterial pellet in cold water. Dissolve one EDTA-free Complete Protease Inhibitor Cocktail Tablet (Roche 04 693 132 001) in 50 ml cold Talon buffer. Resuspend the bacteria in 25 ml of Talon buffer + protease inhibitors and transfer to a 50 ml conical tube on ice.
- Sonicate the suspension to lyse the bacteria. With the Cooney lab's sonicator, I set the amplitude to 30% and the pulse rate to 2 s on, 2 s off. I sonicated four times for 1 min each, letting the sample rest on ice for 1 min between each go.
- Add 10 ml Talon buffer + protease inhibitors and centrifuge at 20,000×g, 4°C for 40 min. Make sure to use tubes that can withstand this g-force.
- Filter the supernatant using a Nalgene Supor machV filter (others will likely clog). Check the pH and adjust it to 7.4 with NaOH if needed.

Talon metal affinity chromatography

- Pack 5 ml (bed volume) Talon metal affinity resin (Clontech) in a 2.5 cm diameter column in the cold room. Equilibrate with 25 ml Talon buffer.
- Load the clarified lysate and adjust the stopcock to reduce the flow rate to < 1 ml/min.
- Wash with 50 ml Talon buffer (with full flow rate).
- Elute with 25 ml Talon buffer + 150 mM imidazole, collecting 5 ml fractions. Check the A280 absorbance of the fractions.

Amylose resin affinity chromatography

- Pack 2 ml (bed volume) amylose resin (New England Biolabs) in a 1 cm diameter column in the cold room. Equilibrate with 10 ml amylose resin buffer.
- Load the protein-containing fractions eluted from the Talon resin. Instead of mixing the fractions, I load them consecutively in order of protein content (least to most).
- Wash with 100 ml amylose wash buffer.
- Wash with 10 ml amylose resin buffer.
- Elute with 10 ml amylose resin buffer + 10 mM maltose.

Concentration

- Check A280 of eluted protein. For MS74NEY2, MW = 100381, $\varepsilon = 112830\ cm^{-1}\ M^{-1}$. Expect a yield of 5-10 mg.
- Concentrate the protein to 60 μM using an Amicon Ultra MWCO 30K centrifugal filter (Millipore). The protein should be stable for several months stored at 4°C.

B.4 Conjugating one or more layers of MS74NEY2 onto SWH100 yeast

Reagents needed for first layer
SWH100 yeast
BG-GLA-NHS (2 mg vial, Covalys BB186)
Dimethylformamide (DMF)
MS74NEY2 protein (60 μM in amylose resin elution buffer, see B.3)
PBS
CHAPS stock solution, 1% (w/v) in PBS
PBS/BSA (PBS + 0.1% BSA)

Reagents needed for subsequent layers
Sfp phosphopantetheinyl transferase, 0.25 mM solution prepared as described by Yin J, Lin AJ, Golan DE, et al. "Site-specific protein labeling by Sfp phosphopantetheinyl transferase" Nat Protoc 2006;1(1):280-5.
BG-CoA, synthesized as described below
1 M $MgCl_2$ stock solution

BG-CoA synthesis
- Dissolve 1 mg of BG-maleimide (BB056, Covalys; MW 489.5) in 0.5 ml DMF.
- Weigh out >1.2 mg of Coenzyme A trilithium salt (C3019, Sigma; MW 785.3) and dissolve in PBS to make a 3 mM solution.
- Add 0.5 ml Coenzyme A solution (1.5 μmoles) drop-wise to the BG-maleimide (2.04 μmoles) while stirring.
- Flush the tube with nitrogen gas, close the cap and place in the 30°C incubator for 24 h.
- Verify by mass spectrometry. Example spectra are shown in Fig. B.1
- Add 1 μl of a 1 M solution of DTT and incubate at 30°C for 2 h to quench the excess BG-maleimide. Store at -20°C.

SWH100 culture and induction
- Inoculate 5 ml of SD-CAA with a colony of SWH100 yeast from a freshly streaked SD-CAA agar plate. Culture in a 30°C shaker until mid-log phase (~18 h). For larger culture volumes, pick more colonies rather than increasing the growth time (e.g. 5 colonies for 50 ml).
- Pellet by centrifugation 5 OD.ml of yeast and resuspend in 5 ml of YPG.
- Shake at 30°C for 12 h, then store at 4°C.
- Optional: check expression levels of aga2p-HA by labeling with α-HA and analyzing by flow cytometry.

BG-SWH100 preparation
- Pellet by centrifugation >10 OD.ml of induced SWH100 yeast split between two microcentrifuge tubes

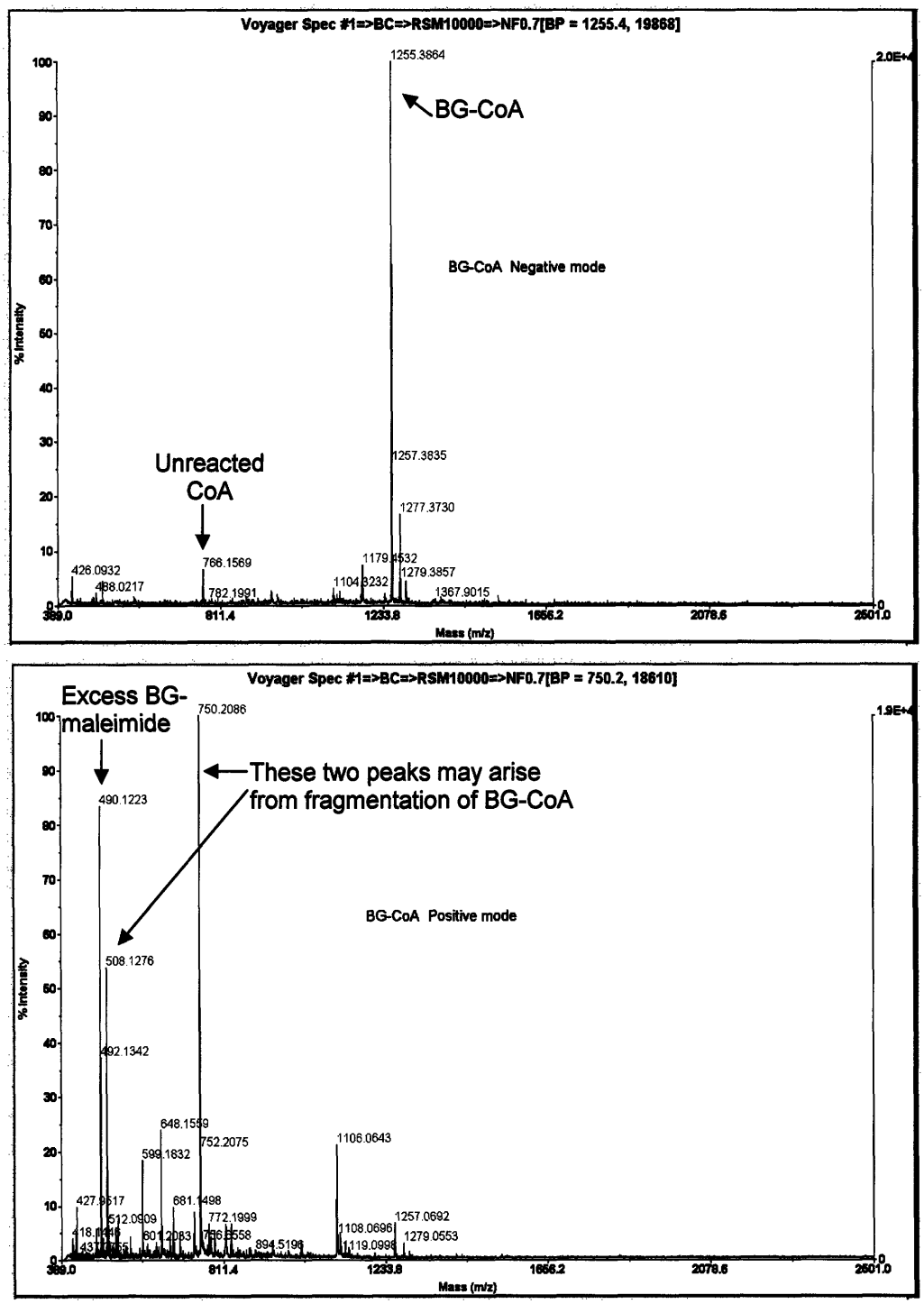

Figure B.1, MALDI mass spectra of BG-CoA in negative and positive modes. The peaks of interest have been annotated.

- Wash each tube 4× with 1 ml PBS + 0.01% CHAPS.
- Resuspend each pellet in 1 ml PBS + 0.01% CHAPS and transfer to a 35 mm Petri dish. UV-irradiate with 1000 J/m^2 in a Stratalinker 1800 (Stratagene). Swirl each Petri dish and UV-irradiate again with 1000 J/m^2.
- Pool the yeast, measure the OD600 and pellet 5 OD.ml of yeast in each of two microcentrifuge tubes.
- Wash each pellet in 0.2 ml DMF, being careful to aspirate completely.
- Dissolve 2 mg of BG-GLA-NHS in 100 µl DMF. Resuspend each yeast pellet in 50 µl of this solution. BG-GLA-NHS is unstable and should be used immediately after dissolving.
- Place the tubes in a 30°C shaker for 2 h.
- Wash each pellet 3× with PBS/BSA. Resuspend in 0.5 ml PBS/BSA and store at 4°C.

Conjugation of the initial layer of antigen

These instructions are written for conjugating antigen to 1 OD.ml of yeast. Scale accordingly.

- Pellet 1 OD.ml of BG-SWH100 in a 0.5 ml tube.
- Resuspend in 400 µl of PBS and add 100 µl of 60 µM MS74NEY2.
- Gently rotate at 30°C for 5 h, using a MACSmix tube rotator (Miltenyi).
- Pellet by centrifugation and aspirate. Since the antigen-conjugated yeast can be quite sticky, centrifuge at maximum speed for 30 s, then rotate the tube 180° (e.g. from having the lid hinge facing the center of the rotor to facing outside) and centrifuge for 30 s. All future centrifugations should be performed in this manner.
- Wash once (if proceeding with subsequent layers) or twice with 0.5 ml PBS/BSA.

Conjugation of subsequent layers of antigen

These instructions are written for conjugating antigen to 1 OD.ml of yeast. Scale accordingly.

- Resuspend 1 OD.ml of yeast coated with one layer of MS74NEY2 in 200 µl of PBS/BSA containing 1 mM $MgCl_2$, 12.5 µM Sfp and 75 µM BG-CoA:
  - 178 µl PBS/BSA
  - 2 µl 1 M $MgCl_2$
  - 10 µl 0.25 mM Sfp
  - 10 µl 1.5 mM BG-CoA
- Incubate at 37°C for 90 min, vortexing every 30 min.
- Pellet by centrifugation, aspirate, and wash twice with 0.5 ml PBS/BSA.
- Resuspend yeast in 400 µl of PBS and add 100 µl of 60 µM MS74NEY2. Gently rotate at 30°C for 2 h.
- Pellet by centrifugation, aspirate, and wash with 0.5 ml PBS/BSA.
- Repeat the steps in this section as desired.

Appendix C –Self-cleaving pH-sensitive Inteins for Antigen Release

C.1 Introduction

In Chapter 2, we demonstrated the importance to cross-presentation of having yeast-attached antigen be released rapidly upon phagocytosis by dendritic cells (DCs). In Chapter 3, the initial antigen release mechanism that we included in the vaccine design, the $(C1)_4$ sequence, had no beneficial effect on cross-presentation. We eventually replaced this with the invariant chain ectodomain that is rapidly cleaved by phagosomal Cathepsin S, but before that, we also investigated an alternative antigen release strategy based upon the acidification of phagosomes as they mature. One potential advantage of pH-triggered antigen release over protease-mediated mechanisms is that the release kinetics will not be limited by protease activity or concentration even at high antigen concentrations.

Inteins are polypeptide sequences within a larger protein that are able to excise themselves and splice together the flanking sequences. Wood et. al engineered a pH-sensitive mini-intein that cleaves at its C-terminus but not the N-terminus and does not perform splicing (1, 2). The cleavage rate of this intein is optimal at pH 6 and is considerably slower at neutral and alkaline pH and at low temperatures. The cleavage rate is also affected by the first amino acid residue (+1 aa) after the C-terminus of the intein, with Cys leading to faster cleavage than Met (2). We hypothesized that replacing the $(C1)_4$ sequence in MSCE with the intein would result in more efficient cross-presentation from the antigen-conjugated yeast, and furthermore, that the release kinetics could be optimized by choosing the appropriate +1 aa.

C.2 Materials and Methods

A plasmid containing the intein sequence (pET/ELP-I-CAT) was generously provided by David Wood. This sequence was PCR-amplified using primers to add flanking *Eco*RI and *Nhe*I

sites and Met or an alternative +1 aa and subcloned into pMSCE. The protein was produced in *E. coli* and purified as described in Chapter 4.3.4, except the chromatography buffers were adjusted to pH 8.5 instead of 7.4. Also, for the faster cleaving inteins (Cys or Ser as the +1 aa), the culture flask was plunged into ice-cold water to cool the contents down to 20°C just before induction, and the induction time was reduced to 2 h at 20°C.

To determine the cleavage kinetics of each intein-containing protein, eight aliquots of 1 µl 60 µM protein added to 19 µl 80 mM sodium phosphate, pH 6.0, 150 mM NaCl were incubated at 37°C for various times, then boiled with SDS-PAGE sample buffer for 5 min. After SDS-PAGE and staining with SimplyBlue Safestain (Invitrogen), the bands were imaged on a Biorad Fluor-S imager and quantified using the automatic band detection function in the Quantity One software. After cleavage, the C-terminal protein fragment (mostly NY-ESO-1) was disproportionately poorly stained. The ratio of the density of the upper band (full length) to the sum of the densities of the upper and middle (N-terminal fragment after cleavage) bands could be fitted to an exponential decay over time (with a constant background term) to determine the cleavage half-life.

Each intein-containing fusion protein was conjugated to BG-SWH100 yeast as described in Appendix B.4, except that the PBS used was adjusted to pH 8.5 and the reaction time was reduced to 2 h to reduce self-cleavage. The cross-presentation assays were performed as described in Chapter 4.3.7.

C.3 Results

For the pilot experiment, we produced the protein MSICE with the self-cleaving intein and Met as the +1 aa between the SNAP-tag and N9V. Conjugating this to yeast, we observed an improvement in cross-presentation over yeast conjugated with protein lacking such a linker or

with $(C1)_4$ as the linker (not shown). This encouraging result prompted us to produce and characterize four other intein-containing fusion proteins, with Cys, Ser, Thr, or Gly as the +1 aa, which varied considerably in their self-cleavage kinetics (Table C.1). However, there was no obvious relationship between the kinetics and the cross-presentation efficiency of the proteins when conjugated to yeast (Fig. C.1). All the intein-containing constructs were slightly improved over the linkerless construct. To investigate the reason for the improvement, we mutated the final residue of the intein from Asn to Ala, preventing the Asn rearrangement necessary for self-cleavage. Yeast-conjugated fusion protein containing this inactive intein was still cross-presented as well as the version containing the functional intein and slightly better than when no linker or $(C1)_4$ was present (Fig. C.2). A lower yeast-to-DC ratio of 7.5:1 was used in this experiment to ensure that the assay output was not saturated.

C.4 Conclusion

Although the insertion of the intein provided a slight but reproducible benefit to cross-presentation, pH-triggered self-cleavage was ruled out as the mechanism. Instead, it is likely that the intein simply contains some sequences that are susceptible to proteases in the early phagosome. When MSICE (functional or inactivated) is digested with Cathepsin S *in vitro*, many more fragments are generated than when MSCE is digested (not shown), supporting this hypothesis. Since the fastest self-cleaving intein has a half-life of only 9 min at pH 6.0, 37°C, it seems quite likely that proteolysis precedes acidification during phagosome maturation.

Table C.1 – Intein self-cleavage half-life at pH 6.0, 37°C

+1 aa	C	S	T	M	G
$t_{1/2}$ (min)	9	16	33	45	166

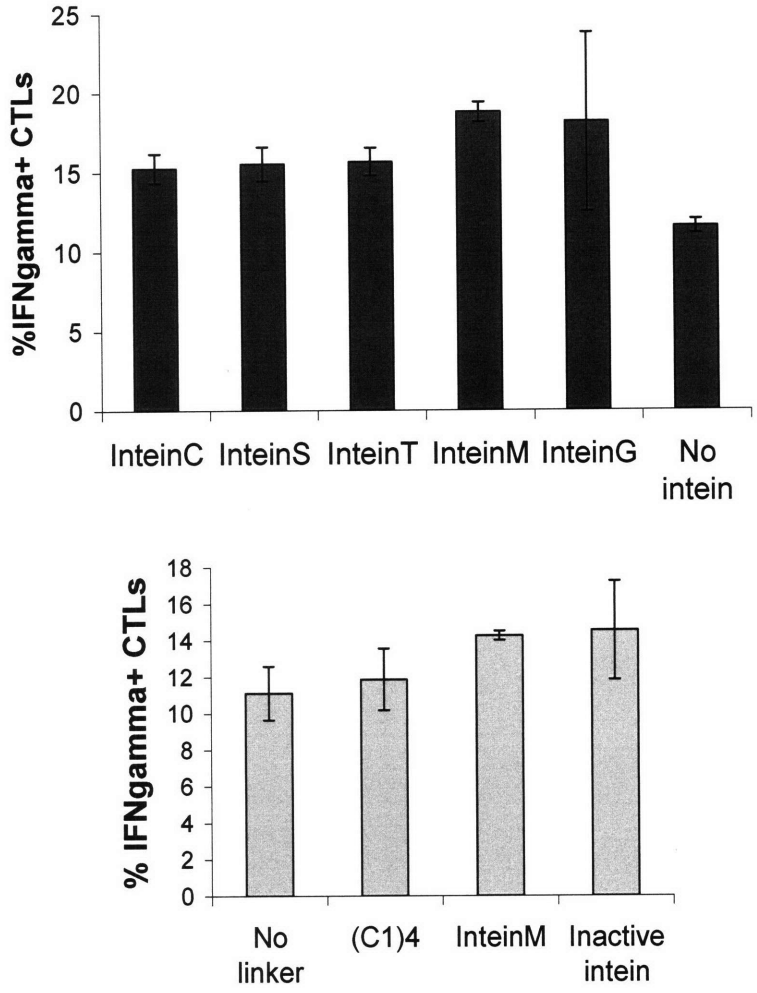

Figure C.1, Improved cross-presentation from intein-containing constructs does not arise from self-cleavage. InteinX indicates X as the +1 aa. Error bars indicate S.D. of duplicate wells.
A, Yeast conjugated to fusion proteins containing the indicated inteins were added to DCs at a 20:1 ratio. The cross-presentation assay was performed after 24 h.
B, Yeast conjugated to fusion proteins with the indicated linkers (between the SNAP-tag and N9V) were added to DCs at a 7.5:1 ratio. The cross-presentation assay was performed after 24 h. The inactive intein has an Ala instead of Asn as its C-terminal residue.

C.5 References

1. Wood, D. W., W. Wu, G. Belfort, V. Derbyshire, and M. Belfort. 1999. A genetic system yields self-cleaving inteins for bioseparations. *Nat Biotechnol* 17: 889-892.
2. Wood, D. W., V. Derbyshire, W. Wu, M. Chartrain, M. Belfort, and G. Belfort. 2000. Optimized single-step affinity purification with a self-cleaving intein applied to human acidic fibroblast growth factor. *Biotechnol Prog* 16: 1055-1063.

Appendix D – Fibronectin Domains for Increasing IgG Binding to Activating over Inhibitory Fc Receptors

D.1 Introduction

The therapeutic effects of many antibodies used to treat cancer have been found to arise from the recruitment of immune effector cells by engaging Fc receptors (FcRs) (1). The Fcγ family of receptors recognizes immunoglobulins (IgGs). In humans, cross-linking of the activating receptors FcγRIA, FcγRIIA (RIIA) and FcγRIIIA (RIIIA) triggers endocytosis and phagocytosis, release of cytokines, chemokines and lytic granules, oxidative burst, and other effector functions, whereas the sole inhibitory receptor FcγRIIB (IIB) regulates and down-modulates these effects. The high affinity FcγRIA is likely occupied by soluble IgG rather than by immune complexes and is not thought to play a significant role in mediating cytotoxic effects (1, 2). In contrast, RIIA, RIIB, and RIIIA have micromolar affinity constants for the various IgG subclasses and are triggered by opsonized antigen. For a given IgG, the ratio of affinities to activating FcγRs over the inhibitory FcγR, termed the A/I ratio, is hypothesized to correlate with antibody efficacy, with the rank order of IgG subclass activity in a murine model reflecting the rank order of A/I ratios (3).

Several lines of evidence suggest that increasing the A/I ratio could be a promising approach to increasing the efficacy of antibody therapeutics. A single nucleotide polymorphism of RIIIA has been correlated with differential outcome in several antibody cancer therapy clinical trials. The 158V form, which has a higher affinity for IgG1 compared to 158F, is associated with better response to rituximab (4-7) and trastuzumab (8), both IgG1 therapeutics. Knockout mice lacking RIIB can be treated with much lower antibody concentrations to reduce tumor growth and metastasis as compared to wild type mice (9). Dhodapkar et. al demonstrated

that selective blockade of RIIB on dendritic cells causes them to mature and to induce T cell immunity much more efficiently when exposed to opsonized tumor cells (10). These studies show the beneficial effects of increasing the A/I ratio by altering the receptor part of the equation, and it is not surprising that several groups have applied protein engineering principles in attempts to achieve the same goal by modifying the IgGs (2).

Mutations in the Fc portion of IgGs that improve A/I ratios have been found by alanine scanning (11), algorithmic prediction (12), and yeast surface display (13, 14). While improved activities in *in vitro* antibody-dependent cellular-mediated cytotoxicity (ADCC) assays were demonstrated, the best clones improved the A/I ratios (either RIIA/RIIB or RIIIA/IIB) by only around 10-fold (12, 13). For one protein surface to achieve simultaneous gains in binding affinity to RIIA and RIIIA while maintaining or decreasing affinity to RIIB is intrinsically difficult; it is made all the more challenging because the extracellular domains of RIIA and RIIB are 93% homologous (2). Instead of Fc engineering, an alternative approach is to create bispecific antibodies where one "arm" engages an activating FcR, as has been achieved with her2-RIIIA specificity in both scFv (15) and IgG (16) formats. In the IgG format, RIIB affinity is undiminished, whereas in the scFv format, RIIB binding is abolished at the cost of also eliminating RIIA binding. For single agent therapy, it would be ideal not to have to choose between activating either RIIA or RIIIA. On one hand, NK cells, which are almost entirely responsible for lysis during *in vitro* ADCC assays using peripheral blood mononuclear cells (PBMCs), express RIIIA but not RIIA or RIIB (2). On the other hand, *in vivo*, the anti-tumor activity of the most effective murine IgG subclass, IgG2a, is primarily dependent on the balance between FcγRIV and FcγRIIB, making it unlikely that NK cells are responsible as they express neither receptor (1, 3).

Here, we present a novel approach for developing IgG-based anti-tumor therapeutics with greatly enhanced A/I ratios by fusing IgGs to two different fibronectin (Fn3) domains, one engineered to bind selectively to RIIA over RIIB and the other to bind selectively to RIIIA. The Fc portion of the IgG is prevented from engaging any of the FcγRs by eliminating the required N-linked glycosylation using the N297Q mutation (14, 17). Aglycosylated Fc, however, retains binding to the neonatal Fc receptor FcRn that recycles IgGs and is responsible for their unusually long serum half-lives (11). The tenth type III domain of human Fn3 is small (~10 kDa), stable, and is a validated scaffold for performing directed evolution to bind to a variety of targets (18-27). Fn3 is a β-sandwich with an immunoglobulin-like fold; three exposed loops termed BC, DE, and FG are structurally analogous to antibody complementarity-determining regions (CDRs). Since each Fn3 domain is engineered separately, the RIIA-binding domain and the RIIIA-binding domain need not bind to the same surface of the FcRs, with the potential to achieve higher A/I ratios than achievable with a single molecule. Another advantage over directly engineering the Fc portion is the ability to "sample" differences in amino acid sequence between RIIA and RIIB that lie outside the Fc-FcR interface, potentially permitting greater discrimination between the highly homologous pair of FcRs.

D.2 Materials and Methods

D.2.1 Naïve Yeast Libraries and Culture Conditions

Three yeast surface display libraries of Fn3 were combined for screening. The G2 library has BC, DE, and FG loops randomized in both length and composition (27); in the G4 library, the amino acid composition of the loops is also biased towards that in antibody CDRs (Hackel, BJ, unpublished). In the YS library, the BC and FG loops consist solely of Tyr and Ser residues (BJ Hackel, unpublished). In general, yeast libraries and individual clones were cultured in SD-CAA (2% dextrose, 0.67% yeast nitrogen base, 0.5% casamino acids, 0.07 M sodium citrate, pH 4.5) at 30°C, 250 rpm to an OD600 of 2-7 and induced in SG-CAA (SD-CAA with galactose replacing dextrose) at an initial OD600 of ~1 for 12-16 h at 30°C, 250 rpm.

D.2.2 Library Screening using Magnetic Beads

Soluble, singly biotinylated human FcRs were provided by the Ravetch group, the Rockefeller University, NY. The method of screening yeast surface display libraries for weak binders using antigen-loaded magnetic beads was developed and validated by Ackerman and colleagues in the Wittrup group (unpublished). Stoichiometric amounts of each FcR were incubated individually with 4×10^6 Biotin Binder Dynabeads (Invitrogen, Carlsbad, CA, ~6×10^6 biotin binding site per bead) overnight at 4°C, then washed twice using the Dynal MPC magnet. Every library sort against an FcR was preceded by two negative sorts to deplete streptavidin and biotin binders. Briefly, yeast cells were incubated for 45 min at 4°C with 8×10^6 untreated beads or beads partially coated with biotin and/or biotin-PEG (Laysan Bio, Arab, AL) in 2 ml PBS + 0.1% bovine serum albumin (PBSA), after which the tube was placed in the magnet for 5 min and the free yeast collected. For positive selection, the depleted library was incubated for 3 h at 4°C with the FcR-coated beads before magnetic separation. The bead-bound

yeast were washed, with the number of wash steps (1-3), duration (1 – 15 min) and temperature (4°C or 20°C) varying as the sorts progressed to maintain the number of retrieved yeast cells at around $10^5 - 5 \times 10^6$. The retrieved yeast cells (with beads) were cultured in 50 ml SD-CAA and the beads were removed using the magnet prior to induction.

In the initial sorts, 8×10^9 yeast cells from the naïve Fn3 libraries were screened against RIIA in a single tube, after which the unbound yeast were screened against RIIIA. For subsequent sorts, enough cells were screened such that the number of expressing cells was approximately ten-fold larger than the maximum library diversity. In addition to varying the washing procedure, the stringency of the selections was also increased by reducing the avidity. From the sixth sort onwards, the number of moles of biotinylated FcR was reduced to ~20% of the number of biotin-binding sites on the beads (although the number of beads used was doubled), which was further reduced to 5% for the final sort against RIIIA. The remaining binding sites were occupied by excess biotin-PEG to reduce streptavidin exposure. Also from the sixth sort onwards, the induction time was reduced to 2.5 h to reduce the number of Fn3 domains expressed per yeast cell. After a total of eight sorts interspersed with four rounds of mutagenesis as described below, the resulting yeast libraries exhibited clear labeling by the respective FcR (in tetrameric form bound to streptavidin) and magnetic bead sorts were abandoned in favor of fluorescence activated cell sorting (FACS).

D.2.3 Fn3 Mutagenesis and Electroporation

After every two sorts (or three in the case of RIIA FACS sorts), the plasmid DNA was rescued from the yeast libraries and subjected to error-prone PCR essentially as described previously (27). Briefly, a 50 µl 15-cycle error-prone PCR reaction was performed to amplify the entire Fn3 gene using 0.5 µM of each primer (see Table D.1), 0.2 mM of each dNTP, 2 mM each

of 8-oxo-dGTP and dPTP (TriLink, San Diego, CA), Taq enzyme and Thermopol buffer (New England Biolabs, Ipswich, MA) and plasmid DNA recovered from 2×10^7 yeast cells (Zymoprep II kit, Zymo Research, Orange, CA). At the same time, three other PCR reactions were performed to mutagenize the BC, DE, and FG loops individually using the appropriate primers (Table D.1) and 20 mM each of 8-oxo-dGTP and dPTP. The error-prone PCR products were extracted from agarose gel and amplified by conventional PCR reactions (400 µl per product) using shortened (23-27 bp) versions of the above primers. The three loop products were precipitated using PelletPaint (Novagen, Madison, WI), dissolved together in 3 µl of water, and mixed with 2 µg of plasmid vector digested to remove the BG loop through the FG loop (*Nco*I/*Sma*I/*Nde*I-cut pCT-Fn3-Loop). The gene product was likewise concentrated down to 1 µl in water and mixed with 2 µg of plasmid vector digested to remove the entire Fn3 gene as well as the $(G_4S)_3$ linker (*Pst*I/*Nde*I/*Bam*HI-cut pCT-Fn3-Gene). From the fourth round of mutagenesis onwards, the mutagenized loops were also mixed with 1-2% of loops derived from the naïve libraries to increase loop diversity. Each DNA mix was electroporated into 100 µl electrocompetent EBY100 yeast (from 25 ml of culture) divided between two cuvettes as described previously (28).

Table D.1. Mutagenesis primers and shortened amplification primers (underlined)

Name	Sequence	Target
W5	CGACGATTGAAGGTAGATACCCATACGACGTTCCAGACTACGCTCTGCAG	Fn3 gene
W3	ATCTCGAGCTATTACAAGTCCTCTTCAGAAATAAGCTTTTGTTCGGATCC	
BC5new	GGGACCTGGAAGTTGTTGCTGCGACCCCCACCAGCCTACTGATCAGCTGG	BC loop
Lbc3	TGAACTCCTGGACAGGGCTATTTCCTCCTGTTTCTCCGTAAGTGATCCTGTAATA	
Lde5	CAGGATCACTTACGGAGAAACAGGAGGAAATAGCCCTGTCCAGGAGTTCACTGTG	DE loop
Lde3	GCATACACAGTGATGGTATAATCAACTCCAGGTTTAAGGCCGCTGATGGTAGC	
Lfg5	ACCATCAGCGGCCTTAAACCTGGAGTTGATTATACCATCACTGTGTATGCTGTC	FG loop
FG3new	GATCCCTGGGATGGTTTGTCAATTTCTGTTCGGTAATTAATGGAAATTGG	

D.2.4 Library Screening by FACS

For flow cytometry, biotinylated FcRs were incubated with streptavidin-PE (premium grade, Invitrogen) or streptavidin-Alexa Fluor 647 at a 4:1 molar ratio for at least 30 min at room temperature (RT) before use. After the eighth magnetic bead sort, the library evolved to bind to RIIIA did not display any binding to RIIB tetramer, thus further selections by FACS were focused only on improving affinity to RIIIA. Yeast libraries were incubated with PE-tagged RIIIA tetramer (at decreasing concentrations with successive sorts) in a volume of PBSA ensuring at least 3-fold excess of RIIIA over Fn3 domains for 1 h at RT. The yeast was then centrifuged and all the supernatant except for 0.1-0.5 ml was removed. Chicken α-c-myc-Alexa Fluor 647 (made by using the Microscale Protein Labeling Kit on the unconjugated IgY, both from Invitrogen) was then added prior to incubation on ice for 30 min. The yeast cells were sorted on a BD FACSAria, selecting 0.1-0.5% of the cells with the highest PE to Alexa Fluor 647 fluorescence ratio, which were collected and grown up in 5 ml SD-CAA.

For the library evolved to bind to RIIA, some binding to RIIB tetramer was also seen after magnetic sorting. Therefore, FACS selections for decreased affinity to RIIB were carried out in alternation with selections for increased affinity to RIIA (performed analogously to the RIIIA affinity sorts). For these selectivity sorts, yeast cells were incubated with Alexa Fluor 647-tagged RIIA tetramer and a higher concentration of PE-tagged RIIB tetramer for 1 h at RT prior to FACS. The cells exhibiting high RIIA binding with little or no RIIB binding were selected.

D.2.5 Characterization of Individual Clones

Plasmid DNA was recovered from the later library generations (Zymoprep II kit) and transformed into competent DH5α bacteria (Invitrogen). Individual colonies (usually ten) were grown, miniprepped, and sequenced, as well as re-transformed into EBY100 yeast (EZ Yeast

Transformation Kit, Zymo Research). The resulting clones were cultured in SD-CAA and induced in SG-CAA for analysis. To rapidly compare different clones, 0.1 OD.ml aliquots of yeast were labeled with a low and a high concentration of PE-tagged RIIA (1 nM, 30 nM) or RIIIA (0.3 nM, 10 nM) tetramer for 1 h at RT prior to flow cytometry (Coulter Epics XL). The apparent tetramer K_d was estimated from the ratio of the two mean fluorescence readings. To measure the apparent tetramer K_d more accurately for selected clones, yeast cells were washed and incubated with 7-8 different concentrations of PE-tagged tetramer spanning 3-4 orders of magnitude for 2 h at RT. The labeling volumes (in PBSA) were chosen to give at least a 10-fold excess of FcR over Fn3. The yeast cells were centrifuged and washed with 0.5 ml PBSA for analysis by flow cytometry. The K_d value was determined by fitting the data to the equation $y = A[\text{tetramer}]/([\text{tetramer}] + K_d) + B$.

D.2.6 Expression and Purification of MBP-Fn3 Fusion Proteins

Selected Fn3 domains were subcloned into the pMal-c2x vector (New England Biolabs) for expression in *E. coli* as a C-terminal fusion to maltose-binding protein (MBP). A forward primer adding a flanking *Ava*I restriction site followed by the TEV protease site LGENLYFQS and a reverse primer adding a Stop codon and a *Xba*I site were used to amplify each Fn3 gene sequence. The *Ava*I/*Xba*I-digested PCR product was ligated to the similarly digested pMal-c2x backbone. After sequence confirmation, the resulting plasmid was transformed into either Rosetta(DE3) or Rosetta-gami 2(DE3) (Stratagene, La Jolla, CA) for expression. Freshly transformed colonies were cultured to saturation in 5 ml antibiotic-supplemented LB + glucose (10 g tryptone, 5 g yeast extract, 5 g NaCl, 2 g glucose in 1 L water) at 37°C, 250 rpm. These starter cultures were used to inoculate 100 ml (Rosetta) or 200 ml (Rosetta-gami) of antibiotic-free LB + glucose at a 1:100 ratio, which were then induced with 0.3 mM IPTG when the OD600

reached 0.6. The bacteria were pelleted by centrifugation and frozen after 1 h induction at 37°C. The thawed pellets were resuspended in 5 ml cold column buffer (20 mM Tris-HCl, pH 7.4, 200 mM NaCl, 1 mM EDTA) with Complete Protease Inhibitor Cocktail (Roche Applied Science, Indianapolis, IN) and lysed by sonication. After centrifuging at 20,000 × g, 15 min, 4°C, the supernatant was loaded onto 2 ml amylose resin (New England Biolabs) pre-equilibrated with column buffer, washed with 50 ml column buffer, and eluted with column buffer containing 10 mM maltose. The eluate was concentrated and buffer-exchanged into PBS using an Amicon Ultra-15 device (Millipore, Billerica, MA).

D.2.7 Surface Plasmon Resonance Analysis

Steady state affinity measurements were performed on a Biacore T100 biosensor by Rene Ott of the Ravetch group. MBP-Fn3 fusion proteins were immobilized to CM5 sensor chips (Biacore) by standard amine coupling. Soluble RIIA, RIIB or RIIIA were injected in 5 different concentrations through flow cells at room temperature in HBS-EP running buffer (Biacore) for 3 min at a flow rate of 30 µl/ min and dissociation was observed for 10 min. Dissociation constants were calculated after subtraction of background binding to a control flow cell using Biacore T100 Evaluation software.

D.3 Results

D.3.1 Selection and Affinity/Selectivity Maturation of Fn3 Binders to FcRs

To select for Fn3 domains that bind weakly to RIIA and RIIIA from naïve yeast surface display libraries, we performed magnetic bead sorting using streptavidin-coated beads loaded with biotinylated FcR, capitalizing on the highly multivalent interactions between yeast cells and beads. The libraries were mutagenized by error-prone PCR (the entire Fn3 gene as well as focused mutagenesis of the BC, DE, and FG loops) on average after every two sorts. As the selections progressed, in addition to increasing the wash stringency, the avidity was reduced by decreasing the surface density of both Fn3 and FcR. Unless otherwise stated, the 131R allele of RIIA and the 158F 176F allele of RIIIA were used. After eight magnetic sorts and four rounds of mutagenesis, both libraries were highly enriched for yeast cells that were clearly labeled by 25 nM of their respective FcR target in tetrameric form (complexed with streptavidin-PE). The RIIIA-binding library showed no binding to RIIB tetramer at 100 nM (not shown); therefore, continued affinity maturation by FACS was performed by standard methods (28, 29). To avoid unwanted side reactions between FcR and any mammalian IgG, a fluorescently tagged chicken IgY was used for expression labeling. The RIIA-targeted library displayed some binding to RIIB tetramer, albeit at a reduced level compared to RIIA tetramer (not shown), which was unsurprising given the high level of homology between the two receptors. Alternating sorts for affinity maturation and selectivity were performed. For the selectivity sorts, libraries were co-labeled with a high concentration of PE-tagged RIIB tetramer and a low concentration of Alexa Fluor 647-tagged RIIA tetramer to enrich clones that discriminated between the two receptors.

D.3.2 Analysis of Selected Clones

Our goal was to engineer Fn3 domains with roughly the same affinity for RIIA and RIIB as native IgGs ($K_d \sim 10^{-5}$-10^{-6} M), such that the eventual IgG-Fn3 fusions would activate immune cells after antigen opsonization but not in soluble form. After four FACS sorts (with one round of mutagenesis), the RIIIA-binding library was clearly labeled by 1 μM of monovalent RIIIA (not shown) and the K_d was estimated to be in the range of 0.5-5 μM (necessarily a poor estimate since saturation could not be reached and dissociation was rapid compared to handling time). Individual clones from this and previous libraries were sequenced and their relative affinities were estimated by determining the ratio of mean fluorescence intensities when labeled with a low versus high concentration of FcR tetramer. The tightest binder was IIIA626 (sequence in Fig. D.1A), which was then further characterized by titration to yield an apparent K_d of 0.13 nM for RIIIA tetramer (Fig. D.1B). Another clone with roughly five-fold lower tetramer affinity was also selected for further characterization in case the monovalent K_d of IIIA626 turned out to be too low. The apparent K_d of IIIA537 for RIIIA tetramer was found to be 0.67 nM (Fig. D.1B).

For the RIIA-binding library, no improvement in apparent K_d was seen during the eighth FACS sort (an affinity sort). Of the individual clones that were analyzed, IIA726 from the seventh FACS sort had the highest affinity for RIIA tetramer. From the titration curve, the apparent K_d for RIIA tetramer was 1.2 nM, whereas binding to RIIB tetramer was undetectable even at 100 nM (Fig. D.1C). A new library was subsequently created by mutagenizing IIA726. After two sorts, clone IIA827 with a single mutation (I88S) was identified as having improved affinity for RIIA tetramer (0.54 nM apparent K_d) while retaining undetectable binding for 100 nM RIIB tetramer (not shown). Unlike the cysteine-free RIIIA binders, IIA726 and IIA827 contain a pair of Cys residues in the BC and DE loops (Fig. D.1A).

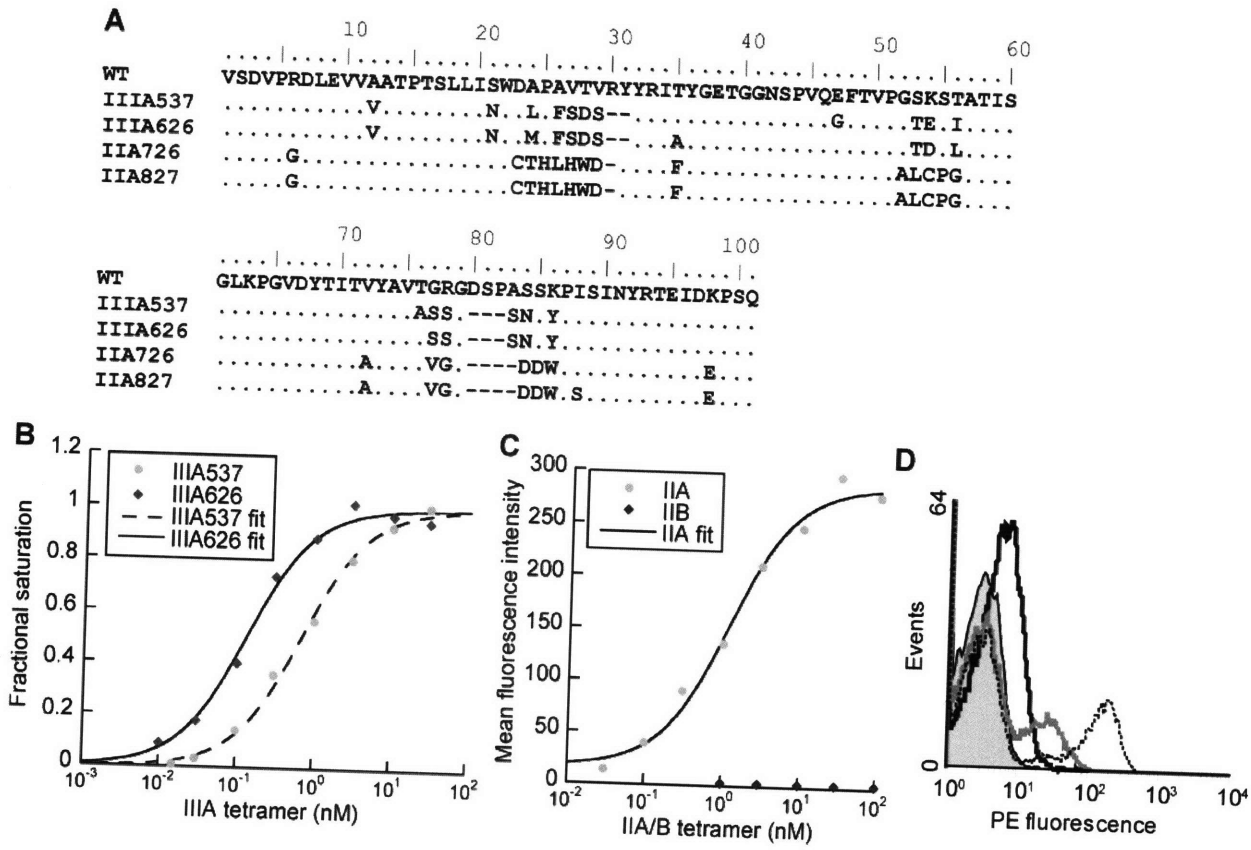

Fig. D.1, Sequences and binding curves of selected Fn3 domains to target FcRs.
A, Sequence alignment with wild type Fn3. Dots indicate conserved positions whereas dashes indicate deletions.

B, Yeast surface-displaying clones IIIA537 and IIIA626 were incubated with various concentrations of RIIIA$^{158F\ 176F}$ tetramer (complexed to streptavidin-PE) for 2 h at RT. The yeast cells were washed and analyzed by flow cytometry. The mean PE fluorescence intensities were fitted to binding isotherms (with proportionality and background constants) to give apparent RIIIA tetramer K_d values of 0.67 nM for IIIA537 and 0.13 nM for IIIA626.

C, Yeast surface-displaying clone IIA726 were incubated with various concentrations of either RIIA^{131R} or RIIB tetramer (complexed to streptavidin-PE) for 2 h at RT. The yeast cells were washed and analyzed by flow cytometry. The curve fit for the RIIA data points is to a binding isotherm (apparent K_d = 1.2 nM) with proportionality and background constants.

D, Each Fn3 domain was produced as a C-terminal fusion to MBP and biotinylated. Pre-incubated mixtures of each biotinylated MBP-Fn3 with streptavidin-PE were used to label human PBMCs for analysis by flow cytometry. Cells were gated by forward and side scatter to exclude lymphocytes. Gray fill histogram: MBP alone, black line: MBP-IIA726, gray line: MBP-IIIA537, dotted line: MBP-IIIA626.

D.3.3 Soluble MBP-Fn3 Fusion Proteins

The selected Fn3 domains were each produced as C-terminal fusions to MBP for determining the affinities for FcRs using surface plasmon resonance (SPR). MBP was chosen as a fusion partner because it contains many lysine residues available for amine coupling and acts as a chaperone, increasing the yields of soluble protein expressed in *E. coli* (30). MBP fusions of IIIA537, IIIA626 and IIA726 were initially expressed in the strain Rosetta(DE3) at high yields (3-5 mg from 100 ml of culture) and purified by amylose affinity chromatography. MBP-IIIA537 and MBP-IIIA626 were able to block the binding of PE-tagged RIIIA tetramer to yeast surface-displaying IIIA537 (not shown). The ability of MBP-IIA726 to block RIIA tetramer binding to yeast surface-displaying IIA726 was much lower (not shown), leading us to hypothesize that disulfide bond formation between the BC and DE loops was important for binding activity but had failed to occur. Accordingly, after MBP-IIA726 was incubated with 10 μM of $CuSO_4$ for 1 h at RT (cupric-catalyzed oxidation (31)), the blocking ability was significantly enhanced (not shown). MBP-IIA726 was then produced in Rosetta-gami 2, a strain containing mutations to promote disulfide bond formation in the cytosol. The blocking ability of this preparation was high and not significantly improved by incubation with $CuSO_4$ (not shown).

To determine whether the Fn3 domains were able to recognize FcRs expressed on cell surfaces, each MBP-Fn3 fusion protein was biotinylated, complexed with streptavidin-PE and used to label human peripheral blood mononuclear cells (PBMCs). Since B and T cells do not express RIIA or RIIIA, lymphocytes were excluded by forward and side scatter during flow cytometry analysis. MBP-IIA726 labeled the non-lymphocyte PBMCs more than the control of MBP alone, and a subpopulation of cells were distinctly labeled by MBP-IIIA537 and MBP-IIIA626 (Fig. D.1D). Although the shift in fluorescence intensity for MBP-IIA726 was small

(not unexpected because of the low avidity of streptavidin complexes), it was unlikely to be non-specific because no such shift was observed with the lymphocytes (not shown).

These three MBP-Fn3 fusion proteins as well as MBP-IIA827 (also produced in Rosetta-gami 2) were subjected to SPR analysis to determine the monovalent dissociation constants for the FcRs (Table D.1). MBP-IIIA537 and MBP-IIA626 each have single-digit micromolar affinities for their respective antigens, similar to the affinity of IgG1 for the activating FcRs, whereas MBP-IIIA626 and MBP-IIA827 (for RIIA 131R) have sub-micromolar dissociation constants. The RIIIA binders showed no binding to RIIA and RIIB, and the RIIA binders were also highly selective for RIIA over RIIB. Except for MBP-IIA827, the proteins had similar affinities for the two tested isoforms of their target FcR.

Table D.1. Dissociation constants of MBP-Fn3 fusion proteins for FcRs.

Protein	K_d (μM) for FcR				
	RIIA 131H	RIIA 131R	RIIB	RIIIA 158F 176F	RIIIA 158F 176V
MBP-IIIA537	nb	nb	nb	4.9	3.9
MBP-IIIA626	nb	nb	nb	0.53	0.54
MBP-IIA726	3.3	3.2	nb	nb	nb
MBP-IIA826	6.2	0.85	ud	nb	ud

nb: no binding observed ud: binding was too weak for K_d to be determined (>10 μM)

D.4 Conclusion and Future Work

Using yeast surface display, we have engineered Fn3 domains that selectively bind to the activating FcRs RIIA or RIIIA with little or no binding to the inhibitory RIIB receptor. Fusing these to antibodies represents a promising strategy to produce cancer therapeutics with heightened abilities to recruit immune effectors.

The B16-F10 melanoma lung metastasis mouse model has been used by Ravetch and colleagues to study tumor cytotoxicity effects mediated by antibodies and FcRs (3, 9, 32). The injected melanoma cells express the gp75 antigen, which is recognized by the TA99 monoclonal antibody. The Ravetch group is currently developing FcγR humanized mice (transgenic mice with individual human FcRs are already available), which will allow human IgGs and our human FcR-binding Fn3 domains to be investigated *in vivo* (33). We have already grafted the TA99 heavy and light variable regions onto human aglycosylated IgG1 (N297Q) heavy and light chain expression vectors. We have also created light chain-Fn3 expression cassettes for each of the four selected Fn3 domains. We plan to co-transfect two light chain-Fn3 plasmids (IIIA537 paired with IIA726 or IIIA626 paired with IIA827) and the heavy chain plasmid into HEK293 cells to secrete assembled IgG fusion proteins with the ability to bind gp75, RIIA and RIIIA. Since complexes with two identical light chain-Fn3 fusions will also be formed, purification of the trispecific complex will be facilitated by using different tags on on the IIA binders versus the IIIA binders (His6 and Strep-tag II). A control IgG-Fn3 fusion protein bearing irrelevant lysozyme-binding Fn3 domains will also be produced. An alternative format for attaching two different Fn3 domains to one IgG molecule is to fuse each Fn3 to the C-terminus of one heavy chain. Heterodimeric assembly of the heavy chains can be promoted using the "knobs-into-holes" technique (complementary mutations in the CH3 domains) (34).

We have shown that the selected Fn3 domains bind epitopes of the FcRs that are accessible on the cell surface, but is is as yet unknown if the topology of either IgG-Fn3 format in an immune complex is amenable to productively engaging and cross-linking FcRs. Therefore, it is likely that *in vitro* experiments will be performed on either human immune cells (using a donor with the appropriate FcR alleles), cells derived from the FcR humanized mouse, or cell lines transgenic for the FcRs. Dendritic cell maturation can also be studied *in vitro* to investigate the consequences of engaging activating FcRs without applying the RIIB brakes.

D.5 References

1. Nimmerjahn, F., and J. V. Ravetch. 2007. Antibodies, Fc receptors and cancer. *Current Opinion in Immunology* 19: 239-245.
2. Desjarlais, J. R., G. A. Lazar, E. A. Zhukovsky, and S. Y. Chu. 2007. Optimizing engagement of the immune system by anti-tumor antibodies: an engineer's perspective. *Drug Discov Today* 12: 898-910.
3. Nimmerjahn, F., and J. V. Ravetch. 2005. Divergent Immunoglobulin G Subclass Activity Through Selective Fc Receptor Binding. *Science* 310: 1510-1512.
4. Cartron, G., L. Dacheux, G. Salles, P. Solal-Celigny, P. Bardos, P. Colombat, and H. Watier. 2002. Therapeutic activity of humanized anti-CD20 monoclonal antibody and polymorphism in IgG Fc receptor Fcgamma RIIIa gene. *Blood* 99: 754-758.
5. Weng, W.-K., and R. Levy. 2003. Two Immunoglobulin G Fragment C Receptor Polymorphisms Independently Predict Response to Rituximab in Patients With Follicular Lymphoma. *J Clin Oncol* 21: 3940-3947.
6. Treon, S. P., M. Hansen, A. R. Branagan, S. Verselis, C. Emmanouilides, E. Kimby, S. R. Frankel, N. Touroutoglou, B. Turnbull, K. C. Anderson, D. G. Maloney, and E. A. Fox. 2005. Polymorphisms in Fc{gamma}RIIIA (CD16) Receptor Expression Are Associated With Clinical Response to Rituximab in Waldenstrom's Macroglobulinemia. *J Clin Oncol* 23: 474-481.
7. Kim, D. H., H. D. Jung, J. G. Kim, J.-J. Lee, D.-H. Yang, Y. H. Park, Y. R. Do, H. J. Shin, M. K. Kim, M. S. Hyun, and S. K. Sohn. 2006. FCGR3A gene polymorphisms may correlate with response to frontline R-CHOP therapy for diffuse large B-cell lymphoma. *Blood* 108: 2720-2725.
8. Musolino, A., N. Naldi, B. Bortesi, D. Pezzuolo, M. Capelletti, G. Missale, D. Laccabue, A. Zerbini, R. Camisa, G. Bisagni, T. M. Neri, and A. Ardizzoni. 2008. Immunoglobulin G Fragment C Receptor Polymorphisms and Clinical Efficacy of Trastuzumab-Based Therapy in Patients With HER-2/neu-Positive Metastatic Breast Cancer. *J Clin Oncol* 26: 1789-1796.
9. Clynes, R. A., T. L. Towers, L. G. Presta, and J. V. Ravetch. 2000. Inhibitory Fc receptors modulate in vivo cytoxicity against tumor targets. *Nat Med* 6: 443-446.
10. Dhodapkar, K. M., J. L. Kaufman, M. Ehlers, D. K. Banerjee, E. Bonvini, S. Koenig, R. M. Steinman, J. V. Ravetch, and M. V. Dhodapkar. 2005. Selective blockade of inhibitory Fc{gamma} receptor enables human dendritic cell maturation with IL-12p70 production and immunity to antibody-coated tumor cells. *Proc Natl Acad Sci U S A* 102: 2910-2915.
11. Shields, R. L., A. K. Namenuk, K. Hong, Y. G. Meng, J. Rae, J. Briggs, D. Xie, J. Lai, A. Stadlen, B. Li, J. A. Fox, and L. G. Presta. 2001. High Resolution Mapping of the Binding Site on Human IgG1 for Fcgamma RI, Fcgamma RII, Fcgamma RIII, and FcRn and Design of IgG1 Variants with Improved Binding to the Fcgamma R. *J. Biol. Chem.* 276: 6591-6604.

12. Lazar, G. A., W. Dang, S. Karki, O. Vafa, J. S. Peng, L. Hyun, C. Chan, H. S. Chung, A. Eivazi, S. C. Yoder, J. Vielmetter, D. F. Carmichael, R. J. Hayes, and B. I. Dahiyat. 2006. Engineered antibody Fc variants with enhanced effector function. *Proc Natl Acad Sci U S A* 103: 4005-4010.

13. Stavenhagen, J. B., S. Gorlatov, N. Tuaillon, C. T. Rankin, H. Li, S. Burke, L. Huang, S. Johnson, E. Bonvini, and S. Koenig. 2007. Fc Optimization of Therapeutic Antibodies Enhances Their Ability to Kill Tumor Cells In vitro and Controls Tumor Expansion In vivo via Low-Affinity Activating Fc{gamma} Receptors. *Cancer Res* 67: 8882-8890.

14. Sazinsky, S. L., R. G. Ott, N. W. Silver, B. Tidor, J. V. Ravetch, and K. D. Wittrup. 2008. Aglycosylated immunoglobulin G1 variants productively engage activating Fc receptors. *Manuscript in progress*.

15. McCall, A. M., G. P. Adams, A. R. Amoroso, U. B. Nielsen, L. Zhang, E. Horak, H. Simmons, R. Schier, J. D. Marks, and L. M. Weiner. 1999. Isolation and characterization of an anti-CD16 single-chain Fv fragment and construction of an anti-HER2/neu/anti-CD16 bispecific scFv that triggers CD16-dependent tumor cytolysis. *Molecular Immunology* 36: 433-446.

16. Xie, Z., N. Guo, M. Yu, M. Hu, and B. Shen. 2005. A new format of bispecific antibody: highly efficient heterodimerization, expression and tumor cell lysis. *Journal of Immunological Methods* 296: 95-101.

17. Tao, M., and S. Morrison. 1989. Studies of aglycosylated chimeric mouse-human IgG. Role of carbohydrate in the structure and effector functions mediated by the human IgG constant region. *J Immunol* 143: 2595-2601.

18. Koide, A., C. W. Bailey, X. Huang, and S. Koide. 1998. The fibronectin type III domain as a scaffold for novel binding proteins. *J Mol Biol* 284: 1141-1151.

19. Koide, A., S. Abbatiello, L. Rothgery, and S. Koide. 2002. Probing protein conformational changes in living cells by using designer binding proteins: application to the estrogen receptor. *Proc Natl Acad Sci U S A* 99: 1253-1258.

20. Xu, L., P. Aha, K. Gu, R. G. Kuimelis, M. Kurz, T. Lam, A. C. Lim, H. Liu, P. A. Lohse, L. Sun, S. Weng, R. W. Wagner, and D. Lipovsek. 2002. Directed evolution of high-affinity antibody mimics using mRNA display. *Chem Biol* 9: 933-942.

21. Richards, J., M. Miller, J. Abend, A. Koide, S. Koide, and S. Dewhurst. 2003. Engineered fibronectin type III domain with a RGDWXE sequence binds with enhanced affinity and specificity to human alphavbeta3 integrin. *J Mol Biol* 326: 1475-1488.

22. Karatan, E., M. Merguerian, Z. Han, M. D. Scholle, S. Koide, and B. K. Kay. 2004. Molecular recognition properties of FN3 monobodies that bind the Src SH3 domain. *Chem Biol* 11: 835-844.

23. Parker, M. H., Y. Chen, F. Danehy, K. Dufu, J. Ekstrom, E. Getmanova, J. Gokemeijer, L. Xu, and D. Lipovsek. 2005. Antibody mimics based on human fibronectin type three domain engineered for thermostability and high-affinity binding to vascular endothelial growth factor receptor two. *Protein Eng Des Sel* 18: 435-444.

24. Huang, J., A. Koide, K. W. Nettle, G. L. Greene, and S. Koide. 2006. Conformation-specific affinity purification of proteins using engineered binding proteins: application to the estrogen receptor. *Protein Expr Purif* 47: 348-354.

25. Koide, A., R. N. Gilbreth, K. Esaki, V. Tereshko, and S. Koide. 2007. High-affinity single-domain binding proteins with a binary-code interface. *Proc Natl Acad Sci U S A* 104: 6632-6637.

26. Lipovsek, D., S. M. Lippow, B. J. Hackel, M. W. Gregson, P. Cheng, A. Kapila, and K. D. Wittrup. 2007. Evolution of an interloop disulfide bond in high-affinity antibody mimics based on fibronectin type III domain and selected by yeast surface display: molecular convergence with single-domain camelid and shark antibodies. *J Mol Biol* 368: 1024-1041.

27. Hackel, B. J., A. Kapila, and K. D. Wittrup. 2008. Picomolar affinity fibronectin domains engineered utilizing loop length diversity, recursive mutagenesis, and loop shuffling. *Manuscript in progress.*

28. Chao, G., W. L. Lau, B. J. Hackel, S. L. Sazinsky, S. M. Lippow, and K. D. Wittrup. 2006. Isolating and engineering human antibodies using yeast surface display. *Nat. Protocols* 1: 755-768.

29. Colby, D. W., B. A. Kellogg, C. P. Graff, Y. A. Yeung, J. S. Swers, and K. D. Wittrup. 2004. Engineering Antibody Affinity by Yeast Surface Display. *Methods Enzymol.*: 348-358.

30. Kapust, R., and D. Waugh. 1999. Escherichia coli maltose-binding protein is uncommonly effective at promoting the solubility of polypeptides to which it is fused. *Protein Sci* 8: 1668-1674.

31. Yamada, T., A. Fujishima, K. Kawahara, K. Kato, and O. Nishimura. 1987. Importance of disulfide linkage for constructing the biologically active human interleukin-2. *Archives of Biochemistry and Biophysics* 257: 194-199.

32. Clynes, R., Y. Takechi, Y. Moroi, A. Houghton, and J. V. Ravetch. 1998. Fc receptors are required in passive and active immunity to melanoma. *Proc Natl Acad Sci U S A* 95: 652-656.

33. Nimmerjahn, F., and J. V. Ravetch. 2008. Fc[gamma] receptors as regulators of immune responses. 8: 34-47.

34. Ridgway, J. B. B., L. G. Presta, and P. Carter. 1996. 'Knobs-into-holes' engineering of antibody CH3 domains for heavy chain heterodimerization. *Protein Eng.* 9: 617-621.